



FINAL REPORT

Ecosystem model comparison at multiple scales and sites

Project#: RC-201702

Dr. Melissa Lucash, Portland State University
Dr. Robert Scheller, North Carolina State University
Dr. Matthew Duvaneck, Harvard University

Version 1.0

TABLE OF CONTENTS

LIST OF ACRONYMS	3
LIST OF FIGURES	3
LIST OF TABLES	4
Acknowledgments	5
ABSTRACT	6
EXECUTIVE SUMMARY	7
1.0 INTRODUCTION	12
1.1 BACKGROUND	12
1.2 OVERALL OBJECTIVES	13
1.3 REGULATORY DRIVERS	14
2.0 TECHNOLOGY/METHODOLOGY DESCRIPTION	15
2.1 TECHNOLOGY/METHODOLOGY OVERVIEW	15
2.2 ADVANTAGES AND LIMITATIONS OF THE TECHNOLOGY/ METHODOLOGY	19
3.0 PERFORMANCE OBJECTIVES	21
4.0 SITE DESCRIPTION	23
4.1 SITE SELECTION	23
4.2 SITE LOCATION AND HISTORY	23
4.3 SITE CHARACTERISTICS	23
5.0 TEST DESIGN	25
5.1 CONCEPTUAL TEST DESIGN	25
5.2 BASELINE CHARACTERIZATION AND PREPARATION	25
5.3 DESIGN AND LAYOUT OF TECHNOLOGY AND METHODOLOGY COMPONENTS	31
5.4 FIELD TESTING	31
5.5 SAMPLING PROTOCOL	31
5.6 SAMPLING RESULTS	31
6.0 PERFORMANCE ASSESSMENT	37
6.1 Test Phase	37
6.2 Demonstration Phase	37
7.0 COST ASSESSMENT	46
8.0 IMPLEMENTATION ISSUES	47
9.0 REFERENCES	48
APPENDICES	52
Appendix A: Point of Contact	52
Appendix B: Erickson and Strigul (2019).	52

LIST OF ACRONYMS

ACUB	Army Compatible Use Buffer
Co-I	Co-investigator
DoD	Department of Defense
ENCSLP	Eastern North Carolina Sentinel Landscapes Partnership
ESTCP	Environmental Security Technology Certification Program
FBDPWED	Ft. Bragg Directorate of Public Works, Environmental Division
FIA	USDA Forest Inventory and Analysis data
FORCES	Forest Opportunities for Resource Conservation and Environmental Security
HASP	Health and Safety Plan
LANDIS-II	LANDscape DIsturbance and Succession model, variant 2
LANDSIM	LANDscape SIMulator
NCSCP	North Carolina Sandhills Conservation Partnership
NECN-Hydro	Net Ecosystem Carbon and Nitrogen with Hydrology
PI	Principal Investigator
PPA	Perfect Plasticity Approximation
PPA-SiBGC	PPA with Simple Biogeochemistry
PnET	Photosynthesis and EvapoTranspiration model of plant growth
QA/QC	Quality assurance / quality checking
RCW	Red-cockaded woodpecker (<i>Leuconotopicus borealis</i>)
RMSE	Root mean squared error
SERPPAS	Southeast Regional Partnership for Planning and Sustainability
SORTIE	SORTIE gap model

LIST OF FIGURES

Figure 1. Schematic diagram of the PPA-SiBGC model structure. From Erickson and Strigul (2019).

Figure 2. Schematic diagram of the Net Ecosystem Carbon Nitrogen Succession ('NECN') model structure. From Scheller et al. (2011).

Figure 3. Schematic diagram of the PnET model as ported into the LANDIS-II framework. From de Brujin et al. (2014).

Figure 4. Locations of the Jones Center, Ft. Bragg, and Harvard Forest.

Figure 5. The presence of old-growth longleaf pine (left, green) and loblolly pine (right) imputed from Ft. Bragg Natural Resource Division inventory data. These data were integrated into baseline conditions.

Figure 6. Baseline estimated age distributions of nine species within the Ft. Bragg, NC landscape.

Figure 7. A comparison of baseline biomass as imputed into NECN and as derived from FIA data for NC, SC, and VA.

Figure 8. Baseline vegetation types for Ft. Bragg, NC, representing vegetation types circa 2018.

Figure 9. Baseline fire zone maps at Ft. Bragg, NC. Zones are burned either every 1, 2 or 3 years in the current Rx fire regime.

Figure 10. The distribution of hurricane wind speeds in hurricanes that strike GA, SC, NC, or VA, from 1969 – 2018.

Figure 11. Growth calibration of nine tree species using the PnET model. Within each subplot, the longevity value represents the age of each tree species expected senescence; the species-group value listed represents the species-group published within Smith et al. (2006). Data represent growth trajectories of a single species growing by itself.

Figure 12. Establishment calibration of nine tree species using the PnET model. Establishment generally declines as a function of shade represented by biomass. Black symbols represent PnET. Colored lines represent site condition: Blue = high site index, Red = medium site index, Green = low site index.

Figure 13. Growth calibration of nine tree species using NECN. Blue lines are NECN; Black dots represent FIA data and green dots are from Smith et al. (2006). Data represent growth trajectories of a single species growing by itself.

Figure 14. Growth trends over time simulated by NECN (blue) and PnET succession (gold). FIA plots are represented by the black dots, while Smith et al (2016) is represented by the green dots.

Figure 15. Total aboveground biomass (g m^{-2}) as simulated by the NECN and PnET model from 2010 – 2060 for Ft. Bragg, NC.

Figure 16. Aboveground biomass (g m^{-2}) for longleaf pine and loblolly pine as simulated by the NECN and PnET model from 2010 – 2060 for Ft. Bragg, NC.

Figure 17. Aboveground biomass (g m^{-2}) for white oak and red maple as simulated by the NECN and PnET model from 2010 – 2060 for Ft. Bragg, NC.

Figure 18. Hectares harvested for NECN and PnET models, two climate scenario, simulated for 2010 – 2060 for Ft. Bragg, NC.

Figure 19. Mortality caused by prescribed fire for NECN, two climate scenarios, simulated for 2010 – 2060 for Ft. Bragg, NC.

Figure 20. Area burned by prescribed fire (ha) for NECN, two climate scenarios, simulated for 2010 – 2060 for Ft. Bragg, NC.

Figure 21. Number of prescribed fire per year for NECN, two climate scenarios, simulated for 2010 – 2060 for Ft. Bragg, NC.

Figure 22. Aboveground biomass (g m^{-2}) simulated with (HUR) and without (NO_HUR) a contemporary hurricane regime, using NECN and two climate scenarios, simulated for 2010 – 2060 for Ft. Bragg, NC.

LIST OF TABLES

Table 1. Tree species and key life history attributes simulated for Ft. Bragg, NC.	9
Table 2. Performance Objectives for Test Phase and Demonstration Phases.	21
Table 3. Number of hurricanes per year in GA, SC, NC, or VA from 1969-2018.	29
Table 4. Cost Model for a Monitoring Technology	44

Acknowledgments

The Ft. Bragg Directorate of Public Works, Environmental Division was instrumental in the development and delivery of this report: Rod Fleming, Jason Monroe, T. Kevin Crawford. Drs. Adam Erickson and Nicholas Strigul contributed substantially to the Test Phase comparison of models. Paul Pettus provided valuable assistance with running scenarios, maps, and graphing. Paul Schrum lead the hurricane simulation effort.

ABSTRACT

1. Objective:

Ensuring the long-term sustainability of eastern US forests in the face of climate variability and change will require that forest managers have the best available climate change research to make sound management decisions. Ecosystem process models are now able to project forest landscape conditions in response to anticipated climate, natural disturbance, forest management, and their interactions; these projections can inform forest management decisions. However, there is no single scale which is perfectly suited to addressing all climate change and management related questions. Critical patterns which emerge at fine-scales may be over-averaged at larger scales and vice-versa. Our objectives were to, a) compare model outcomes from two modeling frameworks against empirical data and to each other, b) examine climate change, disturbance, and management interactions at Ft. Bragg, North Carolina; translate these procedures; and prepare a roadmap for deployment across other forested military installations.

2. Technology Description:

We executed a two-stage approach for integrating climate, disturbance, and management projections at multiple scales. First, we calibrate and compared two models, a stand-scale model (PPA-SiBGC) and a landscape-scale model (NECN operating within a landscape change framework), against empirical data collected from two pine-dominated sites in the eastern US. Second, we applied the NECN and PnET models to the Ft. Bragg landscape in central North Carolina under multiple projections of climate change, prescribed fires, and hurricanes. We assessed the strengths and weakness of each model and their respective capacity to project a suite of ecosystem processes, including succession, disturbance and nutrient cycling, given current and potential management practices and anticipated climate change.

We worked closely with the Ft. Bragg natural resource management team to refine data inputs and to develop scenarios via an iterative process that identified goals and scenarios, data needs, and desired outputs. Our models will be delivered to Ft. Bragg fully parameterized and prepared for subsequent use, including full documentation and access to the open-source code for each model.

3. Expected Benefits:

Successful demonstration and validation of landscape change models will help decision-makers integrate a multitude of management strategies into the context of the military mission and installation-specific natural resources management plans. Forest managers will be able to use either NECN or PnET to estimate the effects of different management practices on the local installations over varying time horizons and spatial scale resolutions. Upon completion, this technology can be applied immediately at Ft. Bragg's more than 89,000 acres of longleaf pine forests and at other DoD installations with forested habitats..

EXECUTIVE SUMMARY

Introduction

Episodic extremes and directional climatic change may threaten the long-term composition, structure, and function of eastern US forests. Forests are coupled to the climate through feedbacks including surface energy fluxes, hydrology, carbon cycling, vegetation dynamics, land-use, and urbanization. Forests currently sequester substantial global carbon emissions yet are sensitive to climatic changes. Forests also produce local cooling effects, increase ecosystem water storage, and improve water quality. And forests provide critical habitat and support local economic activities, from extractive industry to recreation. Whether these benefits will persist is a key scientific and management question, given evidence of increased temperatures and frequency of extreme events.

Changes to climate and management regimes have broad implications for the future of forests, across local and global scales. Optimizing the management of these forests for projected climatic conditions necessitates that managers have access to accurate and timely forecasts of forest change. Forest change models now have the capacity to project future forest conditions in response to climate, disturbance, and management regimes, as well as their interactions, making them for informing long-term management. However, there is no single model or scale that is suited to addressing all climate-, disturbance-, and management-related questions.

Changes to climate reduce the benefits of forests, including the military mission to provide diverse landscapes for training. In the United States, DoD is the fifth largest federal land manager, managing 11.4 million acres, or 2% of all federal lands. Unlike other federal agencies, DoD manages an additional 12,487 acres overseas, for a total of 11.6 million acres. These lands are critical to the military mission, providing diverse landscapes for training. DoD lands are also of high biological importance, as they are often in pristine condition due to access restrictions and the maintenance of rare fire-prone ecosystems in artillery ranges.

For example, Ft. Bragg, NC, is home to a number of at-risk, threatened, and endangered species under the Endangered Species Act, including red-cockaded woodpecker (*Leuconotopicus borealis*) and Saint Francis' satyr butterfly (*Neonympha mitchellii francisci*). Management activities at Ft. Bragg are designed to meet multiple-use goals and include biodiversity monitoring, prescribed burning, thinning, harvesting, and reforesting. Ft. Bragg serves as a model for forest management for other military installations. Management practices that meet multiple objectives are particularly valuable. Whether these benefits will continue into the future is, however, unknown. New technologies are required to assess potential risks due to climate change and extreme events and to assess potential management activities that could mitigate these risks. Changes to management are expensive and carry a degree of risk (i.e., failure). Our goal was to assess multiple technologies for projecting forest change and assess their performance.

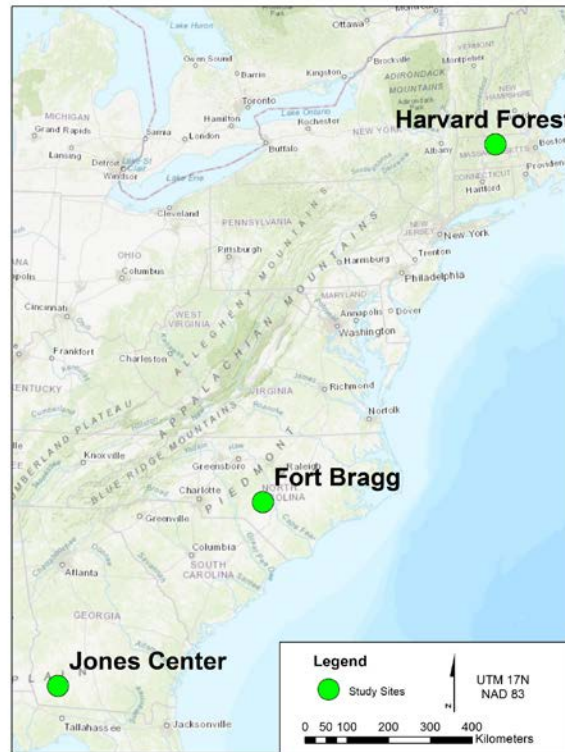
Objectives

Our objectives were to: (a) compare the performance of three forest change models to empirical measurements and to each other; (b) demonstration model performance when projecting climate

change, disturbance, and management interactions at Ft. Bragg, NC; (c) translate these procedures and prepare a roadmap for deployment across other forested military installations.

Successful demonstration and validation of these models will help DoD natural resource managers consider and compare a multitude of management strategies into the context of the military mission and installation-specific natural resources management plans. Our intention is that forest managers will be able to readily apply one or more models to estimate the effects of different management regimes at DoD installations over varying spatiotemporal scales.

We conducted our technology comparison in two stages with two distinct tasks. In the stage one (the **Test Phase**), we parameterized, calibrated, and compared PPA-SiBGC (a variant of the SORTIE model) and NECN models and empirical data collected for two well-characterized sites in the eastern US: Harvard Forest, MA and Jones Ecological Research Center, GA. In stage two (the **Demonstration Phase**), we applied the NECN and PnET models to Ft. Bragg, NC, to simulate the effects of projected changes to climate. For both phases, we assessed the strengths and weakness of each model and their respective capacities to simulate a suite of processes that influence forests and forest change. Processes include forest management (prescribed fire, clearcutting, and thinning), succession, disturbance, and biogeochemical cycling, under alternate climatic conditions.



Technology Description

Forest change models are primary technology being evaluated (although some ancillary tools are also necessary). Model selection was constrained by the need to achieve objectives at two scales: (1) stand-scale (< 10 ha) for comparison with 5-25 years of flux tower data at two sites; (2) landscape-scale for simulation of management, disturbance and climate scenarios for 50-100 years across Ft. Bragg, NC. Many models satisfy one but not both of these objectives, or operate only at broader scales. To be included, models must produce data that can be objectively compared against empirical data, particularly biogeochemical cycling (e.g., growth and autotrophic respiration rates), succession, and disturbances. Where possible, we compared models with different architectures to capture variability attributable to model design. We emphasized mature models with evidence of successful application in the literature.

Based on our criteria, we selected three forest change models: (1) the PPA-SiBGC model, a variant of the SORTIE gap model reduced with the Perfect Plasticity Approximation (PPA); (2)

the Net Ecosystem Carbon and Nitrogen model (NECN; operating within the LANDIS-II framework); and (3) the Photosynthesis and Evapotranspiration model (PnET; operating within the LANDIS-II framework). All three models operate at a cohort resolution (representing not individual trees but instead binning trees into cohorts defined by their species, age, and other pertinent attributes) and can scale from stands to landscapes. The scale of their primary interactions distinguish the three models. PPA-SiBGC emphasizes interactions among cohorts within stands. NECN emphasizes an ecosystem (i.e., mass balance) approach to allocating Carbon and Nitrogen. PnET emphasizes a mechanistic approach to simulate photosynthesis based on light, water, temperature, and competition through vertical layers in a canopy.

Both NECN and PnET have been implemented within the LANDIS-II landscape change framework. LANDIS-II is an open-source framework allows the development of user-defined sub-models that interact with a simulation core. This design specification has facilitated the rapid development of many new sub-models operating within the LANDIS-II framework. The sub-models are primarily comprised of succession, management, and disturbance models but also include other model functionality. LANDIS-II benefits from a large user base and extensive model calibration-validation efforts, providing model maturity and flexibility. LANDIS-II inputs include climate, stand composition and age, life history attributes, and disturbance regimes.

In the **Test Phase**, we compared the performance of PPA-SiBGC and NECN and with empirical data collected at two research sites on the east coast of the United States: (1) Harvard Forest, MA; and (2) Jones Ecological Research Center, GA (Figure 4). We implemented an innovative approach that leverages all available data by sampling from distributions of parameters, rather than flattening the variance into mean values, at the start of each simulation run. This allowed us to produce confidence intervals and/or uncertainties for the simulations using Monte Carlo methods.

In the **Demonstration Phase**, we applied the NECN and PnET models to forecast future management and climate scenarios across the Ft. Bragg, NC landscape (Figure 4). We iteratively created final scenarios via direct collaboration with Ft. Bragg Directorate of Public Works, Environmental Division (FBDPWED). They provided available data and helped to resolve any localized parameter needs.

Performance Assessment

For the **Test Phase**, we compared PPA-SiBGC and NECN against empirical data and therefore the success criterion for each objective was the Pearson correlation coefficient (r) across the vector of annual simulated and empirical values. Performance metrics focused on near-term projections of ecological processes (not including climate change, management, or disturbance) that could be compared against 5-25 years of empirical data collected at Harvard Forest and the Jones Center.

The overall performance for both models was comparable. In general, both models accurately predicted biomass, Carbon, and Nitrogen pools. PPA-SiBGC better predicted soil respiration and NECN better predicted NEE. Overall R^2 values were similar: 0.73 (PPA-SiBGC) vs. 0.69 (NECN). Both models performed better at the Harvard Forest site than the Jones Center.

For the **Demonstration Phase**, we simulated 50 years of forest change based on scenarios developed in collaboration with the FBDPWED. Because our scenarios represent future potential conditions, there are not empirical data for comparison. Performance metrics therefore focused on the capacity to successfully integrate multiple processes and to produce reasonable projections that reflect expected changes given the scenarios. These scenarios were collaboratively developed scenarios with Ft. Bragg natural resource managers. Therefore, our performance assessment included:

- Climate change: How will temperature and precipitation change? There are many Global Circulation Models (GCMs) and carbon emissions projections to choose. We selected one climate future that represents highest mean annual temperature (MAT) and lowest mean annual precipitation (MAP), labeled “Hot-Dry”. Another represents highest MAT with the highest MAP. We selected these two from 15+ downscaled climate data from USGS.
- Management: Ft. Bragg is very actively managed and this will continue to shape vegetation patterns. We simulated prescribed fire occurrence in multiple prescription blocks at 2, 3, and 5 years. We held thinning constant at 2500 acres per year and clearcutting to convert slash pine (*Pinus elliottii*) to longleaf pine (*P. palustris*).
- Hurricanes: Hurricanes have the potential to cause substantial loss of critical biodiversity habitat. Based on historic hurricane extent and mortality patterns (from the past 20 years of data available), we simulated hurricanes under a historic conditions and ‘high’ hurricane conditions. High hurricanes doubled the probability of a hurricane occurring in any given year and will also increase the intensity by 50%.

Table 1. Tree species and key life history attributes simulated for Ft. Bragg, NC.

Species	Longevity	Sexual maturity	Shade tolerance	Effective seed dispersal distance	Max seed dispersal distance	Post-fire regeneration
<i>Pinus taeda</i>	300	30	1	30	200	None
<i>P. palustris</i>	400	30	1	100	200	None
<i>P. echinata</i>	200	20	1	60	500	Resprout
<i>P. elliottii</i>	200	10	1	46	100	Resprout
<i>Quercus alba</i>	300	40	3	30	3000	Resprout
<i>Q. laevis</i>	200	20	1	100	200	Resprout
<i>Lyquidambar styraciflua</i>	300	25	1	100	200	Resprout
<i>Acer rubrum</i>	150	10	4	100	1000	None
<i>Liriodendron tulipifera</i>	250	15	1	150	300	Resprout

Our performance assessments are ongoing due to implementation issues (below). However, the preliminary results suggest that NECN and PnET are sensitive to different climatic drivers and different forest types (conifer vs. deciduous) have differing sensitivity to climate. Another substantial difference in performance is the difference in achieving baseline conditions. PnET currently uses a ‘spin-up’ method whereby the model must run prior to scenario execution in order to estimate baseline conditions of aboveground biomass. NECN uses inventory data to estimate baseline conditions. PnET baseline conditions were substantially higher than in NECN. Likely PnET is underestimating the background disturbance rate during spin-up (particularly given the active management regime at Ft. Bragg). It is also possible – but less likely - that our inventory data over-estimate initial biomass due to the necessity of sampling inventory data from the broader southeast region (NC, SC, and VA). The consequence of differing baseline conditions is that PnET growth is constrained by competition sooner than in NECN. However, the model estimates of aboveground biomass converge over time, achieving parity for the most important species within 30 years.

Regarding disturbance and management, neither model estimates of aboveground was particularly sensitive to variation in the prescribed fire management regime. This is in part because prescribed fire targets sub-canopy deciduous trees that have low biomass. Future work that will focus on endangered red-cockaded woodpecker (*Leuconotopicus borealis*) habitat is expected to show greater sensitivity to prescribed fire. Both models are highly sensitive to simulated hurricanes, highlighting model differences in regeneration and growth. This work is ongoing.

Cost Assessment

Our cost assessment is primarily focused on labor. The forest change models assessed are all open-source and freely available. All of the necessary supporting software is also free (or free equivalents can be found). The input data are also freely available from US agencies or free local natural resource managers.

The primary labor expenses are (1) a competent GIS technician (with additional skills in data manipulation via R), (2) a modeling expert. Both are required to operate the methods described above. Within our demonstration plan, we were able to produce the projections using ~8 months of GIS technician effort and ~2 months of model expert effort. The final cost will vary depending on labor costs for the technician and modeling experts.

Implementation Issues

We encountered numerous implantation issues including technical and scheduling issues. Originally we intended to use the PPA-SiBGC model in both phases. However, the technology was not mature and did not continue necessary management and disturbance routines for simulating a large base. Therefore we had to replace the model (with PnET) and recruit and onboard a new Co-I with PnET experience. In addition, we had to replace the original technician. As a result, there were numerous transition and funding delays although we anticipate meeting all performance objectives by project conclusion.

1.0 INTRODUCTION

1.1 BACKGROUND

Episodic extremes and directional climatic change may threaten the long-term composition, structure, and function of eastern US forests (Aber et al. 1995, Iverson et al. 2004, Dukes et al. 2009). Forests are coupled to the climate through feedbacks including surface energy fluxes, hydrology, carbon cycling, vegetation dynamics, land-use, and urbanization (Bonan 2008). Forests currently exhibit the capacity to sequester substantial global carbon emissions yet are sensitive to climatic changes (Luyssaert et al. 2008, Pan et al. 2011). Forests also produce local cooling effects, increase ecosystem water storage, and improve water quality (Bonan 2008, Ellison 2017). And forests provide critical habitat and support local economic activities, from extractive industry to recreation. Whether these benefits will persist is a key scientific and management question, given evidence of increased temperatures and frequency of extreme events.

Changes to climate and management regimes have broad implications for the future of forests, across local and global scales. Forest management is an integral component of the global carbon cycle, growing in importance since early agricultural land clearing 8,000 years ago (Ruddiman 2003, Kaplan et al. 2011). While the share of natural forests continues to decline globally, the share of managed forests continues to increase (FAO 2016). Adapting forest management for projected climatic conditions (Millar et al. 2007, D'Amato et al. 2011) requires that managers have access to accurate and timely ecological forecasts for different timescales (Clark et al. 2001). Forest change models now have the capacity to project future forest conditions in response to climate, disturbance, and management regimes, as well as their interactions, making them ideal for informing climate adaptive management practices. However, there is no single scale or model that is perfectly suited to addressing all climate-, disturbance-, and management-related questions (Scheller 2018). Fine-scale patterns in forests are lost when simulating broad scales, compressing spatiotemporal variation through averaging (Wiens et al. 2002). Yet, the net effect of fine-scale variability has been shown to produce emergent properties at larger scales, altering estimates of forest properties important to managers (Johnsen et al. 2001, Seidl et al. 2013).

Changes to climate threaten many benefits of forests, most critical to the military mission of which is the availability of diverse landscapes for training. In the United States, DoD is the fifth largest federal land manager, managing 11.4 million acres, or 2% of all federal lands. Unlike other federal agencies, DoD manages an additional 12,487 acres overseas, for a total of 11.6 million acres (Vincent et al. 2017). These lands are critical to the military mission, providing diverse landscapes for training. DoD lands are also of high biological importance, as they are often in pristine condition due to access restrictions and the maintenance of rare fire-prone ecosystems in artillery ranges (Douglas and Leslie 1997).

As an example, Ft. Bragg, NC, is home to a number of at-risk, threatened, and endangered species under the Endangered Species Act, including red-cockaded woodpecker (RCW: *Leuconotopicus borealis*) (Kuefler et al. 2008) and Saint Francis' satyr butterfly (*Neonympha*

mitchellii francisci) (Lipscomb and Williams 2006). Management activities at Ft. Bragg are designed to meet multiple-use goals and include biodiversity monitoring, prescribed burning, thinning, harvesting, and reforesting. These goals are threatened by climate change and its ancillary effects including increased hurricane activity and limitations to prescribed burning due to shifting burn windows. Ft. Bragg can serve as a model for other military installations attempting to adapt their management plans for global change if the appropriate technologies (forest change models) can be integrated into their planning activities.

1.2 OVERALL OBJECTIVES

Our objectives were to: (a) compare outcomes produced by two models of forest ecosystems to empirical measurements and to each other; (b) examine modeled climate change, disturbance, and management interactions at Ft. Bragg; (c) translate these procedures and prepare a roadmap for deployment across other forested military installations.

We assessed the capabilities of appropriate forest change models to simulate future climate, disturbance, and management conditions at multiple scales. We utilized three distinct models of forests change; these models represent an advancement from previous generation ‘growth-and-yield’ and process-based ‘gap’ models (Shifley et al. 2017). Forest change models typically operate at cohort resolution (i.e., whereby individual trees are grouped into tree species and size/age classes) to enable efficient simulation through reduced model dimensionality. Unlike terrestrial biosphere models, these models operate at a species taxonomic resolution, capturing more precise trait variation than plant functional types.

Successful demonstration and validation of these models will help decision-makers integrate a multitude of management strategies into the context of the military mission and installation-specific natural resources management plans. Our intention is that forest managers will be able to readily apply one or more model to estimate the effects of different management regimes at DoD installations over varying spatiotemporal scales. The technology was demonstrated and applied at Ft. Bragg’s 89,000 acres of longleaf pine forests with the intention that the approach will be replicable across other DoD installations containing forested habitats with similar data sources.

We conducted our research in two stages with two distinct tasks. In the stage one (the **Test Phase**), we parameterized, calibrated, and compared two models against empirical data collected for two well-characterized sites in the eastern US: Harvard Forest, MA and Jones Ecological Research Center, GA (Erickson and Strigul 2018). In stage two (the **Demonstration Phase**), we applied two models to Ft. Bragg, NC, to simulate the effects of projected changes to climate, management, and disturbance.

For both phases, we assessed the strengths and weakness of each model and their respective capacities to simulate a suite of processes that drive forest change. These processes included management, succession, disturbance, biogeochemical cycling, and changing climatic conditions.

1.3 REGULATORY DRIVERS

An array of regulatory and programmatic drivers exist that support the need for the development of this new environmental management technology. Drivers include the following:

- Relevant federal law includes the following: Endangered Species Act of 1973, Clean Water Act of 1972, National Environmental Policy Act of 1970.
- Relevant DoD programs include the following: Army Regulation 200-1 Environmental Protection and Enhancement, and Army Compatible Use Buffer (ACUB) Program.
- Relevant Ft. Bragg programs include the following: Sustainability Management System, Cultural Resource Management...
- Relevant combined federal-state programs include the following: NC Forest Service – DoD partnership, including Southeast Regional Partnership for Planning and Sustainability (SERPPAS), NC Working Lands Group, and Sentinel Landscapes, including the Eastern North Carolina Sentinel Landscapes Partnership (ENSLP) and Forest Opportunities for Resource Conservation and Environmental Security program (FORCES), and North Carolina Sandhills Conservation Partnership (NCSCP).
- Relevant state programs include the following: NC Plant Conservation Program, NC Forest Action Plan, NC Wildlife Action Plan, and NC Forest Service Strategic Plan (*under revision*).
- Within NC Forest Service, relevant programs include the following: Forest Management Program, Technical Development, Planning, and Utilization (*applied research*), Forest Development Program (*reforestation*), and the Water Quality Program.
- Other relevant programs include the following: National Arbor Day's Tree City USA.

2.0 TECHNOLOGY/METHODOLOGY DESCRIPTION

2.1 TECHNOLOGY/METHODOLOGY OVERVIEW

Model selection was constrained by the need to achieve objectives at two scales: (1) stand-scale (< 10 ha) for comparison with 5-25 years of empirical data at two sites; (2) landscape-scale for projections of forest change due to management, disturbance and climate scenarios for 50 years across Ft. Bragg, NC. Many models satisfy one but not both of these objectives, or operate only at broader scales (~0.5 degree grids), such as Terrestrial Biosphere Models (Bugmann 2001, Scheller and Mladenoff 2007). The selected models must produce data that can be objectively compared between models and with empirical data. Furthermore, to the degree possible we compared models with different architectures to capture variability attributable to model design. We emphasize mature models with evidence of successful application in the literature.

Based on our criteria, we selected three forest change models: (1) the PPA-SiBGC model, a variant of the SORTIE gap model reduced with the Perfect Plasticity Approximation (PPA) (Strigul et al. 2008, Purves et al. 2008, Erickson and Strigul 2019); (2) the Net Ecosystem Carbon and Nitrogen model (NECN; operating within the LANDIS-II framework) (Scheller et al. 2007, Scheller et al. 2011); and (3) the Photosynthesis and Evapotranspiration model (PnET; operating within the LANDIS-II framework) (De Bruijn et al. 2014).

All three models operate at cohort resolution and can scale from stands to landscapes. The models are distinguished by the scale of their primary interactions. PPA-SiBGC emphasizes interactions among cohorts within stands. NECN emphasizes an ecosystem (i.e., mass balance) approach to allocating Carbon and Nitrogen. PnET emphasizes a mechanistic approach to simulate photosynthesis based on light, water, temperature, and competition through vertical layers in a canopy.

SORTIE with PPA reduces the classical SORTIE gap model using a well-grounded assumption based on empirical observations and simulations of crown plasticity (Mitchell 1975) and phototropism (Umeki 1995, Umeki 1997). PPA obviates the computational expense of detailed canopy light models, allowing for accelerated simulations with simple growth, mortality, and regeneration models applied to aspatial cohorts, rather than individual trees in Cartesian space. A simplified biogeochemistry focused variant of SORTIE with PPA was used in this work (PPA-SiBGC; Erickson and Strigul 2019). PPA-SiBGC blends a cohort model with the first-principles ‘big-leaf’ representation of energy and biogeochemistry used in terrestrial biosphere models, including: soil C and N accumulation and decomposition and allocation to above and belowground roots (Figure 1). PPA-SiBGC inputs include a list of trees with depth-at-breast-height (DBH) and species-specific values for growth, mortality, fecundity, species physiological attributes, allometric coefficients, and hourly meteorological data.

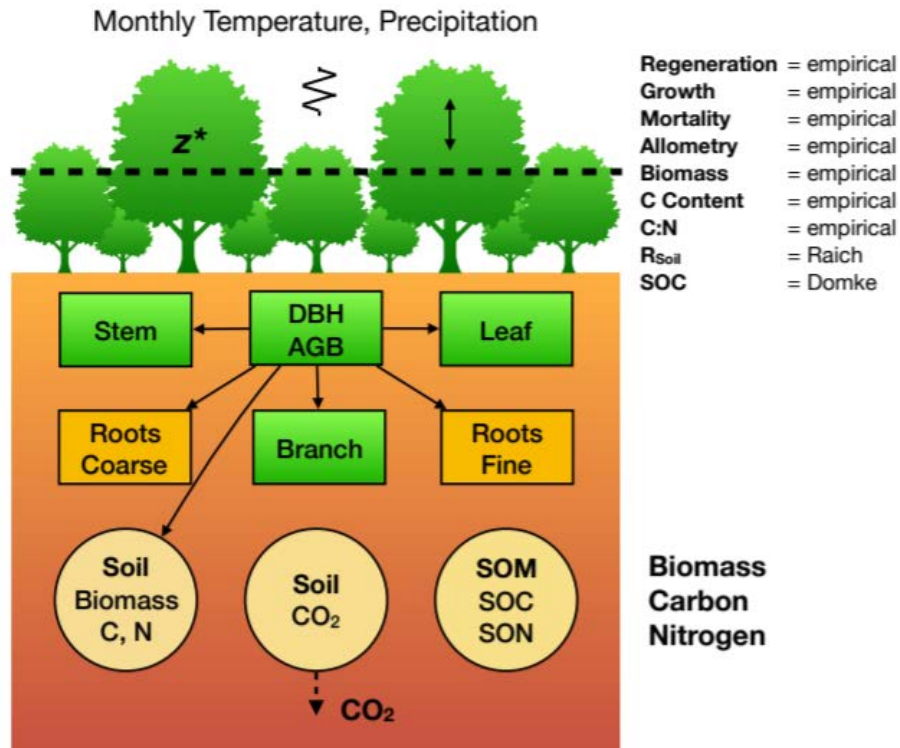


Figure 1. Schematic diagram of the PPA-SiBGC model structure. From Erickson and Strigul (2019).

The Net Ecosystem Carbon and Nitrogen (NECN) model (Scheller et al. 2011) tracks all C and N fluxes across a landscape as a function of climate, soils, disturbances, management, and their interactions. NECN tracks all living (leaves, wood, fine and coarse roots) and dead pools (detritus, organic soils) pools and the fluxes among them (Figure 2). Within NECN, cohort growth is limited by available N, temperature, available water, and leaf area index. NECN estimates Net Ecosystem Exchange (NEE) by tracking above and belowground Net Primary Productivity (NPP) and heterotrophic respiration (Rh). Soil processes follow the CENTURY soils model (Parton et al. 1987) and contains a simple bucket hydrology model. NECN inputs include species-specific values for growth, mortality, fecundity, and species physiological attributes.

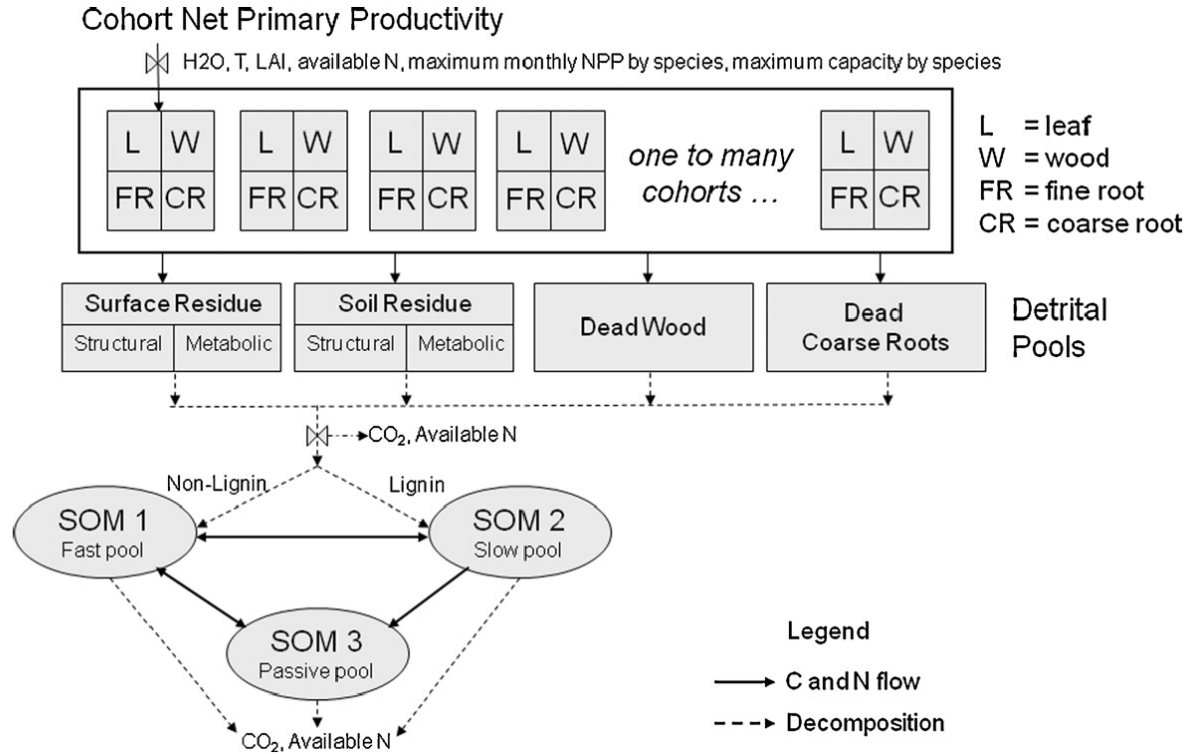


Figure 2. Schematic diagram of the Net Ecosystem Carbon Nitrogen Succession ('NECN') model structure. From Scheller et al. (2011).

The PnET model (as ported to LANDIS-II, v2.1.1, de Bruijn et al. 2014) is based on the PnET-II ecophysiological model (Aber et al. 1995). PnET uses a mechanistic approach to simulate photosynthesis based on light, water, temperature, and competition through vertical layers in a canopy (Figure 3). Photosynthesis drives growth and the accumulation of cohort biomass. Biomass within a cohort is used as a surrogate for canopy height to simulate vertical layers through a canopy. Available soil water, based on precipitation, transpiration, evaporation, runoff, and percolation further affects cohort growth. In addition, growth increases with foliar N, and atmospheric CO₂ concentration, and decreases as cohorts near their longevity age or depart from optimal temperature. Competition among cohorts is simulated by partitioning light through multiple canopy layers. Establishment of new cohorts is regulated based on seed source availability, sub-canopy light, and soil water. Parameterization and use of PnET including calibration, validation, and sensitivity analyses have been described previously (Gustafson et al. 2017, Duvaneck and Thompson 2017, Duvaneck et al. 2017, Liang et al. 2017).

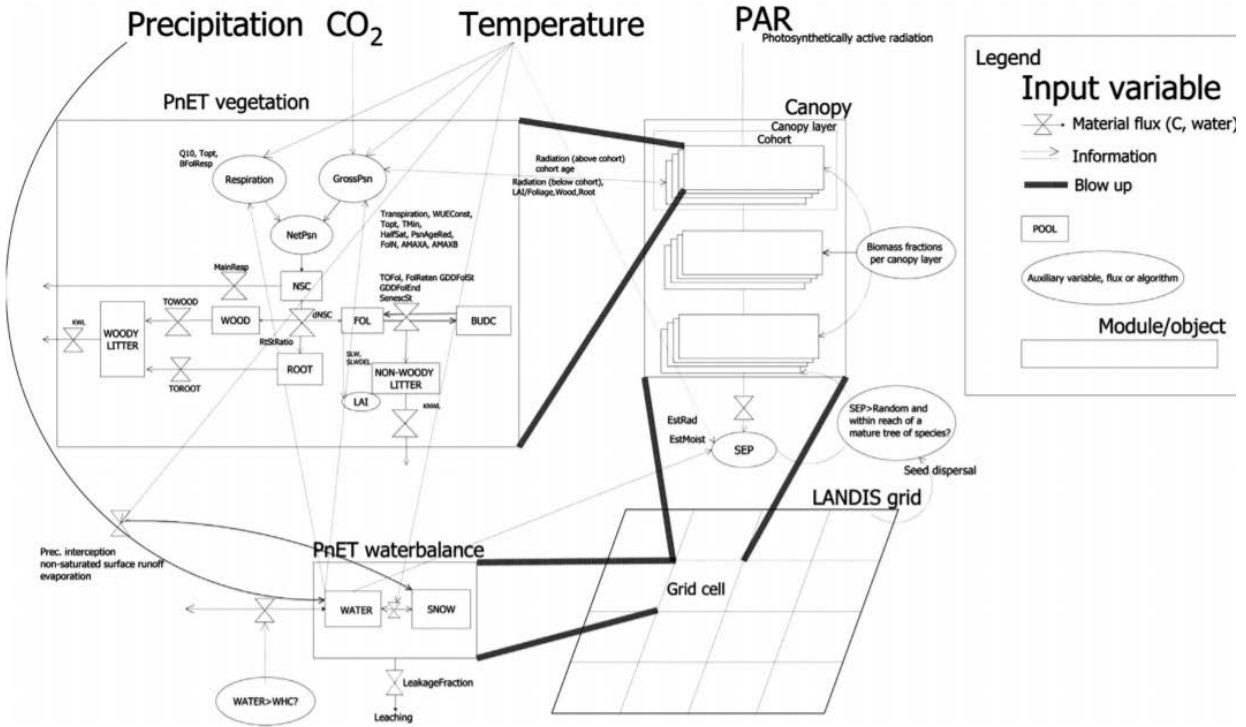


Figure 3. Schematic diagram of the PnET model as ported into the LANDIS-II framework. From de Brujin et al. (2014).

Both NECN and PnET have been implemented within the LANDIS-II landscape change framework. LANDIS-II is an open-source framework allows the development of user-defined sub-models that interact with a simulation core (Scheller et al. 2007). This design specification has facilitated the rapid development of many new sub-models operating within the LANDIS-II framework. The sub-models are primarily comprised of succession and disturbance models but also include other model functionality. LANDIS-II benefits from a large user base and extensive model calibration-validation efforts, providing model maturity and flexibility. LANDIS-II inputs include climate, stand composition and age, life history attributes, and disturbance regimes.

In the **Test Phase**, we compared the performance of PPA-SiBGC and NECN and with empirical data collected at two research sites on the east coast of the United States: (1) Harvard Forest, MA; and (2) Jones Ecological Research Center, GA (Figure 4). We implemented an innovative approach that leverages all available data by sampling from distributions of parameters, rather than flattening the variance into mean values, at the start of each simulation run. This allowed us to produce confidence intervals and/or uncertainties for the simulations using Monte Carlo methods.

In the **Demonstration Phase**, we applied the NECN and PnET models to forecast future management and climate scenarios across the Ft. Bragg, NC landscape (Figure 4). We worked directly with Ft. Bragg Directorate of Public Works, Environmental Division (FBDPWED) to iteratively create scenarios and to determine their specific information needs (Gustafson et al. 2006). They provided available data and helped to resolve any localized parameter needs.

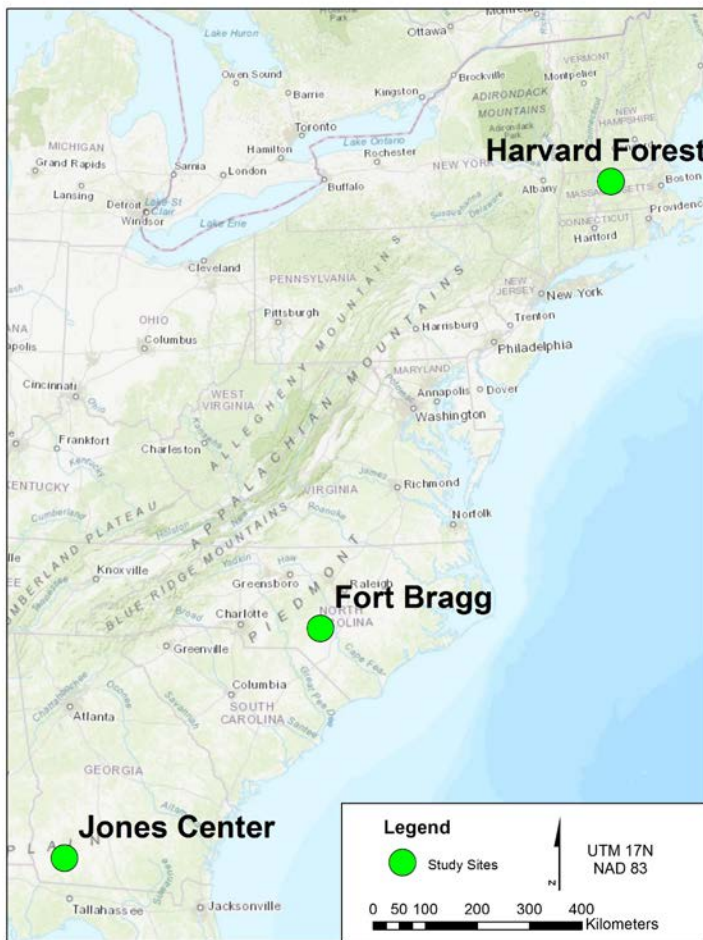


Figure 4. Locations of the Jones Center, Ft. Bragg, and Harvard Forest.

2.2 ADVANTAGES AND LIMITATIONS OF THE TECHNOLOGY/METHODOLOGY

There are limited alternative technologies or methods that met the specific regulatory and stewardship needs of this project. The Forest Vegetation Simulator (FVS) model is a forest growth-and-yield model that is readily available, widely applied across the US, robust, and well-parameterized for the southeastern US (Crookston and Dixon 2005). However, it is only a stand-scale model that lacks dynamic disturbance regimes or biogeochemical processes. In this case, FVS is designed to operate at a fine-scale that is not congruent with our objectives. As such, the FVS model is unable to offer mechanistic representations of competition, disturbance, or growth. The Ecosystem Demography (ED2) model also predicts ecosystem structure (e.g. above and below-ground biomass, forest height and basal area, and soil carbon stocks) and ecosystem fluxes (e.g. NEE, NPP, and evapotranspiration) according to climate, soil, and land-use inputs (Moorecroft et al. 2001). ED2 is an individual-based tree model and contains sub-models for leaf physiology, plant carbon allocation, dispersal, the effects of fire disturbances, soil carbon

dynamics and hydrology. ED2 has been optimized to forecast large-scale landscape changes and has been used to simulate how climate change, soils, disturbances, and human activities alter ecosystem structure and fluxes (Moorcroft et al. 2001). ED2 utilizes Plant Functional Types (PFTs) that are broadly representative of the canopy at a given location. Disturbances are simulated as transitions among primary and secondary vegetation and agriculture (Pereira et al. 2017). ED2 has been successfully used at broad scales (e.g., eastern United States, the Amazon basin) to estimate ecosystem structure and fluxes. However, at a more regional or local scale (e.g., Ft. Bragg), many critical disturbance functions are not represented, including: tree thinning, prescribed fires, spatial allocation of natural resource objectives, and preferences for particular species according to habitat needs (e.g., differentiating among conifers to support red cockaded woodpecker). In this case, EDS is designed to operate at a coarse-scale that is not congruent with our objectives.

The three selected models (PPA-SiBGC, NECN, PnET) represent state-of-the-art formulations of landscape-scale forest ecosystem models (Shifley et al. 2017). They were all designed to operate at a species and cohort resolution and are optimized for the landscape scale, which can have implications for model accuracy (Jin et al. 2016). The landscape scale is also the most appropriate scale for informing management plans.

3.0 PERFORMANCE OBJECTIVES

Our performance objectives varied between the two phases of our research (Table 1).

For the Test Phase, we compared PPA-SiBGC and NECN against empirical data and therefore the success criterion for each objective was the Pearson correlation coefficient (r) across the vector of annual simulated and empirical values. Pearson's r is used to normalize the success criteria and to assess correctness in the directionality, rather than magnitude, of simulated dynamics in the temporal domain. We chose this method because magnitudes are often easy to adjust with parameters, while directionality is more indicative of the correctness of model structure. This method provides a probabilistic estimate of the support for one model over another, using the full distribution of predictions produced by each model, rather than point estimates. Performance metrics included:

- **Biogeochemistry – Aboveground:** This metric is important for its contribution in calculating net ecosystem exchange (NEE). We will compare simulated and empirical annual rates of change in aboveground biomass, C, and N storage. We will also compare total values at the end of the simulation period. This requires empirical forest inventory (i.e., stem, branch, and leaf), eddy covariance flux tower, and canopy C and N data.
- **Biogeochemistry – Belowground:** This metric is important for its contribution in calculating NEE. We will compare simulated and empirical annual rates of change in belowground biomass, C, and N storage. We will also compare total values at the end of the simulation period. This requires empirical forest inventory (i.e., roots and soils), eddy covariance flux tower, and belowground C and N data.
- **Biogeochemistry – Soil Organic:** This metric is important for its contribution in calculating NEE. We will compare simulated and empirical annual rates of change in soil organic C (SOC) and soil organic N (SON) storage. We will also compare total values at the end of the simulation period. This requires empirical SOC and SON measurements.
- **Biogeochemistry – Soil Respiration:** This metric is important for its contribution in calculating NEE and represents a poorly understood dynamic. We will compare simulated and empirical annual rates of change in soil respiration (i.e., soil CO₂ efflux). We will also compare total values at the end of the simulation period. This requires eddy covariance flux tower data with soil respiration measurements.

For the Demonstration Phase, we projected 50 years of forest change based on scenarios developed in collaboration with the Ft. Bragg Natural Resources Division. Because our scenarios represent potential conditions, there are not empirical data for comparison.

Performance metrics included:

- **Prescribed Fire:** This disturbance metric is important for its contribution in calculating NEE and landscape heterogeneity for biodiversity habitat and training grounds. We will compare simulated and empirical annual fire frequency and severity, for prescribed fires. We will also compare the total number of fires and severity at the end of the simulation period. This requires historical wildfire perimeter data.
- **Hurricane:** This disturbance metric is important for its contribution in calculating NEE and landscape heterogeneity for biodiversity habitat and training grounds. We will compare simulated and empirical annual wind event frequency and severity, for episodic

and linear events. We will also compare the total number of wind events and severity at the end of the simulation period. This requires historical wind damage data.

- **Forest Composition and Structure:** These two metrics are important for understanding successional changes that may carry long-term implications for NEE. The metrics are also vital for biodiversity habitat, economic value, and diverse training environments. We will compare simulated and empirical changes in forest composition and structure at the end of the simulation period. This requires forest inventory data.

Table 2. Performance Objectives for Test Phase and Demonstration Phases.

Performance Objective	Metric	Data Requirements	Success Criteria
Quantitative Performance Objectives (Test Phase)			
Biogeochemistry – Aboveground	<ul style="list-style-type: none"> ● Biomass ● Carbon (C) ● Nitrogen (N) 	<ul style="list-style-type: none"> ● Forest inventory ● Flux tower ● Canopy C, N 	$r > 0.50$ against empirical data ($\text{g m}^{-2} \text{ year}^{-1}$)
Biogeochemistry – Belowground	<ul style="list-style-type: none"> ● Biomass ● Carbon (C) ● Nitrogen (N) 	<ul style="list-style-type: none"> ● Forest inventory ● Flux tower ● Soil C, N 	$r > 0.30$ against empirical data ($\text{g m}^{-2} \text{ year}^{-1}$)
Biogeochemistry – Soil Organic	<ul style="list-style-type: none"> ● Soil organic C (SOC) ● Soil organic N (SON) 	<ul style="list-style-type: none"> ● SOC mass or fraction (%) ● SON mass or fraction (%) 	$r > 0.30$ against empirical data ($\text{mg cm}^{-3} \text{ year}^{-1}$)
Biogeochemistry – Soil Respiration	<ul style="list-style-type: none"> ● CO_2 	<ul style="list-style-type: none"> ● Soil CO_2 efflux 	$r > 0.30$ against empirical data ($\text{g C m}^{-2} \text{ year}^{-1}$)
Quantitative Performance Objectives (Demonstration Phase)			
Disturbance: Prescribed Fire	<ul style="list-style-type: none"> ● Area burned ● Event severity 	<ul style="list-style-type: none"> ● Management plans and maps 	Qualitative assessment.
Disturbance: Hurricane	<ul style="list-style-type: none"> ● Event frequency ● Event severity 	<ul style="list-style-type: none"> ● Historical hurricane events and tree mortality rates 	Qualitative assessment.
Forest Composition and Structure	<ul style="list-style-type: none"> ● Biomass and age class in total and by species 	<ul style="list-style-type: none"> ● Multi-temporal forest inventory 	Qualitative assessment.

4.0 SITE DESCRIPTION

Our research utilized the unique histories and data available at three temperate forests in the eastern USA (Figure 4). The Test Phase utilized two sites, Harvard Forest, MA, which maintains ample relevant data, including forest inventory and biogeochemistry data and the Jones Ecological Research Center, GA, which also maintains sufficient data. The Demonstration Phase utilized Ft. Bragg, NC, a large military base with extensive forests (Figure 4).

4.1 SITE SELECTION

We selected our Test Phase sites based on two primary criteria: (1) representativeness of sites of eastern US forests; (2) availability and quality of data. These Test Phase sites were selected prior to project initiation. The availability of data was critical, as this research required detailed soil biogeochemistry measurements and the availability of data is often a key limiting factor in the calibration and validation of forest biogeochemistry models. We selected the Demonstration Phase site based on its representativeness of forests across the eastern seaboard, its proximity to major universities, the data available that describe the site, and the willingness of on-base natural resource managers to collaborate.

4.2 SITE LOCATION AND HISTORY

The two Test Phase sites have unique forest composition (Jones Center is dominated by Longleaf pine and the Harvard Forest site is dominated by Eastern Hemlock, *Tsuga canadensis*) and structure. The Demonstration Phase was conducted at Ft. Bragg, NC, one of the nation's largest military bases.

4.3 SITE CHARACTERISTICS

Harvard Forest is located in North-central Massachusetts. The climate is temperature, cool and moist with a July mean temperature of 20 degrees C and January mean temperature -7 degrees C. The annual mean precipitation 110 cm. The elevation ranges from 220 to 410 meters above sea level. Bedrock includes granite, gneiss and schist. The soils are mainly well-drained sandy loam glacial till with some alluvial and colluvial deposits. Soils here are acid with a mean depth of 1 meter. Dominant species include red oak (*Quercus rubra*), red maple (*Acer rubrum*), black birch (*Betula lenta*), white pine (*Pinus strobus*), eastern hemlock (*Tsuga canadensis*). Conifer plantations cover about 7% of Harvard Forest land (Harvard University 2018).

Jones Ecological Research Center at Ichauway is a 29,000-acre site located in GA with over 1,100 document vascular plants and 370 vertebrate species. The site includes longleaf pine (*Pinus palustris*), slash pine (*Pinus elliottii*), loblolly pine (*Pinus taeda*), mixed pine-hardwood, and riparian hardwood forests. Ichauway contains two management zones: (1) a multiple-use zone for sustainable forest management; (2) a conservation zone for biological diversity. The site is dominated by well-drained sandy soils and the elevation ranges from 27 to 61 meters.

Ichauway includes an 18,000-acre upland pine-grassland, agricultural fields, wetlands, and riparian hardwoods. Virgin longleaf forests were harvested in the early 20th century; current longleaf stands are dominated by 8-100-year-old trees. Longleaf pine forests dominate upland

sites, with wiregrass or broom sedge understory. Most stands contain mature, uncrowded pines. The site's longleaf pine ecosystems are fire-maintained and were once dominant across the region. Unlike other areas in the southeastern Coastal Plain, there is significant limestone. Much of the ground cover remains undisturbed (Jones Ecological Research Center 2018).

The Ft. Bragg Military Reservation and adjacent areas contain a large contiguous area of longleaf pine and wiregrass ecosystem (*Pinus palustris*–*Aristida stricta*) (Sorrie et al. 2006) and is representative of the longleaf landscape formerly common across the southeastern United States coastal plain (Ware et al. 1993). Frequent low-intensity fires are necessary for maintaining healthy longleaf pine forests because they experience lightning fires every two to five years under natural conditions. These fires are also essential for maintaining the pine forest's characteristic wiregrass ground cover and for preventing scrub oaks and other hardwoods from replacing the pines (Gilliam and Platt 1999). Major threats to longleaf pine forests include fire suppression, conversion to pine plantations, and climate change (Landers et al. 1995, Van Lear et al. 2005). Ft. Bragg also contains a high floristic diversity and a variety of pine forest types (Sorrie et al. 2006). Within Ft. Bragg, 1500-2000 acres of thinning is performed annually, including slash to longleaf pine conversion, and 12,000 acres is also managed at nearby Camp McCall. Ft.

5.0 TEST DESIGN

Simulation models have become essential tools for forecasting and understanding the long-term effects of exogenous drivers (e.g., climate change) and management on the ability of landscapes to continue providing expected or required ecosystem services (Scheller 2018). However, there are many available models each with its own data requirements, optimal scale, application domain (where and what type of vegetation), user base, software testing, and accuracy (compared to empirical data if available). Our test design was created to compare the model performance of forest simulation models at two spatiotemporal scales: (1) the stand-scale (< 10 ha) operating at short durations, and (2) the landscape-scale (> 10,000 ha) operating at long durations. Simultaneously, our test design sought to provide actionable information to the FBDPWED.

5.1 CONCEPTUAL TEST DESIGN

Our test design was based on calibrating validating the PPA-SiBGC, NECN, and PnET models at well-described flux tower sites before applying the validated models to simulate forests at Ft. Bragg, NC. We did not apply treatments in our Test Phase validation experiments, but instead sought to replicate empirical patterns of forest biogeochemistry, composition, and structure. In the Test Phase, we parameterized, calibrated, and validated PPA-SiBGC and NECN for Harvard Forest, MA and Jones Ecological Research Center, GA. We used empirical data including climate, soils, wind and fire disturbance, forest inventory, species trait, vital attributes, and energy, water, C, and N budgets to generate parameters for each model.

After parameterizing, calibrating, and validating models at the Test Phase sites, we applied and compared the NECN and PnET models to Fort Bragg, NC. Because PPA-SiBGC lacked the necessary routines to simulate prescribed fire and harvesting, the PnET model was substituted at the beginning of the Demonstration Phase. Because detailed biogeochemistry and belowground data is unavailable for Ft. Bragg, we focused on aboveground net primary production (ANPP), forest composition and structure, and model usability, performance, and transferability as our performance metrics for this site.

5.2 BASELINE CHARACTERIZATION AND PREPARATION

For the Test Phase, baseline characterization was provided by Harvard Forest and the Jones Center (Erickson and Strigul 2019). These data included flux tower estimates of Net Ecosystem Exchange, climatic data from on-site meteorology stations, descriptions of the dominant vegetation including species and diameters, estimates of above- and belowground biomass, and other empirical data (see Appendix A and B in Erickson and Strigul 2019).

For the Demonstration Phase at Ft. Bragg, we relied on forest inventory data provided by the FBDPWED and USDA Forest Inventory and Analysis (FIA) data. Contemporary (2018) inventory data provided the baseline conditions necessary to initialize the landscape for our scenarios. We included nine tree species in our simulations (Table 1). Bragg consists of numerous forest stands of different age classes growing on different soil types and thus required extensive parameterization efforts.

We created a baseline map of species composition and species' age at a resolution of 1 ha, by imputing FIA data onto a land cover map provided by FBDPWED. The FIA data were necessary because the Ft. Bragg inventory data were not comprehensive and did not include a full species inventory at each plot. The FIA database contains diameter and height for each tree, but not tree age as required for cohort simulation. We used site index curves to calculate age for every tree in the FIA database for VA, SC and NC. We also added old growth longleaf and loblolly pine to the landscape based on the maps of old pines provided by FBDPWED (Figure 5). The resulting age distributions for our nine species on Ft. Bragg were variable although the median ages (< 100 years) reflects the land use history of the base (Figure 6). A comparison of the baseline conditions with FIA data indicates that baseline conditions had lower biomass than the FIA (Figure 7). However, FIA data were drawn from a much wider area that includes many older stands than are found at Ft. Bragg. A review conducted with the FBDPWED team of the relative amounts and areal extent of the estimated baseline conditions indicated that our estimates were broadly accurate; the final baseline forest type distribution was also congruent with their expectations (Figure 8).

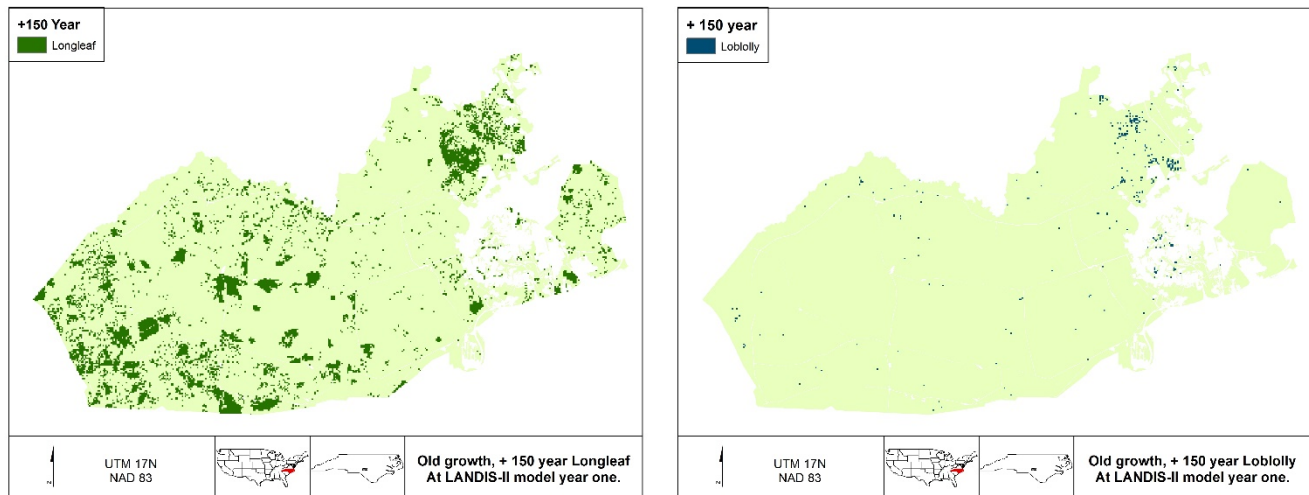


Figure 5. The presence of old-growth longleaf pine (left, green) and loblolly pine (right) imputed from Ft. Bragg Natural Resource Division inventory data. These data were integrated into baseline conditions.

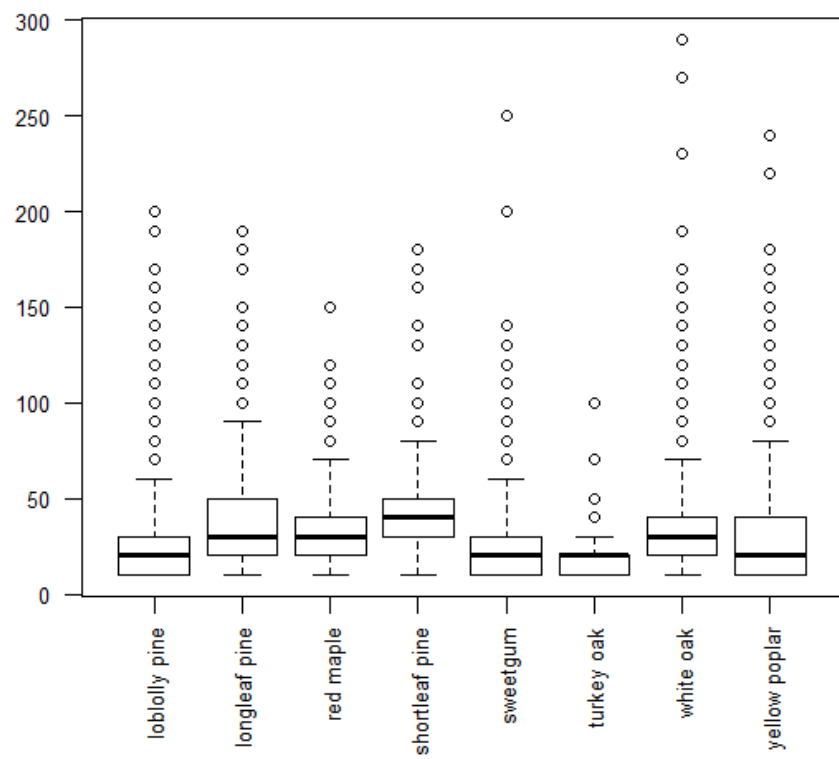


Figure 6. Baseline estimated age distributions of nine species within the Ft. Bragg, NC landscape.

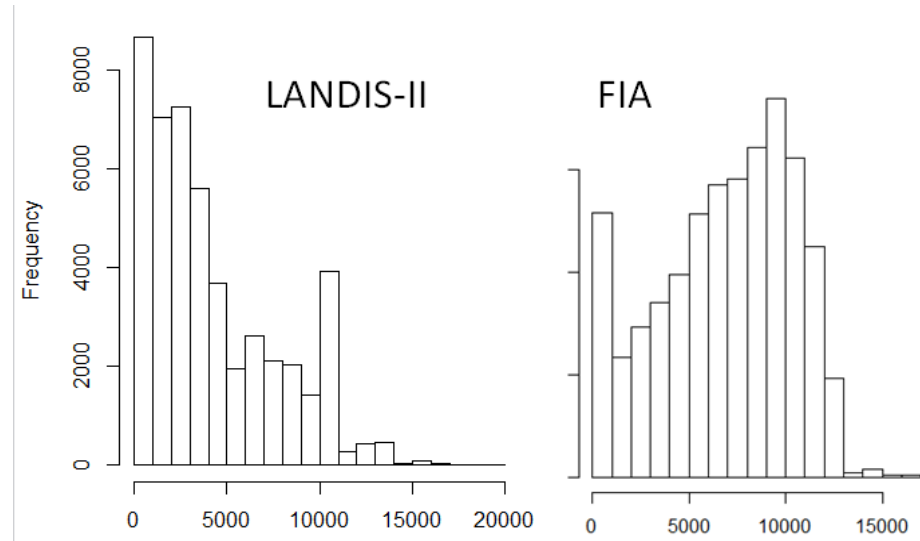


Figure 7. A comparison of baseline biomass as imputed into NECN and as derived from FIA data for NC, SC, and VA.

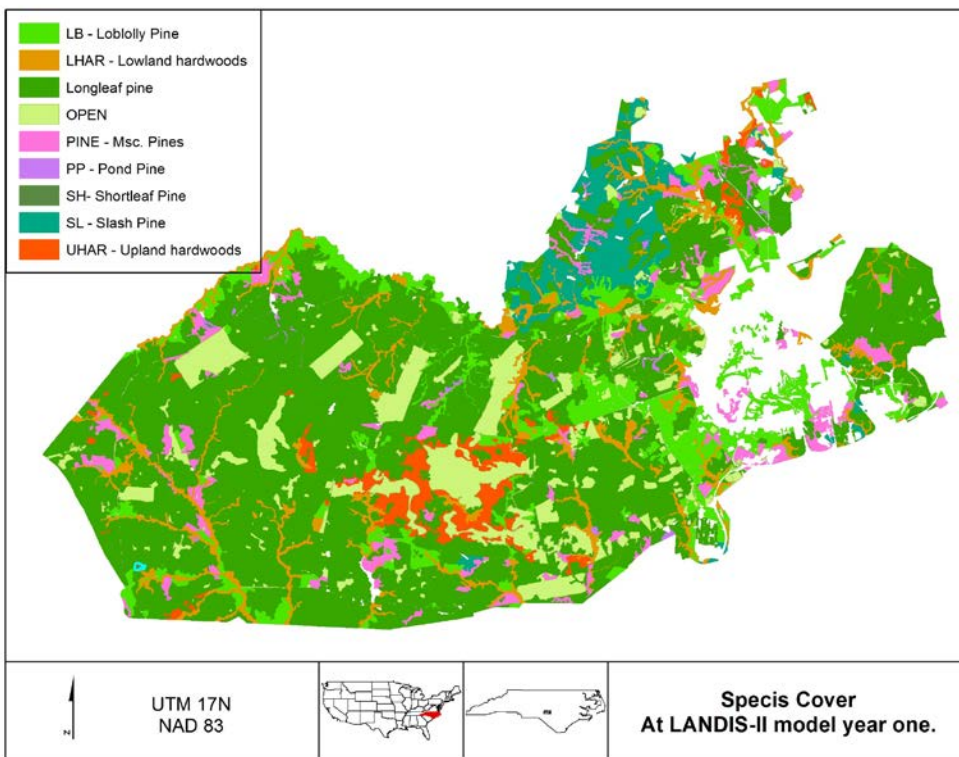


Figure 8. Baseline vegetation types for Ft. Bragg, NC, representing vegetation types circa 2018.

In all our Demonstration Phase simulations, we simulated current forest management practices: thinning and clear-cutting. Thinning had a target 2.4% or about $\sim 1000 \text{ ha yr}^{-1}$ of the entire landscape. Clearcutting is designed to remove large patches of slash pine in the northeastern section of Ft. Bragg. Slash pine is removed every year for the next 20 years. Thinning and clearcutting were simulated using the Biomass Harvest extension for LANDIS-II (Gustafson et al. 2000).

We also simulated three different prescribed fire regimes. Ft. Bragg burns on average every 3 years at the landscape-scale and this was considered the baseline fire regime (Figure 9). To simulate the baseline fire regime, we used fire ‘cycles’ to denote which zones were burned at each time point. The fire ‘cycles’ are based on a year grouping of 1, 2, or 3, and which ‘year cycle’ those stand plots are burned on (1, 2, 3). A fire cycle of 1 year plots burn once every year (‘cycle’ 1 with ‘year cycle’ 1, cycle 2 year plots burn every other year (‘cycle’ 2 year with ‘year cycle’ 1 or 2 years), and cycle 3 year plots every third year (‘cycle’ 3 year with ‘year cycle’ 1, 2, or 3 years. We also simulated a more frequent fire regime (“more fire) with an average burning rate of every two years and a less frequent fire regime with an average burning rate of every five years (“less fire”). Prescribed fire was simulated using the Social Fire extension for LANDIS-II (Scheller et al. 2019). Prescribed fire constraints were dictated by the FBDPWED and include the following: maximum wind speed $< 13.5 \text{ km hr}^{-1}$; maximum temperature $< 35^\circ \text{ C}$; minimum relative humidity 22° C ; maximum flame length $\leq 8 \text{ ft.}$; maximum number prescribed fires = 450; maximum number of fires per day = 3; earliest day = January 1; latest day = August 31.

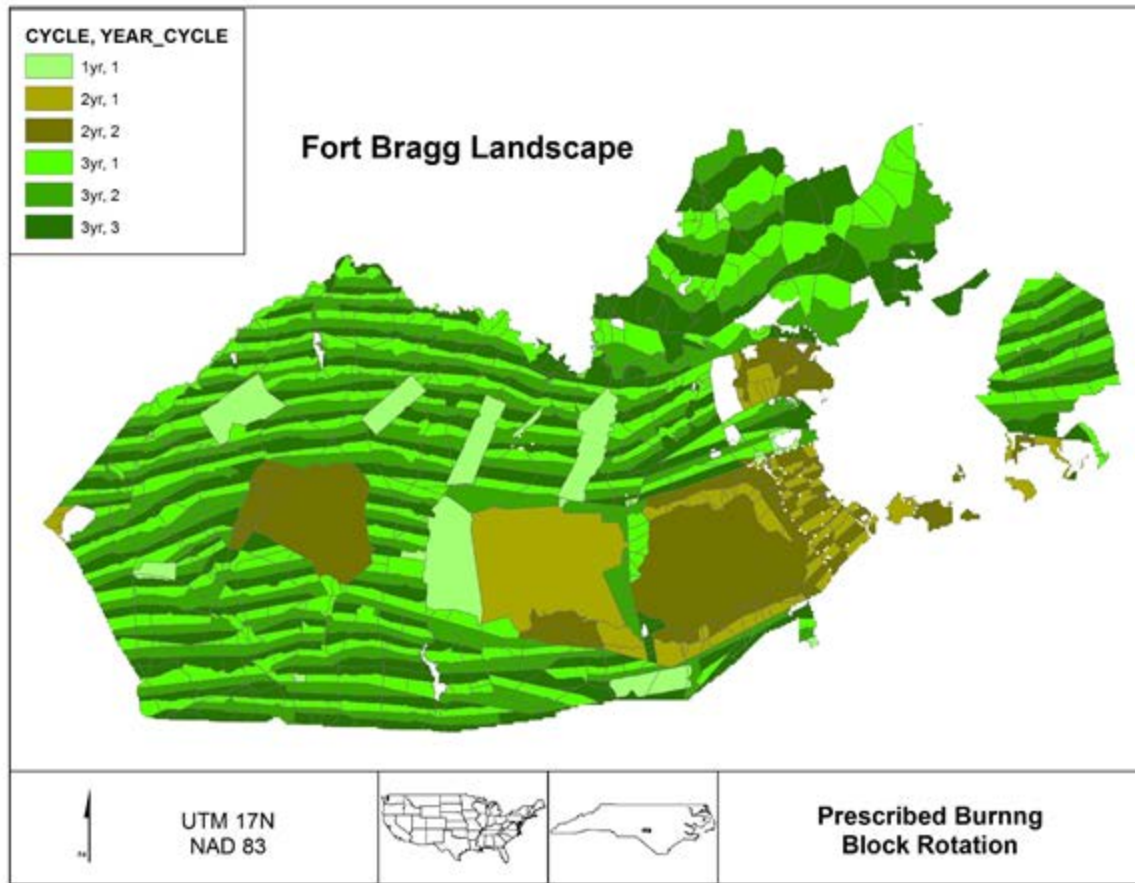


Figure 9. Baseline fire zone maps at Ft. Bragg, NC. Zones are burned either every 1, 2 or 3 years in the current Rx fire regime.

To simulate hurricanes, we developed a new LANDIS-II extension, Base Hurricane (<https://github.com/LANDIS-II-Foundation/Extension-Base-Hurricane>). This extension models tropical cyclones and hurricanes making landfall on the east coast of the United States, including GA, SC, NC, and VA. Historical hurricane track records were retrieved from the National Hurricane Center's Best Track Data (HURDAT2) at <https://www.nhc.noaa.gov/data/#hurdat>, see: <https://github.com/PaulSchrum/Hurdat2FC/tree/master/output>. Using this data, we analyzed the hurricane landfall frequency on the east coast of the US from 1969 to 2018 and determined the historic storm count per year (Table 3). The following table summarizes the findings:

Table 3. Number of hurricanes per year that hit landfall in GA, SC, NC, or VA from 1969-2018.

Number of Hurricanes	Count	Percentage
0	29	58%
1	16	32%
2	5	10%
3	0	0%

To randomize the wind speed at landfall, the historic storms were binned by wind speed (Figure 10). Based on this histogram we selected a log-normal distribution to model landfall wind speeds.

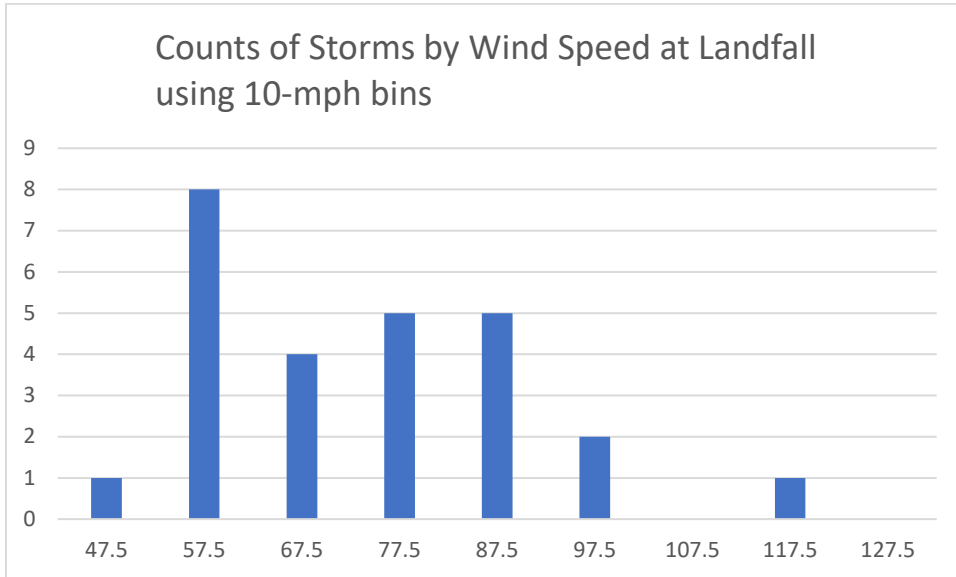


Figure 10. The distribution of hurricane wind speeds in hurricanes that strike GA, SC, NC, or VA, from 1969 – 2018.

Ft. Bragg is inland from the coast and therefore hurricane wind speeds are not as high as they are at landfall. To represent this in the model, we studied exemplar storms in the HURDAT database to see how the wind speed drops as the storm moves inland. From this, a simple equation was developed to represent storm center wind speeds decreasing as the storm moves inland and decreasing over the lateral distance from the storm center:

$$y = \frac{b}{(a^2 + x^2) \sqrt{\frac{x^2}{a^2} + 1}} + baseSpeed$$

Where y = maximum wind speed; a = scale parameter, inflection point; b = scale parameter, back-calculated; x = distance inland from landfall (km); and $baseSpeed$ = speed at final reading (kph). We computed suitable values for a and b to match the equation values with historic values from hurricane Katrina.

Cohort mortality was estimated for each species, age, and wind speed (Hook 1991). For any given storm, the wind speed at landfall is generated, then the wind speed drop is modelled according to a randomized track from landfall moving inland. For each site, the maximum hurricane wind speed was computed and cohort mortalities were determined according to the mortality likelihood from the cohort mortality table.

5.3 DESIGN AND LAYOUT OF TECHNOLOGY AND METHODOLOGY COMPONENTS

The technology and methodology applied in this work is described above.

5.4 FIELD TESTING

No fieldwork was required for this research. However, we visited the field site at Ft. Bragg, NC in spring of 2018. We met with natural resources managers, gathered photographs of the site, and collected any other non-sensitive information useful in conducting our simulation experiments. We reviewed available inventory data necessary for generating baseline conditions, as well as data on biogeochemistry, soils, and meteorology.

5.5 SAMPLING PROTOCOL

N/A. This project does not rely on new data collection for the demonstration of the technology. We rely upon presently available data for each of the validation sites and for Ft. Bragg, NC.

5.6 SAMPLING RESULTS

Test Phase sampling results are provided in Tables 1-4 in Erickson and Strigul (2019)(Appendix B).

For the Demonstration Phase, model calibration and validation were required. Calibration is the process of determining appropriate values for parameters that are unit-less (e.g., shape parameters) or are poorly estimated from empirical data (e.g., tree species data are often lacking for non-commercial tree species). Validation is the comparison of calibrated models against empirical data that were not used in the calibration process.

Tree species attributes are often the most difficult to source and provide point estimates. Where tree attribute parameters were unavailable, we imputed values from similar populations, species, or genera (Table 1). A full list of species data and all other parameters is available on GitHub (<https://github.com/LANDIS-II-Foundation/Project-Fort-Bragg-NC>).

We calibrated PnET growth trajectories of nine common tree species at Ft. Bragg (Figure 11). We calibrated against both inventory data (FIA) and published values (Smith et al. 2006). Our PnET calibration was informed by previous work including a sensitive analysis which identified the most sensitive parameters in PnET (McKensie et al. 2019). Our calibrations represent growth trajectories of a single species growing by itself in the hypothetical absence of competition from other species or older cohorts. We did not attempt to precisely match or predict a specific value or site knowing that variation exists across sites. However, we did attempt to capture the general trajectory for each tree species. These calibrations were subsequently used for model evaluation; they do not represent the Ft. Bragg landscape.

In addition to growth, we calibrated PnET regeneration (the probability of establishment given sufficient light and seed availability). PnET regeneration was compared against the probability

that young seedlings would be present under adult trees in FIA inventory plots (Figure 12). For example, we were able to capture variation in the probability of regeneration by each species (Figure 12). Again, we did not attempt to precisely match the establishment curves rather tried to capture the general trend of and variation of each species. To our knowledge, no one has evaluated landscape model regeneration with inventory data to this extent. We expect this evaluation will inform our own and future modeling projects to improve model behavior.

We also calibrated NECN growth trajectories against the same nine tree species at Ft. Bragg using the same methodology described above for PnET (Figure 13).

Finally, we compared the calibration growth trajectories between NECN and PnET for nine species (Figure 14). Although some model differences are apparent where one model resulted in more or less growth for a species, the growth trends simulated by each model generally capture the expected growth trajectory of each species.

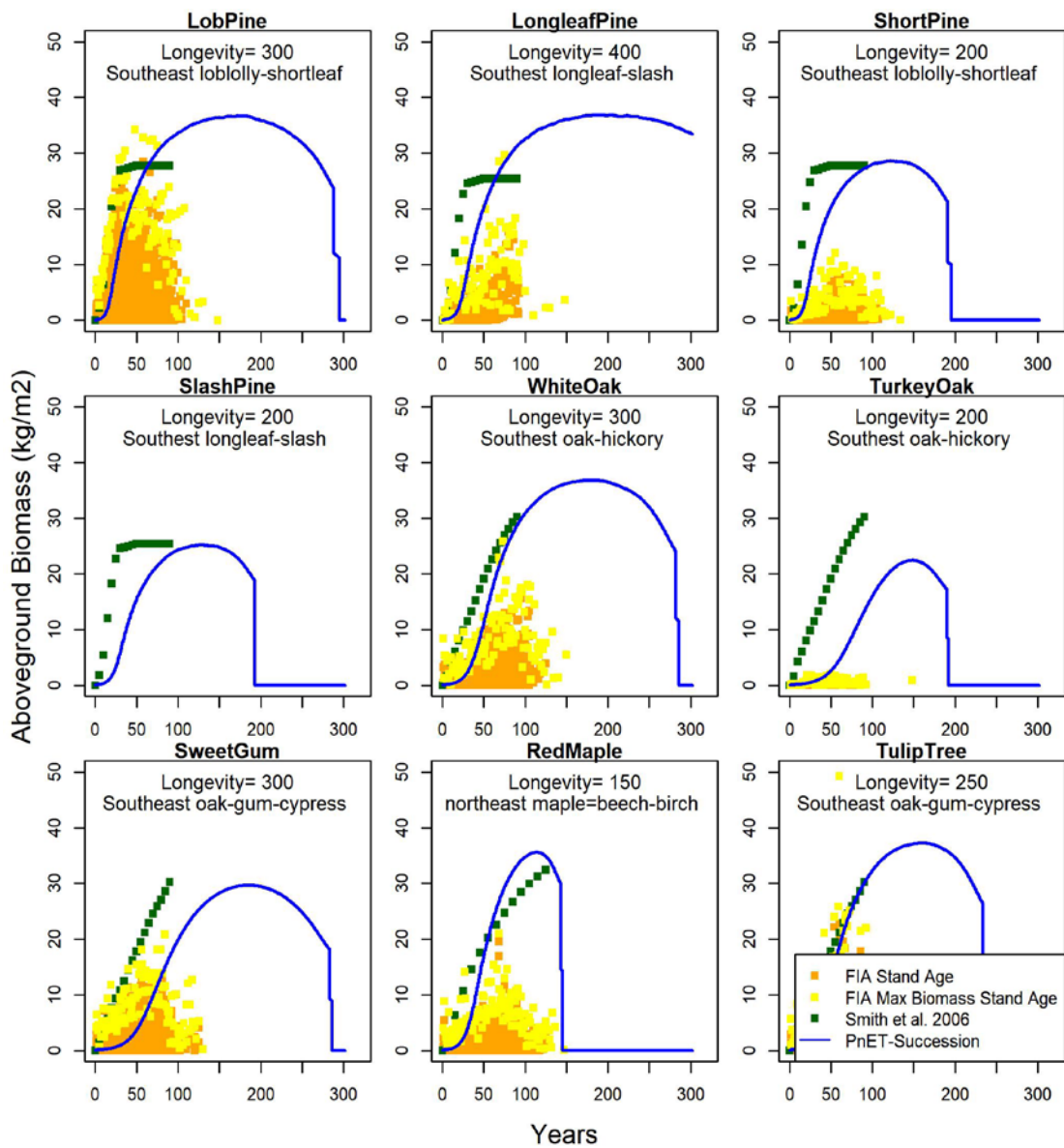


Figure 11. Growth calibration of nine tree species using the PnET model. Within each subplot, the longevity value represents the age of each tree species expected senescence; the species-group value listed represents the species-group published within Smith et al. (2006). Data represent growth trajectories of a single species growing by itself.

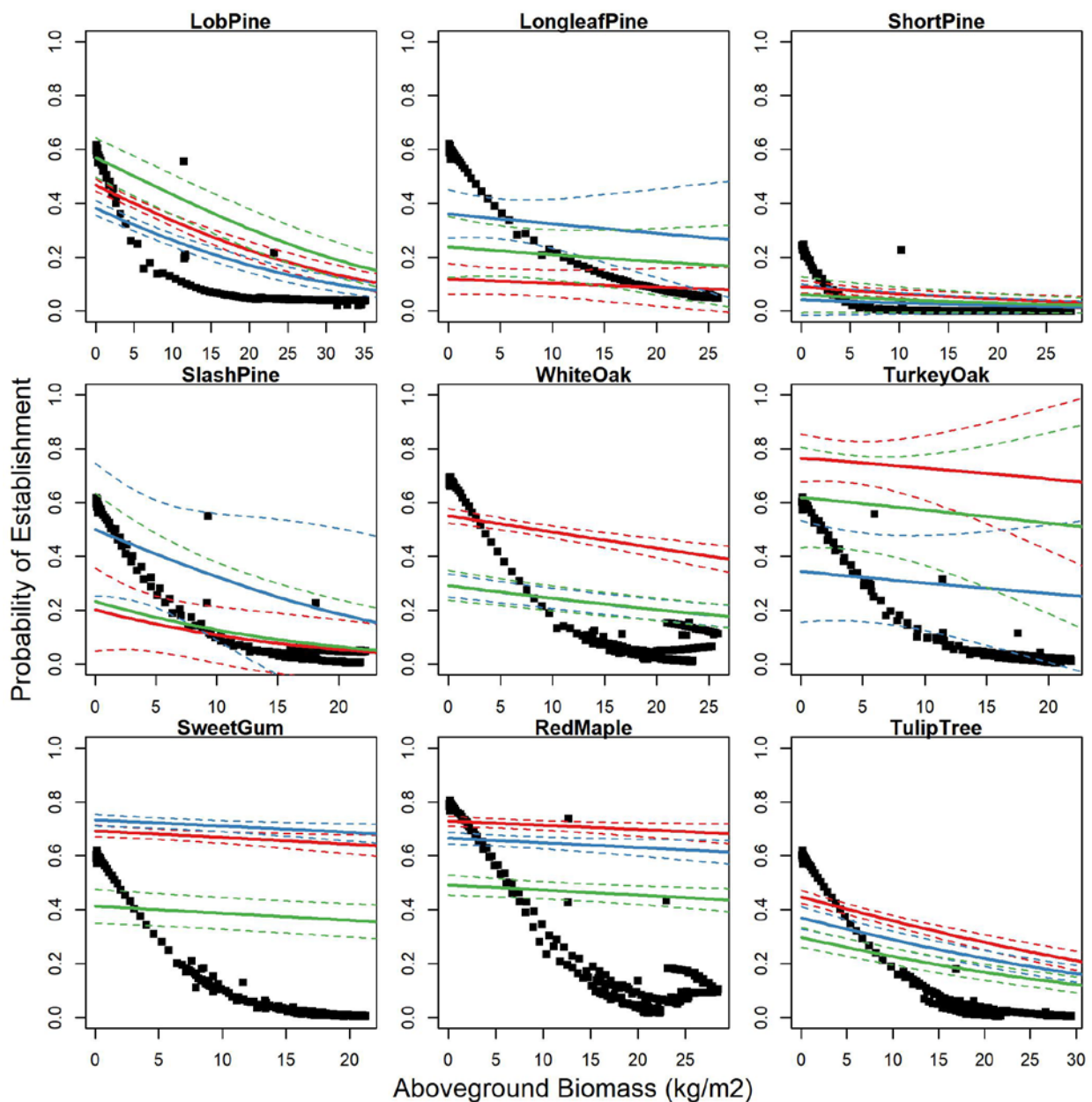


Figure 12. Establishment calibration of nine tree species using the PnET model. Establishment generally declines as a function of shade represented by biomass. Black symbols represent PnET. Colored lines represent site condition: Blue = high site index, Red = medium site index, Green = low site index.

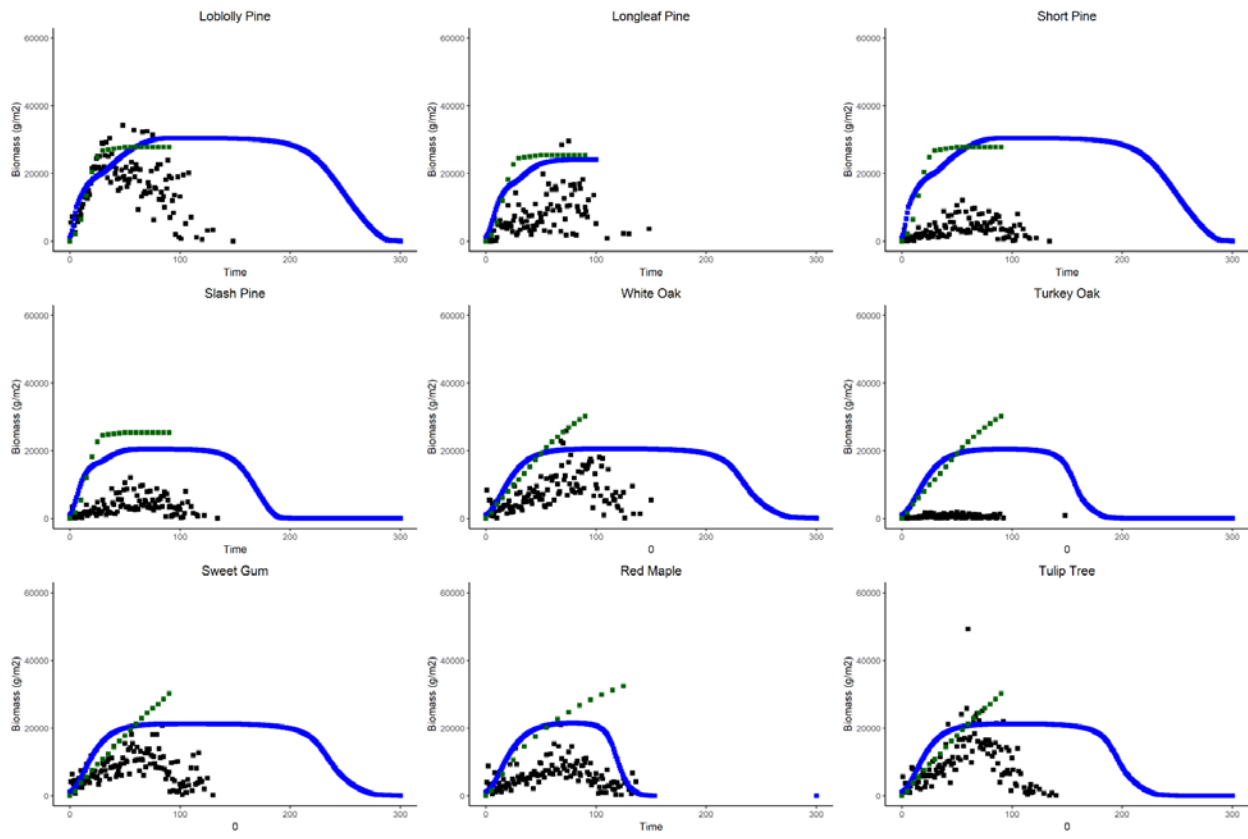


Figure 13. Growth calibration of nine tree species using NECN. Blue lines are NECN; Black dots represent FIA data and green dots are from Smith et al. (2006). Data represent growth trajectories of a single species growing by itself.

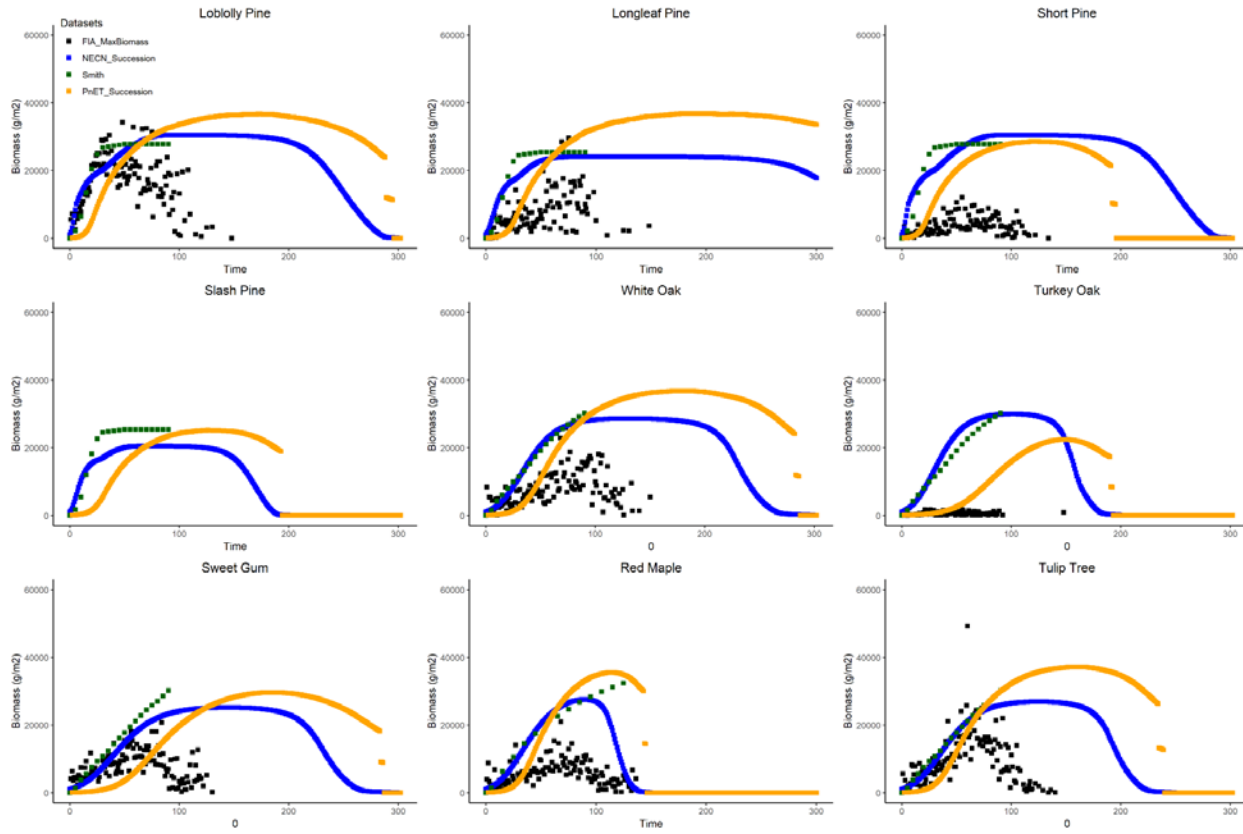


Figure 14. Growth trends over time simulated by NECN (blue) and PnET succession (gold). FIA plots are represented by the black dots, while Smith et al (2016) is represented by the green dots.

6.0 PERFORMANCE ASSESSMENT

6.1 Test Phase

Our Test Phase statistical analysis for assessing model performance in predicting individual metrics of interest focused on the application of the Pearson correlation coefficient (r) to simulated and empirical time-series at annual resolution. We applied Pearson's r and RMSE to check that the net values at the end of the simulation period are correct in both direction and magnitude. Pearson's r is selected over RMSE to hold the time-series metrics to the same assessment scale, placing equal value on each metric, and to ensure that the directionality of model predictions is correctly synchronized with empirical observations.

A lack of correlation between predictions and observations over time was indicative of errors in model architecture or parameterization. Additionally, Bayesian model comparison was applied to the target metrics given distributions of predictions from randomly sampled parameter vectors and given distributions of empirical measurements. To make the comparison even, no priors were assumed for either model in this calculation. Finally, mean r values were computed for each model to assess the overall temporal correlation with observations and the contribution of each variable to such net values.

The overall performance for both models was similar (Appendix B: Figure 5 in Erickson and Strigul 2019). In general, both models accurately predicted biomass, Carbon, and Nitrogen. PPA-SiBGC better predicted soil respiration and NECN better predicted NEE. Overall R^2 values were similar: 0.73 (PPA-SiBGC) vs. 0.69 (NECN). Both models performed better at the Harvard Forest site (Appendix B: Erickson and Strigul 2019).

6.2 Demonstration Phase

We collaboratively developed scenarios with FBDPWED. Scenarios are necessary to constrain future uncertainty when considering time horizons beyond existing or anticipated empirical data collection (Thompson et al. 2012). Our conversations with FBDPWED indicated that their primary interests are in scenarios that inform the use of prescribed fires and management for Red-cockaded woodpecker (*Leuconotopicus borealis*), an endangered species that requires older pines with an open understory. Therefore, our final scenarios included:

- Climate change: How will temperature and precipitation change? There are many Global Circulation Models (GCMs) and carbon emissions projections to choose. We selected one climate future that achieved the highest mean annual temperature (MAT) and the lowest mean annual precipitation (MAP) out of all GCMs available (labeled 'Hot-Dry', GCM provided by the Hadley Climate Centre). A second climate projection achieved the highest MAT with the highest MAP ('Hot-Wet', GCM provided by the Beijing Climate Center). These two climate futures were selected from the 15+ downscaled climate data available from USGS.
- Management: Ft. Bragg is very actively managed and this will continue to shape vegetation patterns. We simulated prescribed fire occurrence in multiple prescription blocks at 2, 3, and 5 years. Current day fire rotation is typically 3 years. We held

thinning constant at 2500 acres per year and will report out tons per acre removed; thinning will target stands with the highest basal area.

- Hurricanes: Hurricanes have the potential to cause substantial loss of RCW habitat. Based on historic hurricane extent and mortality patterns (from the past 20 years of data available), we simulated hurricanes under a historic conditions and ‘high’ hurricane conditions. High hurricanes doubled the probability of a hurricane occurring in any given year and will also increase the intensity by 50%. Hurricanes were simulated using the Saffir-Simpson Hurricane Wind Scale; therefore increasing the intensity will increase the probability of the higher classes by 50%.
- Other processes (e.g., succession and seed dispersal) were simulated but not encapsulated by the scenarios. They respond dynamically to climate change, hurricanes, and management autonomously.

As described, this combination produces $2 \times 2 \times 3 = 12$ distinct scenarios. We simulated forest change for 50 years, out to 2060. We used a 1 ha (2.5 acre) spatial resolution.

LANDSCAPE-SCALE ABOVEGROUND BIOMASS DENSITY

The baseline (year 2018) average aboveground biomass density differed between the PnET and NECN models (Figure 15). PnET used a spin-up phase to simulate growth up to current conditions, whereas NECN used FIA inventory data (species biomass) for starting conditions (see section 8: Implementation Issues). By 2030, the simulated biomass produced by both models converged. Over the 50 year simulation, simulated biomass increased for both NECN and PnET. PnET simulated a smaller increase but with a higher baseline than NECN.

PnET also simulated larger differences between climate scenarios than NECN indicating that PnET is more sensitive to climate, specifically precipitation than NECN (Figure 15). PnET simulated higher biomass in the hot-wet climate scenario than the hot-dry climate scenario. Unlike, PnET, NECN simulated only small difference in average landscape biomass across climate change scenarios.

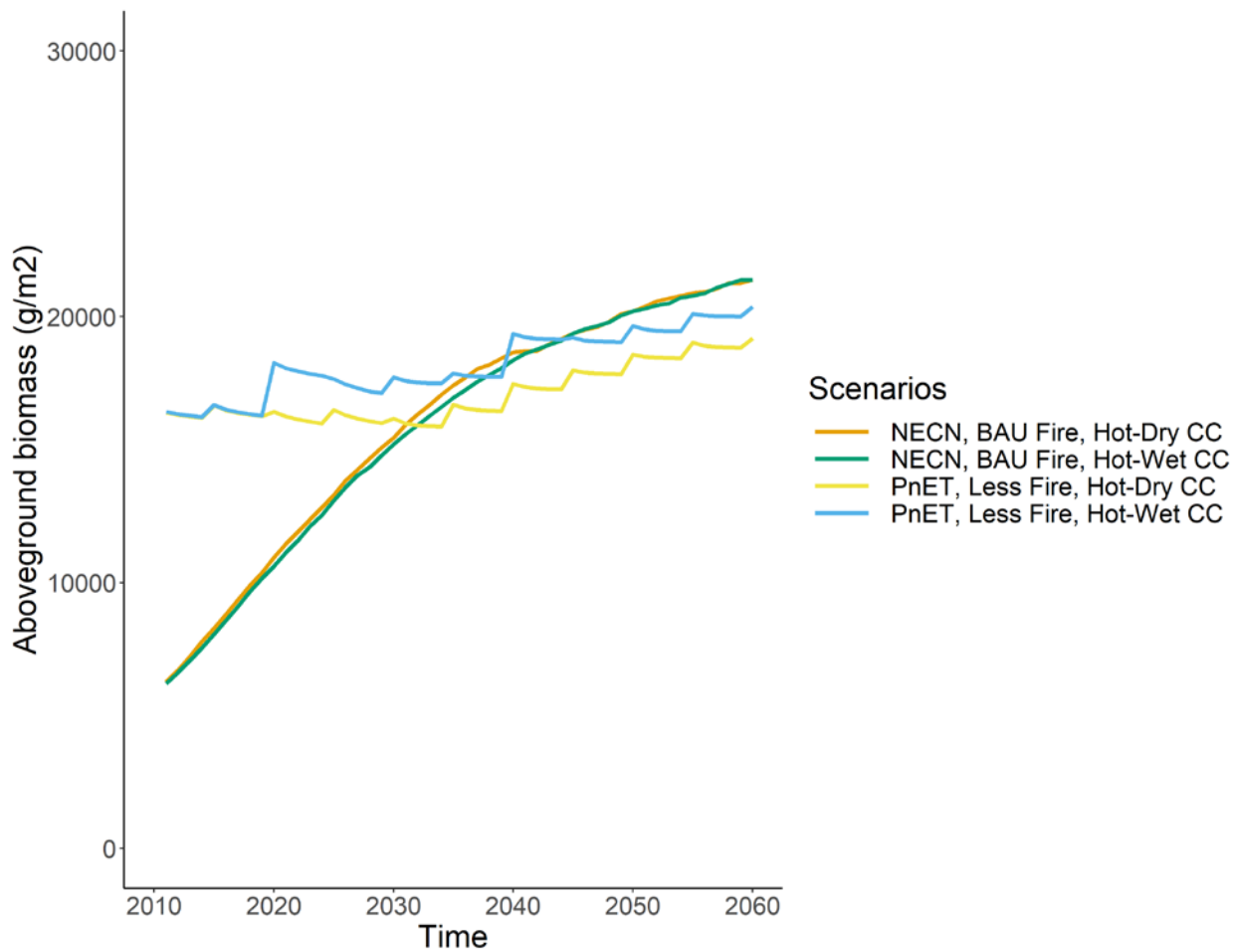


Figure 15. Total aboveground biomass (g m^{-2}) projected using NECN and PnET model, two climate scenarios, simulated from 2010 – 2060 for Ft. Bragg, NC.

SPECIES-SPECIFIC ABOVEGROUND BIOMASS DENSITY

As with aboveground biomass, the initial simulated biomass of both longleaf and loblolly pine varied between the two models (Figure 16). In NECN, simulated longleaf biomass increased over time, while simulated biomass under PnET remained more stable. For loblolly pine, biomass tended to increase over time in both models though more in NECN than PnET. Similar to landscape total biomass, the wetter climate change scenario resulted in more longleaf and loblolly pine in PnET simulations.

The simulated biomass of white oak was much higher in PnET than NECN though they increased over time at approximately the same rate in both models (Figure 17). Trends in biomass of red maple were different between the models; biomass increased slowly in NECN but rapidly in PnET. Model sensitivity to climate change in hardwoods had an opposite pattern to the conifers. For deciduous species, NECN was more sensitive to climate differences than PnET. In NECN, the hot-dry scenario resulted in lower biomass than the hot-wet scenario. In PnET, simulated red maple and white oak biomass differences were small between climate scenarios.

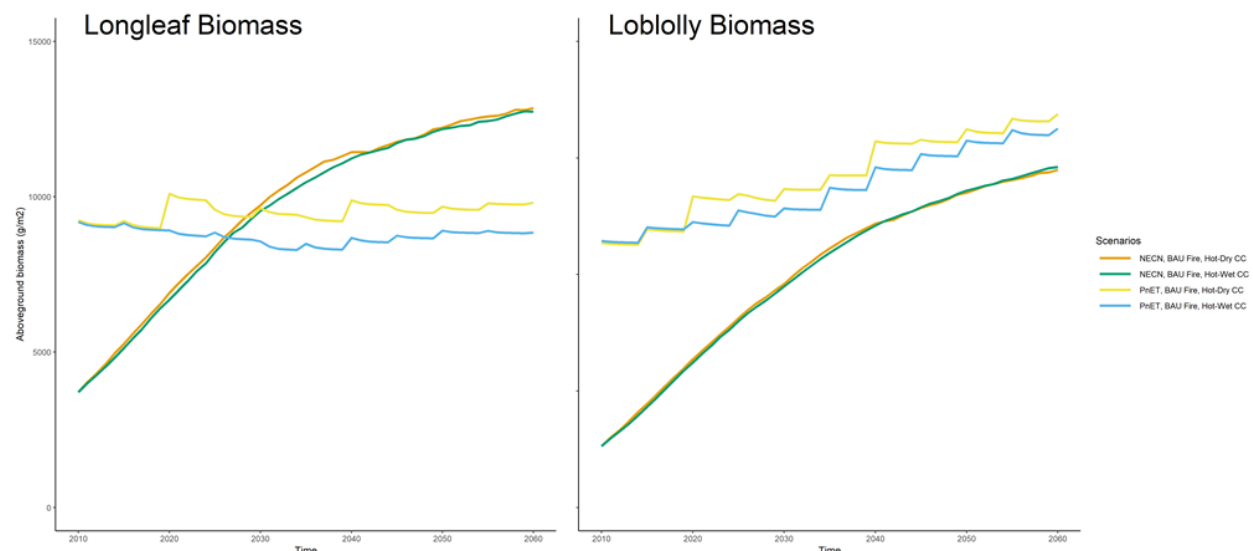


Figure 16. Aboveground biomass (g m^{-2}) for longleaf pine and loblolly pine projected using NECN and PnET model, two climate scenarios, simulated from 2010 – 2060 for Ft. Bragg, NC.

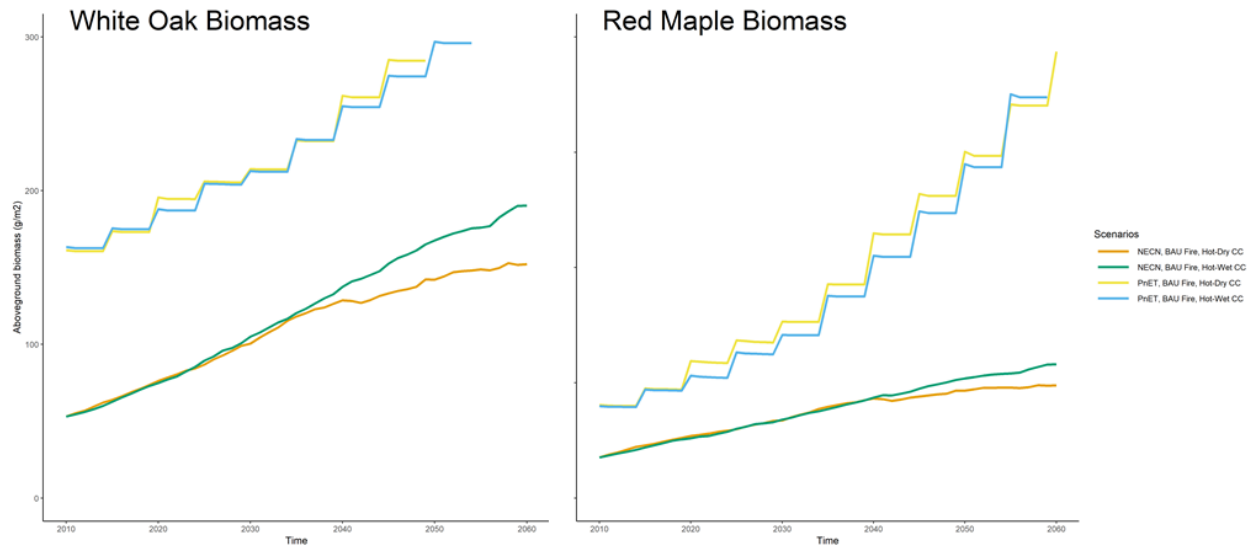


Figure 17. Aboveground biomass (g m^{-2}) for white oak and red maple projected using NECN and PnET model, two climate scenarios, simulated from 2010 – 2060 for Ft. Bragg, NC.

HARVESTED AREA

For all scenario and both models, we used the same harvest prescriptions and harvest model. Therefore, the harvest behavior across models and scenarios was very similar (Figure 18). The area that was thinned was similar between models and across scenarios and was relatively constant over time, indicating that simulated (current management) practices are sustainable over the next 50 years. Annual variability in harvest area was due to the stochastic stand selection within the harvest model.

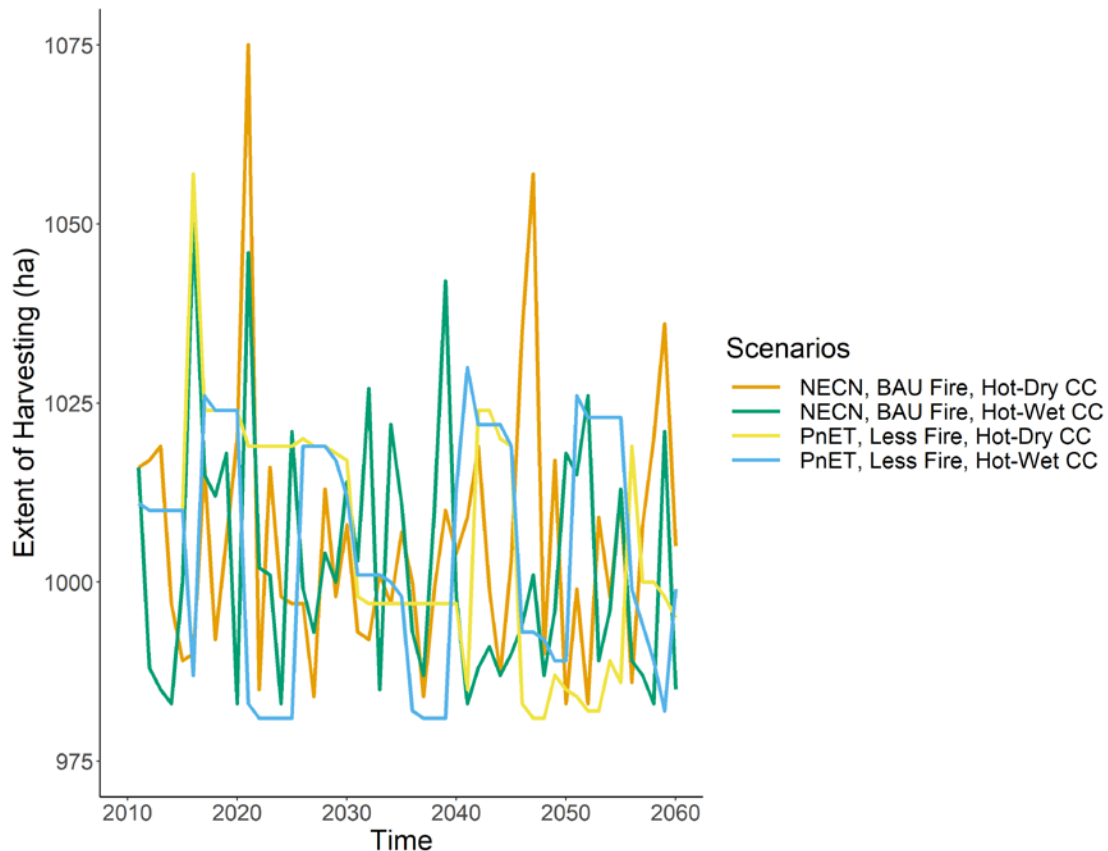


Figure 18. Hectares harvested using NECN and PnET models, two climate scenarios, simulated for 2010 – 2060 for Ft. Bragg, NC.

PREScribed FIRE

NECN simulated approximately the same amount of biomass removed across scenarios (Figure 19). Although mortality varied year-to-year, reflecting the variation in the weather conditions when prescribed burning was applied, there are no larger trends (Figure 19). This is because growth compensates for the minor losses due to prescribed fire, providing a constant amount of biomass for combustion. By comparison, the extent (area) and number of prescribed burning decreased over time for all scenarios (Figures 20 and 21), despite constant prescribed fire goals. We hypothesize that this is due to climate change reducing the ‘burn window’ available for prescribed burning due to restrictions placed on the weather conditions under which prescribed burning can occur. For example, if more days exceed the maximum temperature under which prescribed burning can occur, the number of fires necessarily declines.

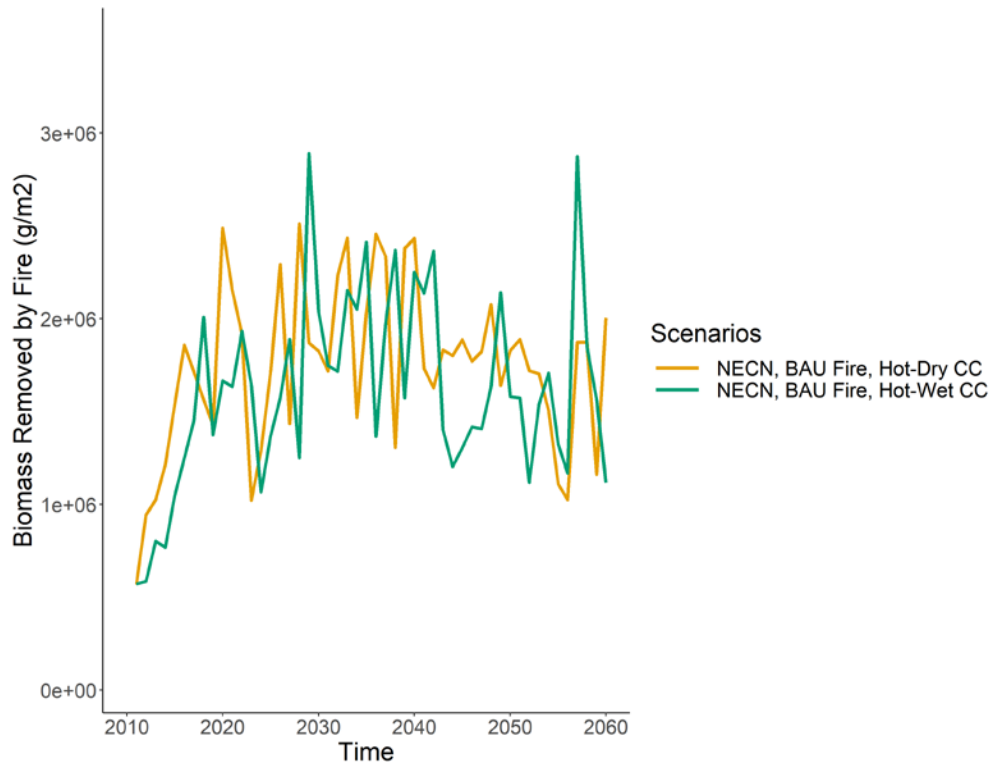


Figure 19. Mortality (g biomass m⁻²) caused by prescribed fire using NECN, two climate scenarios, simulated for 2010 – 2060 for Ft. Bragg, NC.

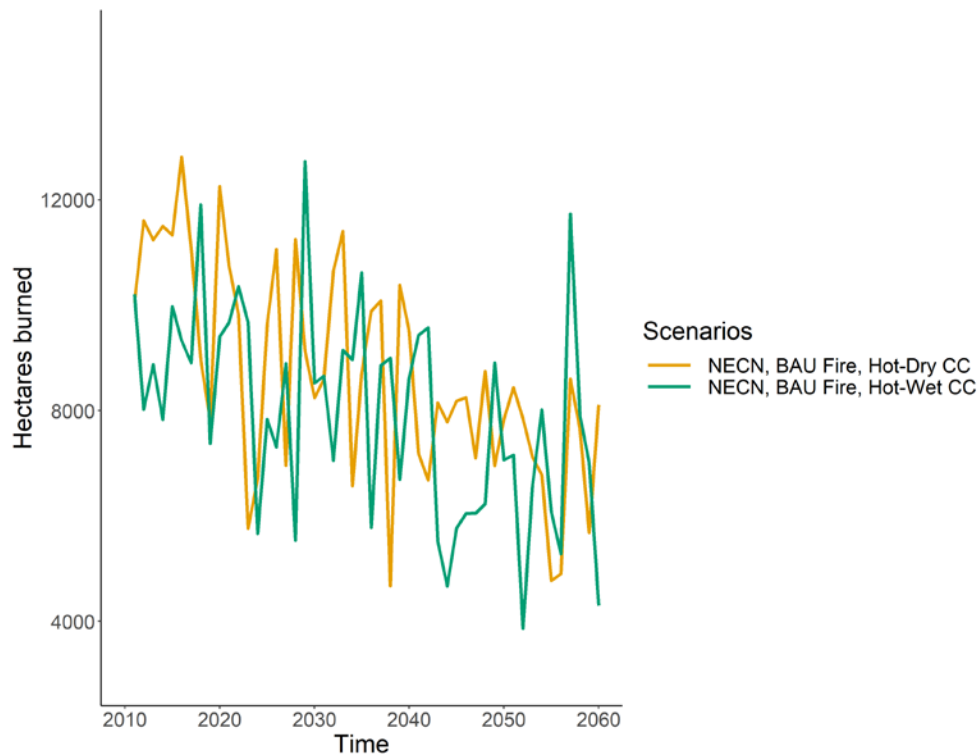


Figure 20. Area burned by prescribed fire (ha) using NECN, two climate scenarios, simulated for 2010 – 2060 for Ft. Bragg, NC.

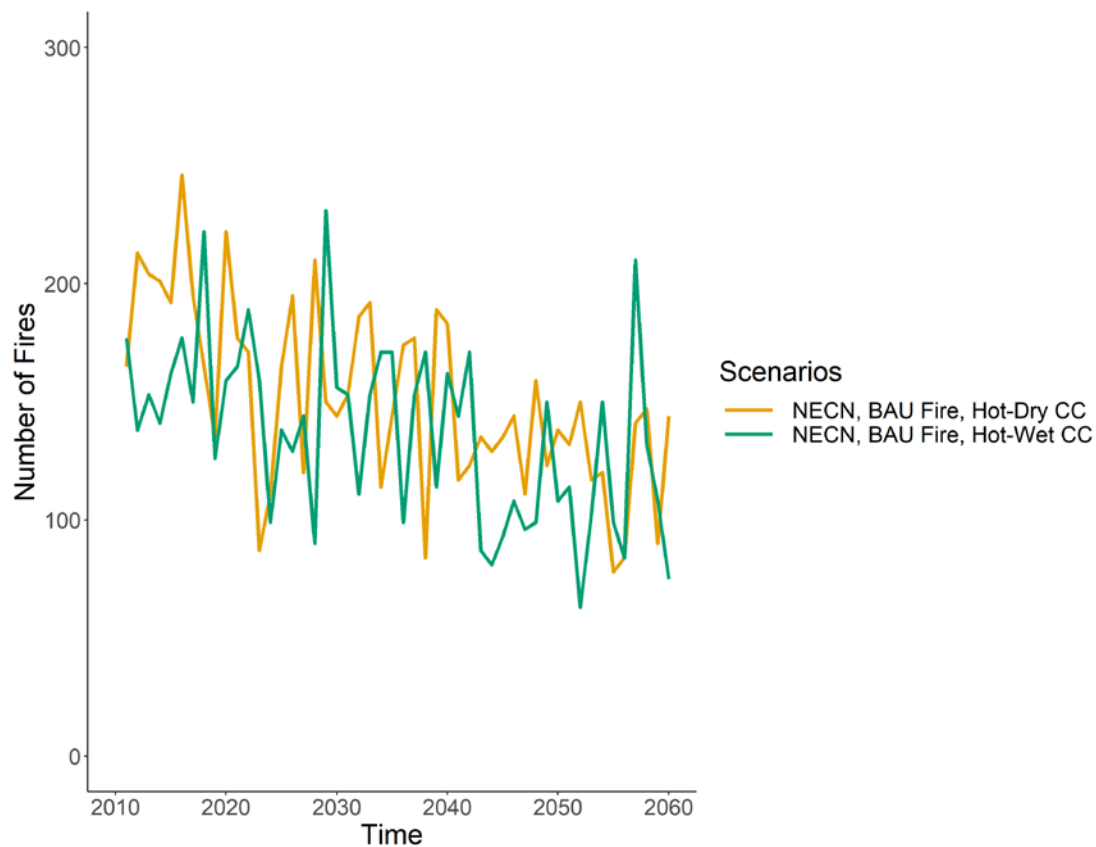


Figure 21. Number of prescribed fire per year using NECN, two climate scenarios, simulated for 2010 – 2060 for Ft. Bragg, NC. The target number of prescribed fires was 450 per year.

HURRICANES

Hurricanes simulated with NECN and with climate change resulted in substantially lower aboveground biomass (Figure 22). Simulated hurricanes also generated larger differences between the climate change scenarios. Whether these differences will persist after hurricanes are replicated 10x will be determined in future analyses.

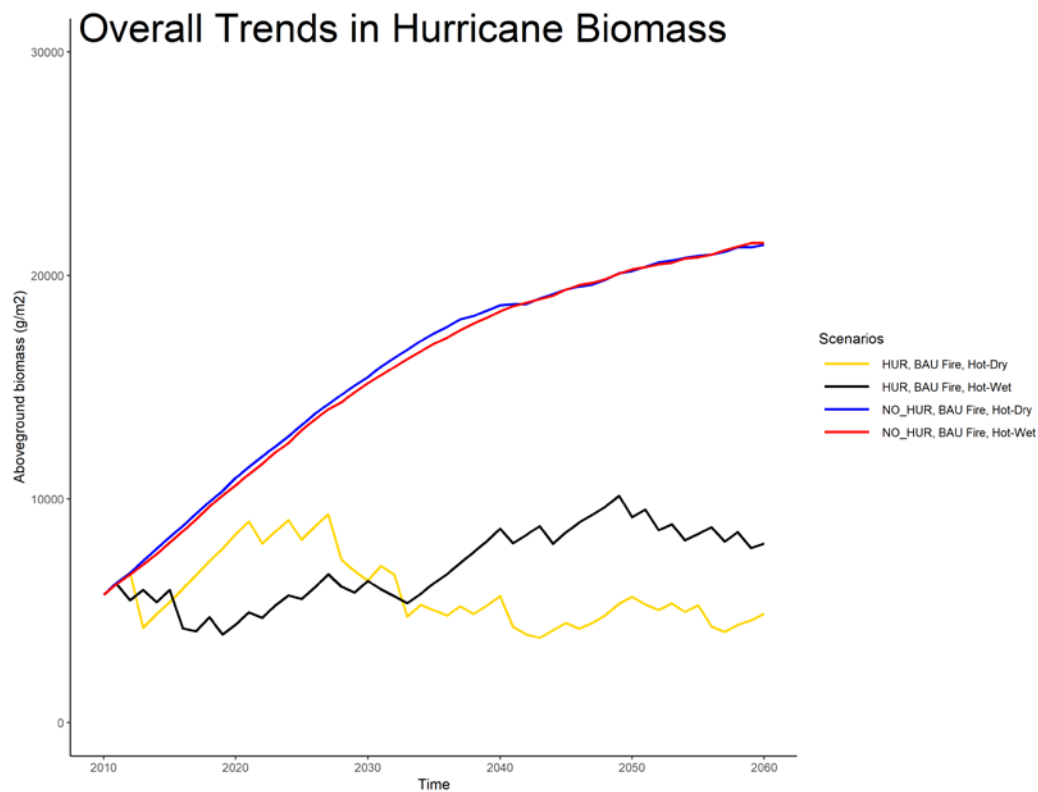


Figure 22. Aboveground biomass (g m^{-2}) simulated with hurricanes (HUR) and without hurricanes (NO_HUR), assuming a hurricane regime similar to the past 50 years. Simulations used NECN and two climate scenarios, simulated for 2010 – 2060 for Ft. Bragg, NC.

7.0 COST ASSESSMENT

Table 4. Cost Model for a Monitoring Technology

Cost Element	Data Tracked During the Demonstration
Sensor procurement	N/A
Installation costs	N/A: All software described above is open-source and freely available. Data must be processed so as to meet the input requirements of each model; these data are freely available or can be readily estimated.
Sensor consumable	N/A
Operation costs	A competent GIS technician with the support of a modeling expert is required to operate the methods described above. Within our demonstration plan, we were able to produce the projections using ~6 months of technician effort and ~2 months of model expert effort.
Maintenance	N/A
Sensor lifetime	N/A

8.0 IMPLEMENTATION ISSUES

1. As noted above, we had to replace the PPA-SiBGC model after the Test Phase due to its incompatibility with the needs of Ft. Bragg; it did not have the capacity to simulate prescribed fire and management as practiced. This substitution had longer-term ramifications as it required that we change both models and personnel.
2. We intended for NECN and PnET models to have identical baseline conditions for the landscape, facilitating comparison. However, the necessary software for eliminating the ‘spin-up’ period in PnET was not completed in time for this final report. We anticipate the software will become available in September and any subsequent reports or publications will have identical baseline conditions.
3. The Base Hurricane extension was not available for implementation until late July 2019 and therefore it was only paired with the NECN model. A subsequent publication is planned that will have a full factorial experimental design including two climate projections, three management projections, two hurricane projections (BAU, high-intensity hurricanes), and at least 10 replications.
4. We have not yet finalized a roadmap allowing for transfer to natural resource management staff. This will be completed in August and September 2019.

9.0 REFERENCES

- Aber, J. D., S. V Ollinger, C. A. Federer, P. B. Reich, M. L. Goulden, D. W. Kicklighter, J. M. Melillo, and R. G. Lathrop. 1995. Predicting the effects of climate change on water yield and forest production in the northeastern United States. *Climate Research* 5:207–222.
- Abramoff, R.Z., Davidson, E.A. and Finzi, A.C., 2017. A parsimonious modular approach to building a mechanistic belowground carbon and nitrogen model. *Journal of Geophysical Research: Biogeosciences*, 122(9), pp.2418-2434.
- Bonan, G.B., 2008. Forests and climate change: forcings, feedbacks, and the climate benefits of forests. *science*, 320(5882), pp.1444-1449.
- Bugmann, H., 2001. A review of forest gap models. *Climatic Change*, 51(3-4), pp.259-305.
- Clark, J.S., Carpenter, S.R., Barber, M., Collins, S., Dobson, A., Foley, J.A., Lodge, D.M., Pascual, M., Pielke, R., Pizer, W. and Pringle, C., 2001. Ecological forecasts: an emerging imperative. *science*, 293(5530), pp.657-660.
- Crookston, N.L. and Dixon, G.E., 2005. The forest vegetation simulator: a review of its structure, content, and applications. *Computers and Electronics in Agriculture*, 49(1), pp.60-80.
- D'Amato, A.W., Bradford, J.B., Fraver, S. and Palik, B.J., 2011. Forest management for mitigation and adaptation to climate change: insights from long-term silviculture experiments. *Forest Ecology and Management*, 262(5), pp.803-816.
- De Bruijn, A., Gustafson, E.J., Sturtevant, B.R., Foster, J.R., Miranda, B.R., Lichti, N.I. and Jacobs, D.F., 2014. Toward more robust projections of forest landscape dynamics under novel environmental conditions: embedding PnET within LANDIS-II. *Ecological Modelling*, 287, pp.44-57.
- Douglas, R.J. and Leslie, M., 1997. Conserving biodiversity on military lands. *Federal Facilities Environmental Journal*, 8(2), pp.93-105.
- Dukes, J.S., Pontius, J., Orwig, D., Garnas, J.R., Rodgers, V.L., Brazee, N., Cooke, B., Theoharides, K.A., Stange, E.E., Harrington, R. and Ehrenfeld, J., 2009. Responses of insect pests, pathogens, and invasive plant species to climate change in the forests of northeastern North America: what can we predict?. *Canadian journal of forest research*, 39(2), pp.231-248.
- Duvaneck, M. J., and J. R. Thompson. 2017. Climate change imposes phenological tradeoffs on forest net primary productivity. *Journal of Geophysical Research - Biogeosciences* 122:1–16.
- Duvaneck, M. J., J. R. Thompson, E. J. Gustafson, Y. Liang, and A. M. G. de Bruijn. 2017. Recovery dynamics and climate change effects to future New England forests. *Landscape Ecology*:1–13.
- Ellison, D., Morris, C.E., Locatelli, B., Sheil, D., Cohen, J., Murdiyarso, D., Gutierrez, V., Van Noordwijk, M., Creed, I.F., Pokorny, J. and Gaveau, D., 2017. Trees, forests and water: Cool insights for a hot world. *Global Environmental Change*, 43, pp.51-61.
- Erickson, A. and Strigul, N., 2019. A forest model intercomparison framework and application at two temperate forests along the East Coast of the United States. *Forests*, 10(2), p.180.
- Food and Agriculture Organization of the United Nations. 2016. *Forests and Climate Change*.
- Gilliam, F.S. and Platt, W.J., 1999. Effects of long-term fire exclusion on tree species composition and stand structure in an old-growth *Pinus palustris* (longleaf pine) forest. *Plant Ecology*, 140(1), pp.15-26.

- Gustafson, E.J., Shifley, S.R., Mladenoff, D.J., Nimerfro, K.K. and He, H.S., 2000. Spatial simulation of forest succession and timber harvesting using LANDIS. Canadian Journal of Forest Research, 30(1), pp.32-43.
- Gustafson, E.J., Sturtevant, B.R. and Fall, A., 2006. A collaborative, iterative approach to transferring modeling technology to land managers. In Forest Landscape Ecology(pp. 43-64). Springer, New York, NY.
- Gustafson, E. J., A. M. G. De Bruijn, B. R. Miranda, B. R. Sturtevant, and M. E. Kubiske. 2017. Do rising temperatures always increase forest productivity? Interacting effects of temperature, precipitation, cloudiness and soil texture on tree species growth and competition. Environmental Modelling and Software.
- Harvard University. Physical and biological characteristics of the Harvard Forest. Harvard Forest 2018. Available at: <http://harvardforest.fas.harvard.edu/research/HF-tract>. (Accessed: 6th March 2018)
- Hook, D.D., Buford, M.A., and Williams, T.M., 1991. Impact of Hurricane Hugo on the South Carolina Coastal Plain Forest. *Journal of Coastal Research*, SI#8, 291-300. Fort Lauderdale (Florida). Spring 1991.
- Iverson, L.R., Schwartz, M.W. and Prasad, A.M., 2004. How fast and far might tree species migrate in the eastern United States due to climate change?. Global Ecology and Biogeography, 13(3), pp.209-219.
- Jin, W., He, H.S. and Thompson III, F.R., 2016. Are more complex physiological models of forest ecosystems better choices for plot and regional predictions?. Environmental modelling & software, 75, pp.1-14.
- Johnsen, K., Samuelson, L., Teskey, R., McNulty, S. and Fox, T., 2001. Process models as tools in forestry research and management. Forest Science, 47(1), pp.2-8.Jospeh W. Jones Ecological Research Center at Ichauway. Ichauway. Jospeh W. Jones Ecological Research Center at Ichauway. 2018. Available at: <http://www.jonesctr.org/about/ichauway.php>. (Accessed: 16th March 2018)
- Kaplan, J.O., Krumhardt, K.M., Ellis, E.C., Ruddiman, W.F., Lemmen, C. and Goldewijk, K.K., 2011. Holocene carbon emissions as a result of anthropogenic land cover change. The Holocene, 21(5), pp.775-791.
- Kuefler, D., Haddad, N.M., Hall, S., Hudgens, B., Bartel, B. and Hoffman, E., 2008. Distribution, population structure and habitat use of the endangered Saint Francis Satyr butterfly, *Neonympha mitchellii francisci*. The American Midland Naturalist, 159(2), pp.298-321.
- Landers, J.L., D.H. Van Lear & W.D. Boyer. 1995. The longleaf pine forests of the Southeast: requiem or renaissance? Journal of Forestry 93: 39-44.
- Liang, Y. Y., M. J. M. J. Duveneck, E. J. E. J. Gustafson, J. M. J. M. Serra-Diaz, and J. R. J. R. Thompson. 2017. How disturbance, competition, and dispersal interact to prevent tree range boundaries from keeping pace with climate change. Global Change Biology:335–351.
- Lipscomb, D.J. and Williams, T.M., 2006. Evaluating some proposed matrices for scoring sub-optimal red-cockaded woodpecker foraging habitat in relation to the 2003 recovery plan. Gen. Tech. Rep. SRS-92. Asheville, NC: US Department of Agriculture, Forest Service, Southern Research Station. pp. 10-16.
- Luyssaert, S., Schulze, E.D., Börner, A., Knohl, A., Hessenmöller, D., Law, B.E., Ciais, P. and Grace, J., 2008. Old-growth forests as global carbon sinks. Nature, 455(7210), p.213.
- McKenzie, P. F., Duveneck, M. J., Morreale, L. L., & Thompson, J. R. 2019. Local and global

- parameter sensitivity within an ecophysiologicaly based forest landscape model. Environmental Modelling & Software, 117, 1-13.
- Millar, C.I., Stephenson, N.L. and Stephens, S.L., 2007. Climate change and forests of the future: managing in the face of uncertainty. Ecological applications, 17(8), pp.2145-2151.
- Mitchell, K.J., 1975. Dynamics and simulated yieldof Douglas-fir. Forest Science, 21(suppl_1), pp.a0001-z0001.
- Moorcroft, P.R., G.C. Hurtt, and S.W. Pacala. 2001. A method for scaling vegetation dynamics: the ecosystem demography model (ED). Ecological Monographs 71: 557-585.
- Pan, Y., Birdsey, R.A., Fang, J., Houghton, R., Kauppi, P.E., Kurz, W.A., Phillips, O.L., Shvidenko, A., Lewis, S.L., Canadell, J.G. and Ciais, P., 2011. A large and persistent carbon sink in the world's forests. Science, 333(6045), pp.988-993.
- Parton, W.J., Schimel, D.S., Cole, C.V. and Ojima, D.S., 1987. Analysis of factors controlling soil organic matter levels in Great Plains Grasslands 1. Soil Science Society of America Journal, 51(5), pp.1173-1179.
- Pereira, F.F., Farinosi, F., Arias, M.E., Lee, E., Briscoe, J. and Moorcroft, P.R., 2017. A hydrological routing scheme for the Ecosystem Demography model (ED2+ R) tested in the Tapajós River basin in the Brazilian Amazon. Hydrology & Earth System Sciences, 21(9).
- Purves, D.W., Lichstein, J.W., Strigul, N. and Pacala, S.W., 2008. Predicting and understanding forest dynamics using a simple tractable model. Proceedings of the National Academy of Sciences, 105(44), pp.17018-17022.
- Ruddiman, W.F., 2003. The anthropogenic greenhouse era began thousands of years ago. Climatic change, 61(3), pp.261-293.
- Scheller, R.M., Domingo, J.B., Sturtevant, B.R., Williams, J.S., Rudy, A., Gustafson, E.J. and Mladenoff, D.J., 2007. Design, development, and application of LANDIS-II, a spatial landscape simulation model with flexible temporal and spatial resolution. ecological modelling, 201(3-4), pp.409-419.
- Scheller, R.M. and Mladenoff, D.J., 2007. An ecological classification of forest landscape simulation models: tools and strategies for understanding broad-scale forested ecosystems. Landscape Ecology, 22(4), pp.491-505.
- Scheller, R.M., Hua, D., Bolstad, P.V., Birdsey, R.A. and Mladenoff, D.J., 2011. The effects of forest harvest intensity in combination with wind disturbance on carbon dynamics in Lake States Mesic Forests. Ecological Modelling, 222(1), pp.144-153.
- Scheller, R.M. 2018. The challenges of forest modeling given climate change. Landscape Ecology 33: 1481-1488.
- Scheller, R.M., A. Kretchun, T.J. Hawbaker, P.D. Henne. 2019. A landscape model of variable social-ecological fire regimes. Ecological Modelling 401: 85-93.
- Scoullar, K., Seely, B., Welham, C., Kimmins, H. and Blanco, J.A., 2010. Forecasting forest futures: a hybrid modelling approach to the assessment of sustainability of forest ecosystems and their values. Routledge.
- Seidl, R., Eastaugh, C.S., Kramer, K., Maroschek, M., Reyer, C., Socha, J., Vacchiano, G., Zlatanov, T. and Hasenauer, H., 2013. Scaling issues in forest ecosystem management and how to address them with models. European Journal of Forest Research, 132(5-6), pp.653-666.
- Shaw, J.D., Vacchiano, G., DeRose, R.J., Brough, A., Kusbach, A. and Long, J.N., 2006. Local calibration of the Forest Vegetation Simulator (FVS) using custom inventory data. In In: Society of American Foresters 2006 National Convention [electronic resource]: Pittsburgh,

- Pennsylvania, October 25-29. Bethesda, MD: Society of American Foresters, 2006: 10 p...
- Shifley, S.R., He, H.S., Lischke, H., Wang, W.J., Jin, W., Gustafson, E.J., Thompson, J.R., Thompson, F.R., Dijak, W.D. and Yang, J., 2017. The past and future of modeling forest dynamics: from growth and yield curves to forest landscape models. *Landscape Ecology*, 32(7), pp.1307-1325.
- Smith, J. E., Heath, L. S., Skog, K. E., & Birdsey, R. A. 2006. Methods for calculating forest ecosystem and harvested carbon with standard estimates for forest types of the United States. Gen. Tech. Rep. NE-343. Newtown Square, PA: US Department of Agriculture, Forest Service, Northeastern Research Station. 216 p., 343.
- Sorrie, B.A., J.B. Gray & P.J. Crutchfield. 2006. The vascular flora of the longleaf pine ecosystem of Fort Bragg and Weymouth Woods, North Carolina. *Castanea* 71: 129-161.
- Strigul, N., Pristinski, D., Purves, D., Dushoff, J. and Pacala, S., 2008. Scaling from trees to forests: tractable macroscopic equations for forest dynamics. *Ecological Monographs*, 78(4), pp.523-545.
- Thompson, J.R., Wiek, A., Swanson, F.J., Carpenter, S.R., Fresco, N., Hollingsworth, T., Spies, T.A. and Foster, D.R., 2012. Scenario studies as a synthetic and integrative research activity for long-term ecological research. *BioScience*, 62(4), pp.367-376.
- Umeki, K., 1995. Modeling the relationship between the asymmetry in crown display and local environment. *Ecological Modelling*, 82(1), pp.11-20.
- Umeki, K., 1997. Effect of crown asymmetry on size-structure dynamics of plant populations. *Annals of Botany*, 79(6), pp.631-641.
- Van Lear, D. H., W.D. Carroll, et al. 2005. History and restoration of the longleaf pine-grassland ecosystem: implications for species at risk. *Forest ecology and Management* 211: 150-165.
- Vincent, C.H., Hanson, L.A. and Bjelopera, J.P., 2014. Federal land ownership: Overview and data (pp. 7-5700). Washington, DC, USA: Congressional Research Service.
- Ware, S., C. Frost, & P.D. Doerr. 1993. Southern mixed hardwood forest: the former longleaf pine forest. p. 447–493. In: W.H. Martin, et al. (eds.). *Biodiversity of the southeastern United States. Lowland terrestrial communities*. J. Wiley and Sons, New York.
- Wiens, J.A., Van Horne, B.E.A.T.R.I.C.E. and Noon, B.R., 2002. Integrating landscape structure and scale into natural resource management. *Integrating landscape ecology into natural resource management*, pp.23-67.

APPENDICES

Appendix A: Point of Contact

POINT OF CONTACT Name	ORGANIZATION Name Address	Phone Fax E-mail	Role in Project
Dr. Melissa Lucash	Portland State U. Department of Geography PO Box 751- GEOG Portland State University Portland, OR 97207-0751	503.725.2170 lucash@pdx.edu	Lead-I
Dr. Robert Scheller	North Carolina State University Campus Box 7106, Raleigh, NC 27695- 7106 USA	919-513-3937 rschell@ncsu.edu	Co-I
Dr. Matthew Duveneck	Harvard University, 324 North Main Street, Petersham, MA 01366	mduveneck@fas.harvard.edu	Co-I

Appendix B: Erickson and Strigul (2019).

Article

A Forest Model Intercomparison Framework and Application at Two Temperate Forests Along the East Coast of the United States

Adam Erickson * and Nikolay Strigul

Department of Mathematics and Statistics, Washington State University, 14204 NE Salmon Creek Avenue, Vancouver, WA 98686, USA; nick.strigul@wsu.edu

* Correspondence: adam.erickson@wsu.edu; Tel.: +1-360-546-9655

Received: 24 December 2018; Accepted: 13 February 2019; Published: 19 February 2019



Abstract: State-of-the-art forest models are often complex, analytically intractable, and computationally expensive, due to the explicit representation of detailed biogeochemical and ecological processes. Different models often produce distinct results while predictions from the same model vary with parameter values. In this project, we developed a rigorous quantitative approach for conducting model intercomparisons and assessing model performance. We have applied our original methodology to compare two forest biogeochemistry models, the Perfect Plasticity Approximation with Simple Biogeochemistry (PPA-SiBGC) and Landscape Disturbance and Succession with Net Ecosystem Carbon and Nitrogen (LANDIS-II NECN). We simulated past-decade conditions at flux tower sites located within Harvard Forest, MA, USA (HF-EMS) and Jones Ecological Research Center, GA, USA (JERC-RD). We mined field data available from both sites to perform model parameterization, validation, and intercomparison. We assessed model performance using the following time-series metrics: Net ecosystem exchange, aboveground net primary production, aboveground biomass, C, and N, belowground biomass, C, and N, soil respiration, and species total biomass and relative abundance. We also assessed static observations of soil organic C and N, and concluded with an assessment of general model usability, performance, and transferability. Despite substantial differences in design, both models achieved good accuracy across the range of pool metrics. While LANDIS-II NECN showed better fidelity to interannual NEE fluxes, PPA-SiBGC indicated better overall performance for both sites across the 11 temporal and two static metrics tested (HF-EMS $\bar{R^2} = 0.73, +0.07$, $\bar{RMSE} = 4.68, -9.96$; JERC-RD $\bar{R^2} = 0.73, +0.01$, $\bar{RMSE} = 2.18, -1.64$). To facilitate further testing of forest models at the two sites, we provide pre-processed datasets and original software written in the R language of statistical computing. In addition to model intercomparisons, our approach may be employed to test modifications to forest models and their sensitivity to different parameterizations.

Keywords: Perfect Plasticity Approximation; SORTIE-PPA; LANDIS-II; forest ecosystem simulation; forest biogeochemistry model; forest landscape model; model intercomparison; Harvard Forest; Jones Ecological Research Center

1. Introduction

1.1. A Brief History of Forest Ecosystem Models

For millenia, timber harvest for economic, militaristic, and social gain was the primary—if not sole—objective of forestry. This focus changed only slightly in the 18th century with the emergence of sustained-yield forest management in Leipzig, Germany (then within the Electorate of Saxony, Holy Roman Empire) [1]. For the first time, controlling the effects of management intensity on land

productivity over time was given primary consideration. This followed a history of deforestation extending back to the loss of *Cedrus* forests across the Middle East, as described in the *Epic of Gilgamesh* in the third millennium BCE [2,3]. While sustained-yield forest management was designed to maximize timber production indefinitely, under the spurious assumption that sustained yield is possible solely through in situ silvicultural treatments, the concept broadly inspired sustainability science, resilience theory [4], and subsequent work on complex adaptive systems [5].

From its inception, sustainability regarded matters economic, social, and ecological in nature [6]. Yet, economic-focused timber production likely accelerated with increased mechanization in the mid-20th century. As our understanding of abiotic and biotic forest interactions expanded, the core assumptions of stationarity underpinning sustained-yield management lost support. The importance of fire ecology [7], structural complexity [8], trophic interactions [9], and their relation to climate, soil, and ecosystem functioning was soon uncovered. Research on climate impacts on regeneration [10,11] further showed that species compositional changes are likely under current climate trajectories, requiring proactive strategies to sustain yields from extant forests.

Research along this line inspired the concepts of adaptive migration [12], assisted gene flow [13], and precise gene editing of trees with CRISPR/Cas9 [14]. Ecological forestry or sustainable forest management is now the dominant management paradigm, where the focus is on emulating natural processes of succession, disturbance, and migration [15]. Mirroring changes in management, modeling forest ecosystems also underwent a paradigm shift from focusing on sustained yield to ecological forestry and multiple-use management. This has required a remarkable increase in the size and complexity of forest ecosystem models in order to simulate a suite of new complex processes.

Forest models likely began 350 years ago in China with yield tables known as the Lung Ch'uan codes, invented by a women of the Kuo family in Suichuan county, Jiangxi [16]. It was not until the 20th century that the first complex mathematical models of forests emerged. Long restricted to simple models developed with mechanical calculators, digital computers enabled researchers to explicitly model forest dynamics. Following the development of matrix models [17] and empirical growth-and-yield models such as Prognosis [18,19], a vast array of gap [20], forest landscape [21–25], and terrestrial biosphere models [26–28] have been developed. Models of forest ecosystems vary substantially in application, abstraction, and system detail. While some models may be entirely statistical or mechanistic, others combine statistical and systems-theoretic process models in a hybrid modeling approach [29,30].

Representation of canopy geometry varies from implicit to a single 'big-leaf' and detailed three-dimensional crown and root geometry (e.g., modern gap models such as MAESPA [31] and LES [32]). Models of growth range from simple allometric equations (e.g., growth-and-yield models) to light-use efficiency models [33] and first-principles mechanistic models of photosynthesis [34]. Belowground process models similarly vary in structure, from simple stoichiometric relations to carbon and nitrogen cycling with microbial dynamics to a fully mechanistic representation of energetic and biogeochemical processes based on thermodynamics. Current belowground models vary considerably in their process representation and accuracy, with much improvement left to be made [35]. Most belowground models in use globally rely on a variant of the classical Century model [36,37].

Model specialization and generalization ranges from pure research applications in narrowly defined areas (e.g., [31]) to simulating multiple loosely coupled landscape processes to modeling biogeochemical fluxes throughout the world's forests. A trade-off is thought to exist between realism, precision, and generality [38], with more detailed models requiring higher parameterization costs. Yet, little is known about the net effects of variation in the structure of these models on the precision and accuracy of their predictions across temporal and spatial scales. While such model intercomparisons are common within classes of models such as terrestrial biosphere models, they are seldom applied to gap or forest landscape models. Models operating at different scales are seldom compared within sites. Yet, much can be learned by comparing models that differ in assumptions and structure.

1.2. Emergence of New Classes of Hybrid Model

Modern forest landscape models are the result of five key model development phases, listed in chronological order: (1) Growth-and-yield models; (2) fire models; (3) gap models; (4) physiological models; (5) hybrid models combining design principles from each [20,29,39]. Terrestrial biosphere models similarly trace their roots back to early one-dimensional physiological models, with land surface models currently in their third generation and dynamic global vegetation models in their second generation [40]. This latest generation of models was intended to address the lack of explicit representation of vegetation dynamics—a critical source of model uncertainty in future climate scenarios [41]. This inspired the aforementioned forest ecosystem model intercomparisons as well as new terrestrial biosphere model designs based on gap models, bypassing the trade-offs of medium-resolution forest landscape models.

Collectively, these efforts yielded a number of new terrestrial biosphere models based on the classical gap model, including the Lund–Potsdam–Jena General Ecosystem Simulator (LPJ-GUESS) [42], the Ecosystem Demography model (ED/ED2) [43,44], and Land Model 3 with PPA (LM3-PPA) [45], based on the Perfect Plasticity Approximation (PPA) [46,47]. These models represent the current state-of-the-art in modeling vegetation dynamics globally, in what we term ‘cohort-leaf’ vegetation models. While individual-based global models have begun to merge, forest landscape models have remained in between, focused on spatial processes of fire, harvest, and biological disturbance. Yet, previous research has shown that such forest landscape models are often insensitive to landscape configuration and are therefore aspatial [48], counter to the main assumption and selling point of these models.

While most forest landscape and terrestrial biosphere models lack individual trees, the SAS [43] and PPA [32,46,49] model reduction strategies have demonstrated an ability to successfully up-scale gap dynamics to forest stands. Other up-scaling strategies exist as well. One recent forest landscape model participating in the CoFoLaMo intercomparison scales from individual trees to stands by pre-computing light tables [50]. Regardless of the model structure, it is clear that gap, forest landscape, and terrestrial biosphere models are beginning to merge into new models of the terrestrial biosphere. This trend is also attributable to improvements in computational efficiency with new processor designs and cluster or cloud computing infrastructure. As few, if any, existing models are designed for highly parallel architectures (e.g., general-purpose graphics processing units, or GPGPUs), there remains much potential for future efficiency gains. Meanwhile, a clear opportunity exists to embed machine learning models within simulators for data-driven, pattern-based processes (e.g., from remote sensing data streams).

1.3. Existing Forest Ecosystem Model Intercomparison Projects

Existing forest model intercomparison projects, or MIPs, in Europe include the stand-level Intersectoral Impact MIP (ISIMIP) regional forests sector [51] and the landscape-level Comparison of Forest Landscape Models (CoFoLaMo) [52] through ISIMIP, both conducted under the European Union Cooperation on Science and Technology (COST) Action FP1304 “Towards robust projections of European forests under climate change” (PROFOUND). Previous MIP efforts in the United States are limited and include the Throughfall Displacement Experiment (TDE) Ecosystem MIP at Walker Branch Watershed in Oak Ridge, Tennessee [53,54]. The TDE MIP involved a large-scale manipulation experiment to assess ecosystem responses to changes in precipitation, utilizing a total of 13 models. The MIP included an array of monthly, daily, and hourly temporal resolution models. Notable models compared include PnET-II [55], SPA [56], Biome-BGC [57], LINKAGES [58], and MAESTRO/MAESTRA [59], in addition to nine other models. Perhaps unsurprisingly, they found that no single model was ideal for predicting a variety of variables while there was substantial disagreement between models in the C response of vegetation to soil water changes. They also found that more mechanistic models operating at shorter temporal resolution generally showed higher fitness [54].

While the TDE MIP provided a thorough model intercomparison using a variety of model structures, it was limited to a single location and was completed nearly two decades ago.

ISIMIP is a protocol that provides a framework for projecting the impacts of climate change across different sectors. The recent ISIMIP2 biome sector MIP involved the following simulation models: CARAIB [60], DLEM [61], JULES [62,63], LPJ-GUESS [64], LPJmL [65], ORCHIDEE [66], VEGAS [67], and VISIT [68]. These models were used to simulate carbon cycling in terrestrial ecosystem in response to climate change and increased atmospheric CO₂ [69]. Shared forcing data was provided at daily temporal and 0.5° spatial resolution. The ISIMIP2 simulation protocol called for model spin-up followed by a transient run forced by historical climate, CO₂ concentration, and land-use [69,70]. ISIMIP2 also involved a regional forests sector, the ISIMIP2/PROFOUND model intercomparison, which included the following models: 3D-CMCC FEM [71,72], 3D-CMCC-CNR-BGC [73], 3-PG [33], 4C or FORESEE [74], ANAFORE [75], BASFOR [76], CARAIB [60], ED2 [43,44], ForClim [20], FORMIND [77], GO+ [78], GOTILWA+ [79], Landscape-DNDC [80], LPJ-GUESS [64], PnET-BGC [81], and PRELES [82].

ISIMIP2/PROFOUND resulted in the release of a database of harmonized data for model intercomparisons, as well as a wrapper library in the R language for statistical computing [83], yet to be released at the time of this writing. For the ISIMIP regional forest model intercomparison, sites were selected in COST Action FP1304 PROFOUND that provide simplified forest model initialization. Modeling experiments mostly encompassed managed forests. Long time-series data from forest inventories and FLUXNET sites were used in model intercomparisons. Meanwhile, CoFoLaMo involved a comparison of the following forest ecosystem models through the ISIMIP framework [52]: LandClim [84], ForHyCS [85], TreeMig [86], LANDIS-II [87], and iLand [50]. Rather than being driven by climate data at 0.5° spatial resolution, temperature and precipitation drivers were downscaled to 100 m resolution in CoFoLaMo. Forest models were compared with respect to their scales, processes, interactions, drivers, disturbances, uncertainties, and implementation details such as data requirements. For model spin-up, the models used observed climate data hindcast to 1600 A.D., while model forecasts used Representative Concentration Pathways (RCPs) from ISIMIP [52].

Given extensive model intercomparison efforts currently underway in Europe, the question remains, is a forest biogeochemistry MIP necessary for North America? Presently, no other current forest biogeochemistry MIP is evident for the Americas, leaving a substantial spatial sampling bias in model implementation. There is a critical need to conduct ongoing forest biogeochemistry model comparisons in this and other regions of the world in order to establish the regional foundation for robust global C cycle projections. While model initialization and validation data may be relatively difficult to come by in other regions, North America enjoys some of the most thorough forest inventory data in the world, with wide coverage and repeat sampling. This is particularly true for vast temperate and boreal forests in the US and Canada that are critical to the global C cycle. Meanwhile, Mexico, Puerto Rico, and the state of Hawaii contain tropical forests critical for improving models in these systems globally. In this work, we aim to begin this process for North America with a comparison of the Perfect Plasticity Approximation with Simple Biogeochemistry (PPA-SiBGC) and Landscape Disturbance and Succession with Net Ecosystem Carbon and Nitrogen (LANDIS-II NECN) models, which provide contrasting model structures for representing demographic and biogeochemical processes.

In this forest biogeochemistry MIP, we focus on two sites on the East Coast of the United States, Harvard Forest (HF), Massachusetts and Jones Ecological Research Center (JERC), Georgia. The two sites were selected for their representativeness of the United States Eastern Seaboard and for the availability of data needed to parameterize and validate the models. Harvard Forest is one of the most-studied forests in the world, with Google Scholar returning 12,700 results for the site. We focus on results for the Environmental Measurement Station (EMS) eddy covariance (EC) flux tower site within the Little Prospect Hill tract - the longest-running eddy covariance flux tower in the world. While there have been fewer studies at Jones Ecological Research Center, Georgia, USA, Google Scholar returns

1370 results for the site, reflecting its growing role in forest sciences research. Our study focuses on the Red Dirt (RD) EC flux tower site within the mesic sector.

In this work, we aim to establish a foundation for future forest biogeochemistry model intercomparisons. This includes open-source object-oriented software to facilitate model parameterization, validation, intercomparison, and simplified reproducibility of results, based on our Earth-science Research and Development Environment (Erde), a library implemented in R and Python (Erickson and Strigul, in preparation). We perform the model intercomparison for two key research forests in the United States to assess the ability of each model to reproduce observed biogeochemistry pools and fluxes over time. We hypothesize that the inclusion of forest growth, compositional change, and mortality processes in both models will allow for accurate predictions of biomass and NEE dynamics, as suggested in previous research Urbanski et al. [88]. Accordingly, we compare both models to observations and to each other for a host of metrics related to biomass, C, N, and forest composition at the two research sites.

2. Materials and Methods

LANDIS-II NECN and PPA-SiBGC were parameterized for two forested sites in the eastern United States, Harvard Forest, Massachusetts and Jones Ecological Research Center, Georgia. At the HF site, we focus on Little Prospect Hill and the EMS EC flux tower (HF-EMS). At the JERC site, we focus on the mesic zone and RD EC flux tower (JERC-RD). Both sites provided local EC and meteorological measurements to conduct this study. Plots of EC flux and meteorological tower measurements for both sites are located in Appendix A (Figures A1–A4); maps of both sites are provided in the site descriptions.

Both models were parameterized using data available for each site, including local (i.e., field measurements) and general information sources (e.g., species compendiums and other published sources). As these empirical or observational values were used to parameterize both models, further model calibration (i.e., parameter tuning) was not necessary. This is because tuning parameters away from measured values to improve model performance, or defining a separate set of tuning parameters, is known to produce model over-fitting (i.e., reduced generality) and thus false improvements in model accuracy through reduced parsimony [89]. We explicitly avoided this practice, as it is only appropriate when fitting empirical growth-and-yield models such as Prognosis, also known as the Forest Vegetation Simulator (FVS) [18,19]. All model parameters are provided in Appendix B (Tables A1–A30). We close the methodology section with descriptions of the metrics, models, and criteria used in the intercomparisons.

2.1. Model Descriptions

In the following sections, we provide a brief overview of the two forest ecosystem models used in this intercomparison study. For detailed information on each model, readers are encouraged to refer to the original publications.

2.1.1. LANDIS-II NECN

The LANDIS-II model is an extension of the original LANdscape DIsturbance and Succession (LANDIS) model [90–92] into a modular software framework [87]. Specifically, LANDIS-II is a model core containing basic state information that interfaces or communicates with external user-developed models known as “extensions” using a combination of object-oriented and modular design. This design makes LANDIS-II a modeling framework rather than a model. The LANDIS family of models, which also includes LANDIS PRO [93] and Fin-LANDIS [94,95], are stochastic hybrid models [29] based on the vital attributes/fuzzy systems approach of the LANDSIM model genre [96]. This genre borrows heavily from cellular automata [97] and thus Markov Chains by applying simple heuristic rule-based systems, in the form of vital attributes, across two-dimensional grids.

Models of the LANDSIM genre focus on landscape-scale processes and assume game-theoretic vital attribute controls over successional trajectories following disturbance [98]. The LANDSIM model genre is thus a reasonable match for the classical forest fire model [99], given its local two-dimensional cellular basis. In contrast to the original LANDIS model, LANDIS-II is implemented in Microsoft C# rather than ISO C++98 [100], simplifying model development in exchange for a proprietary single-vendor software stack [87].

The latest version of LANDIS-II (v7) supports Linux through use of the Microsoft .NET Core developer platform. The modular design of LANDIS-II is intended to simplify the authorship and interaction of user-provided libraries for succession and disturbance. The centralized model core stores basic landscape and species state information and acts as an interface between succession and disturbance models. While there have been numerous forest landscape models over the years [21–25], the LANDIS family of models has enjoyed notable longevity and is currently united under the LANDIS-II Foundation. Part of its longevity is attributable to the prioritization of model functionality over realism in order to appeal to application-minded managers seeking a broad array of functionality.

The Net Ecosystem Carbon and Nitrogen (NECN) model [101] is a simplified variant of the classical Century model [36,37]. The original ten soil layers in Century have been replaced by a single soil layer, with functions for growth and decay borrowed directly from Century v4.5. The NECN succession model Figure 1 is thus a process-based model that simulates C and N dynamics along the plant-soil continuum at a native monthly timestep.

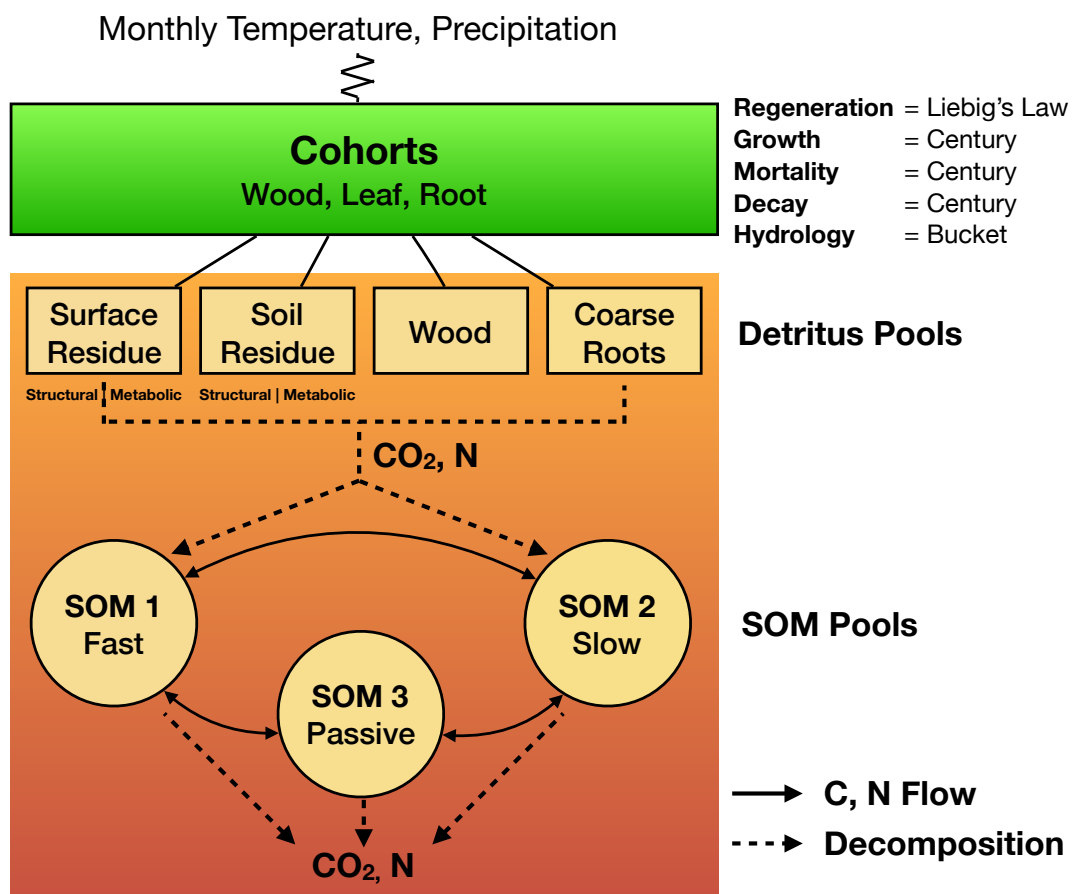


Figure 1. LANDscape DIsturbance and Succession II Net Ecosystem Carbon and Nitrogen (LANDIS-II NECN) model structure.

Atmospheric effects are included through monthly climate (i.e., temperature maxima, minima, means, and standard deviations, and precipitation means and standard deviations). Explicit geometric representation of tree canopies is forgone in favor of bounded statistical growth models based

theoretically on Liebig's Law of the Minimum. Functions for growth, mortality, and decay are adopted from Century [36] while hydrology is based on the simple bucket model [102]. The regeneration function is the only new process in NECN and is also based on Liebig's Law. For a detailed description of the NECN model, readers may refer to the original model publication [101]. Parameterization of the LANDIS-II model for both sites was based on updating parameters used in recent [103–106] and ongoing (Flanagan et al., in review) work.

2.1.2. PPA-SiBGC

The PPA-SiBGC model belongs to the SORTIE-PPA family of models [46,49] within the SAS-PPA model genre, based on a simple and analytically tractable approximation of the classical SORTIE gap model [107,108]. The Perfect Plasticity Approximation, or PPA [46,47], was derived from the dual assumptions of perfect crown plasticity (e.g., space-filling) and phototropism (e.g., stem-leaning), both of which were supported in empirical and modeling studies [49]. The discovery of the PPA was rooted in extensive observational and *in silico* research [46]. The PPA model was designed to overcome the most computationally challenging aspects of gap models in order to facilitate model scaling from the landscape to global scale.

The PPA and its predecessor, the size-and-age structured (SAS) equations [43,109], are popular model reduction techniques employed in current state-of-the-art terrestrial biosphere models [28]. The PPA model can be thought of metaphorically as Navier–Stokes equations of forest dynamics, capable of modeling individual tree population dynamics with a one-dimensional von Foerster partial differential equation [46]. The simple mathematical foundation of the PPA model is provided in Equation (1).

$$1 = \int_{z^*}^{\infty} \sum_{j=1}^k N_j(z) A_j(z^*, z) dz \quad (1)$$

where k is the number of species, j is the species index, $N_j(z)$ is the density of species j at height z , $A_j(a^*, z)$ is the projected crown area of species j at height z , and dz is the derivative of height. In other words, we discard the spatial location of individual trees and calculate the height at which the integral of tree crown area is equal to the ground area of the stand. This height is known as the theoretical z^* height, which segments trees into overstory and understory classes [46].

The segmentation of the forest canopy into understory and overstory layers allows for separate coefficients or functions for growth, mortality, and fecundity to be applied across strata, whose first moment accurately approximates the dynamics of individual-based forest models. Recent studies have shown that the PPA model faithfully reduces the dynamics of the more recent neighborhood dynamics (ND) SORTIE-ND gap model [110] and is capable of accurately capturing forest dynamics [111,112].

In this work, we applied a simple biogeochemistry variant of the SORTIE-PPA model, PPA-SiBGC (Erickson and Strigul, in review) Figure 2.

Empirical observations were relied upon for the C and N content of tree species compartments. Stoichiometric relations were used to estimate N from C, based on empirical measurements provided for both sites. All values were calculated directly from observations. Previously published equations [113] and parameters [114] were used to model crown allometry. Together with inventory data, general biomass equations were used to estimated dry weight mass (kg) for tree stems, branches, leaves, and, fine and coarse roots [115]. Carbon content was assumed to be 50% of dry mass, generally supported by data. Monthly soil respiration was modeled using the approach of Raich et al. [116], while soil organic C was modeled using the simple generalized approach of Domke et al. [117]. Species- and stratum-specific parameters for growth, mortality, and fecundity were calculated directly from field data for both sites. Net ecosystem exchange, or NEE, was modeled as $NEE = r_{soil} - ANPP$ following previous studies, which note associated challenges in connecting field and flux tower measurements [118,119]. Here, ANPP, or annual net primary production, is the total site biomass increment adjusted for the C fraction. This is necessary given the current field-measurement basis of the PPA, which may be replaced by LiDAR measurements and/or process models in future work.

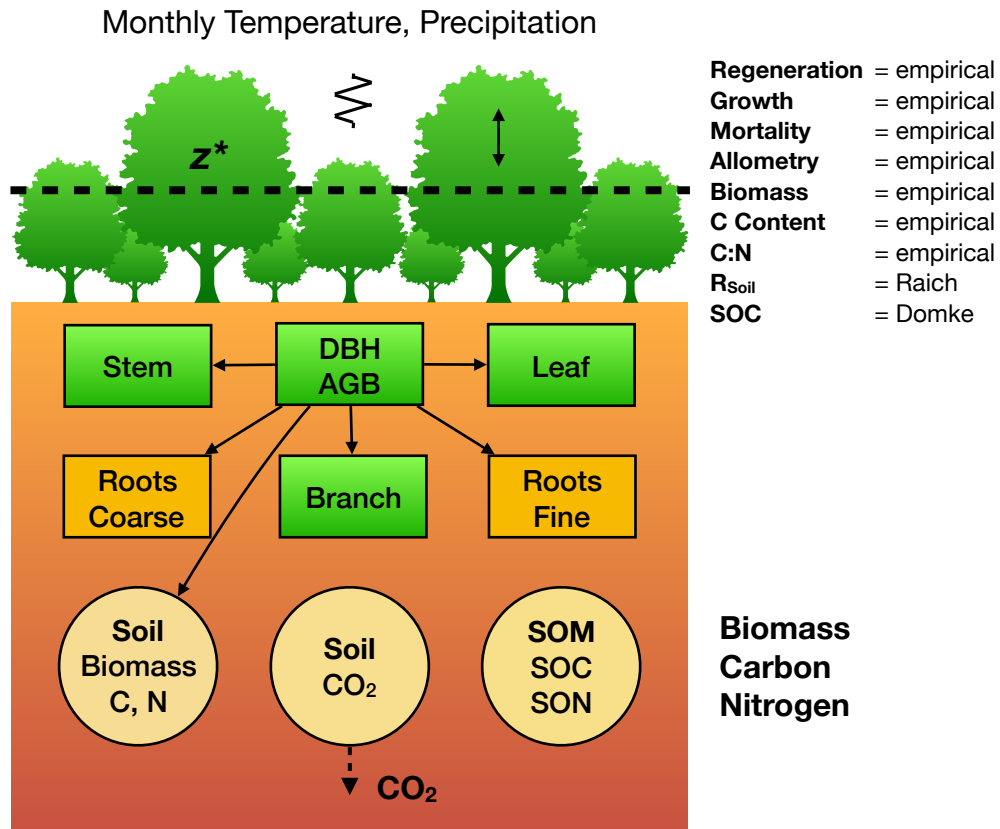


Figure 2. Perfect Plasticity Approximation with Simple Biogeochemistry (PPA-SiBGC) model structure; Raich et al. [116]; Domke et al. [117].

2.2. Site Descriptions

In the following sections, we describe the two forested sites on the East Coast of the United States: HF-EMS and the JERC-RD. A critical factor in the selection of the sites was the availability of eddy covariance flux tower data needed to validate NEE in the models.

2.2.1. HF-EMS

The HF-EMS EC flux tower is located within the Little Prospect Hill tract of Harvard Forest (42.538° N, 72.171° W, 340 m elevation) in Petersham, Massachusetts, approximately 100 km from the city of Boston [88]. A map of the site is shown in Figure 3. The tower has been recording NEE, heat, and meteorological measurements since 1989, with continuous measurements since 1991, making it the longest-running eddy covariance measurement system in the world. The site is currently predominantly deciduous broadleaf second-growth forests approximately 75–95 years in age, based on previous estimates [120]. Soils at Harvard Forest originate from sandy loam glacial till and are reported to be mildly acidic [88].

The site is dominated by red oak (*Quercus rubra* L.) and red maple (*Acer rubrum* L.) stands, with sporadic stands of Eastern hemlock (*Tsuga canadensis* (L.) Carrière), white pine (*Pinus strobus* L.), and red pine (*Pinus resinosa* Ait.). When the site was established, it contained 100 Mg C ha^{-1} in live aboveground woody biomass [120]. As noted by Urbanski et al. [88], approximately 33% of red oak stands were established prior to 1895, 33% prior to 1930, and 33% before 1940. A relatively hilly and undisturbed forest (since the 1930s) extends continuously for several km² around the tower. In 2000, harvest operations removed $22.5 \text{ Mg C ha}^{-1}$ of live aboveground woody biomass about 300 m S-SE from the tower, with little known effect on the flux tower measurements. The 40 biometric plots were designated via stratified random sampling within eight 500 m transects Urbanski et al. [88]. The HF-EMS tower site currently

contains 34 biometric plots at 10 m radius each, covering 10,681 m², or approximately one hectare, in area. Summary statistics for the EMS tower site for the year 2002 are provided in Table 1.

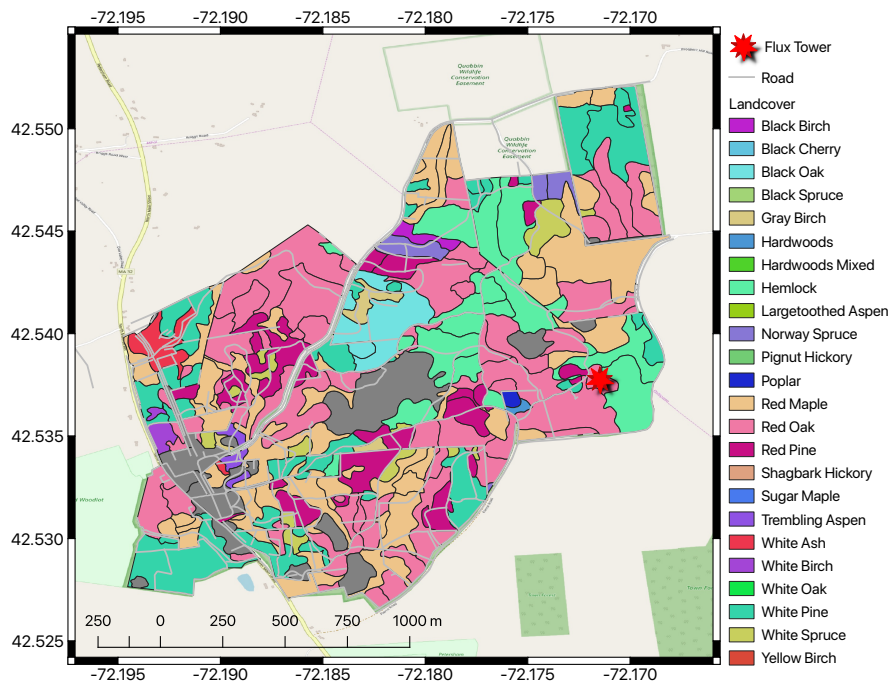


Figure 3. Harvard Forest (HF) EMS flux tower and landcover classes.

Table 1. HF-EMS forest inventory summary for the 34 tower plots in 2002; DBH = depth at breast height (cm); BA = basal area per hectare (m²); Stocking = *n_{trees}* per hectare; QMD = quadratic mean diameter (cm); SDI = Reineke's stand density index [121].

Statistic	N	Mean	St. Dev.	Min	Pctl(25)	Pctl(75)	Max
DBH _{Mean}	34	24.64	3.50	17.32	22.39	27.13	31.97
DBH _{St.Dev.}	34	10.92	2.74	6.11	8.60	12.51	16.88
BA	34	35.29	11.55	13.78	25.98	42.34	57.31
Stocking	34	639.43	232.38	318.31	421.76	787.82	1145.92
QMD	34	26.87	4.00	18.34	23.91	29.64	34.39
SDI	34	680.13	214.45	280.56	531.35	853.97	1071.37

A table of observed species abundances for the year 2002 are provided in Table 2, using tree species codes from the USDA PLANTS database (<https://plants.usda.gov>).

Previous research at the EMS EC flux tower site found unusually high rates of ecosystem respiration in winter and low rates in mid-to-late summer compared to other temperate forests [122]. While the mechanisms behind these observed patterns remains poorly understood, this observation is outside the scope of the presented research. Between 1992 and 2004, the site acted as a net carbon sink, with a mean annual uptake rate of 2.5 Mg C ha⁻¹ year⁻¹. Aging dominated the site characteristics, with a 101–115 Mg C ha⁻¹ increase in biomass, comprised predominantly of growth of red oak (*Quercus rubra*). The year 1998 showed a sharp decline in net ecosystem exchange (NEE) and other metrics, recovering thereafter [88]. As Urbanski et al. [88] note of the Integrated Biosphere Simulator 2 (IBIS2) and similar models at the time, “the drivers of interannual and decadal changes in NEE are long-term increases in tree biomass, successional change in forest composition, and disturbance events, processes not well represented in current models.” The two models used in the intercomparison study,

a SORTIE-PPA [46,47] variant and LANDIS-II with NECN succession [87,101], are intended to directly address these model shortcomings.

Table 2. HF-EMS species abundance for the 34 tower plots in 2002.

Species	Count
ACPE	56
ACRU	4924
BEAL	729
BELE	239
BEPO	116
CADE	1
FAGR	277
FRAM	258
ILVE	86
PIGL	397
PIRE	638
PIST	582
PRSE	270
QURU	2485
QUVE	247
TSCA	1926

2.2.2. JERC-RD

Jones Ecological Research Center at Ichauway is located near Newton, Georgia, USA (31° N, 84° W, 25–200 m elevation). A map of the JERC-RD flux tower with landcover classes is shown in Figure 4. The site falls within the East Gulf Coastal Plain and consists of flat to rolling land sloping to the southwest. The region is characterized by a humid subtropical climate with temperatures ranging from 5–34 °C and precipitation averaging 132 cm year⁻¹. The overall site is 12,000 ha in area, 7500 ha of which are forested [123]. The site also exists within a tributary drainage basin that eventually empties into the Flint River. Soils here are underlain by karst Ocala limestone and mostly Typic Quartzipsamments, with sporadic Grossarenic and Aquic Arenic Paleudults [124]. Soils here often lack well-developed organic horizons [123–125].

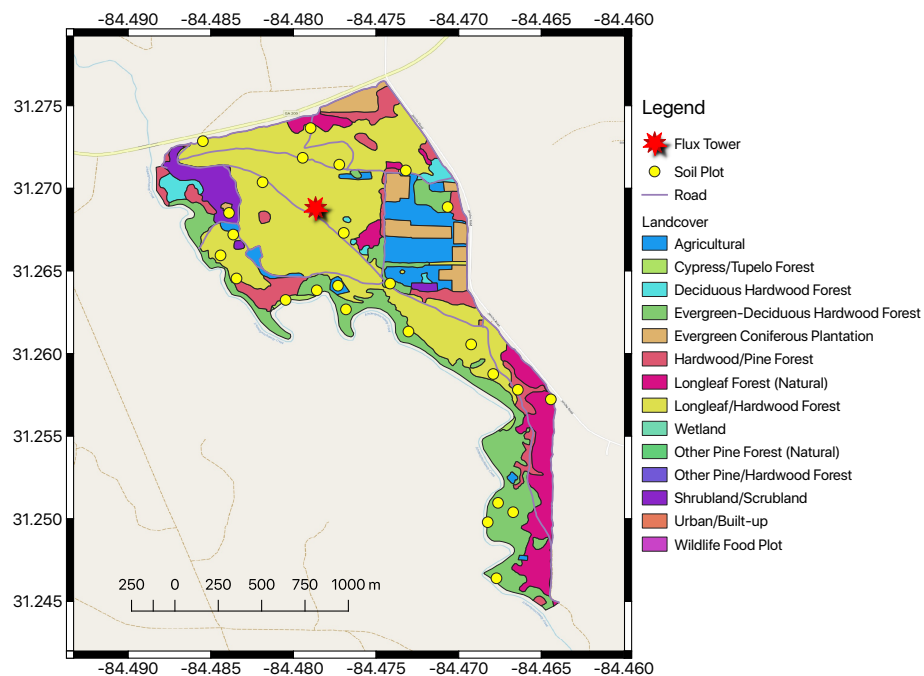


Figure 4. Jones Ecological Research Center (JERC) RD flux tower and landcover classes.

Forests here are mostly second-growth, approximately 65–95 years in age. Long-leaf pine (*Pinus palustris* Mill.) dominates the overstory, while the understory is comprised primarily of wiregrass (*Aristida stricta* Michx.) and secondarily of shrubs, legumes, forbs, immature hardwoods, and regenerating long-leaf pine forests [126]. Prescribed fire is a regular component of management here, with stands often burned at regular 1–5 year intervals [123]. This has promoted wiregrass and legumes in the understory, while reducing the number of hardwoods [123]. The RD EC flux tower is contained within the mesic/intermediate sector. This site consists of only four primary tree species from two genera: Long-leaf pine (*Pinus palustris*), water oak (*Quercus nigra* L.), southern live oak (*Quercus virginiana* Mill.), and bluejack oak (*Quercus incana* W. Bartram). Measurements for the RD tower are available for the 2008–2013 time period. Summary statistics for the RD tower site for the year 2008 are provided in Table 3.

Table 3. JERC-RD forest inventory summary for the four tower plots in 2009; DBH = depth at breast height (cm); BA = basal area per hectare (m^2); Stocking = n_{trees} per hectare; QMD = quadratic mean diameter (cm); SDI = Reineke's stand density index [121].

Statistic	N	Mean	St. Dev.	Min	Pctl(25)	Pctl(75)	Max
DBH _{Mean}	4	31.498	2.870	27.426	30.530	33.392	33.719
DBH _{St.Dev.}	4	12.733	2.737	10.525	11.293	13.285	16.714
BA	4	17.604	1.662	15.764	16.780	18.273	19.756
Stocking	4	201.000	60.871	164	170	205	292
QMD	4	33.968	3.374	29.350	32.665	35.987	37.152
SDI	4	310.965	39.514	278.001	291.255	318.514	368.254

A table of observed species abundances for the year 2009 are provided in Table 4.

Table 4. JERC-RD species abundance for the four tower plots in 2009.

Species	Count
PIPA	2063
QUIN	14
QUNI	22
QUVI	66

Two recent studies [127,128] indicate that the mesic sector of this subtropical pine savanna functions as a moderate carbon sink ($\text{NEE} = -0.83 \text{ Mg C ha}^{-1} \text{ year}^{-1}$; $-1.17 \text{ Mg C ha}^{-1} \text{ year}^{-1}$), reduced to near-neutral uptake during the 2011 drought ($\text{NEE} = -0.17 \text{ Mg C ha}^{-1} \text{ year}^{-1}$), and is a carbon source when prescribed burning is taken into account. NEE typically recovered to pre-fire rates within 30–60 days. The mechanisms behind soil respiration rates here again appear to be complex, site-specific, and poorly understood [128].

Overall, existing research highlights the importance of fire and drought to carbon exchange in long-leaf pine (*Pinus palustris*) and oak (*Quercus spp.*) savanna systems [127–129] at JERC. This is in contrast to the secondary growth-dominated deciduous broadleaf characteristics of Harvard Forest. Species diversity at the EMS tower site is 350% greater than that of the JERC-RD site, with 14 species from a variety of genera compared to four species from only two genera, *Pinus* and *Quercus*.

2.3. Site Data

Data collection methods may be accessed through the below data provider websites. Both sites provided a metadata file along with each data file, as is typically available to data users for the two sites. To conduct this model intercomparison exercise at HF-EMS, we leveraged the large amount of data openly available to the public through the Harvard Forest Data Archive:

<http://harvardforest.fas.harvard.edu/harvard-forest-data-archive>

Data were collected here for a range of studies, as evidenced by the Harvard Forest Data Archive. Datasets used in model validation include HF001-04, HF004-02, HF069-09, HF278-04, HF069-06, HF015-05, HF006-01, and HF069-13. These include weather station and forest inventory time-series, eddy covariance flux tower measurements, soil respiration, soil organic matter, and studies on C:N stoichiometry. Standard measurement techniques were used for each. For both sites, local tree species, age, depth-at-breast-height (DBH), biomass, soil, and meteorological data were primarily used to parameterize the models.

The Jones Ecological Research Center has hosted multiple research efforts over the years, collectively resulting in the collection of a large data library. However, JERC-RD site data are not made openly available to the public and are thus only available by request. One may find contact information located within their website:

<http://www.jonesctr.org>

Datasets used in model validation at JERC-RD include JC010-02, JC010-01, JC003-04, JC004-01, JC003-07, and JC011-01. These include weather station and eddy covariance flux tower measurements, forest inventory data, soil respiration, soil organic matter, and studies on C:N stoichiometry. Standard measurement techniques were also used for each of these.

2.4. Scales, Metrics, and Units

The selection of simulation years was based on the availability of EC flux tower data used in model validation. Thus, we simulated the HF-EMS site for the years 2002–2012 and the JERC-RD site for the years 2009–2013. For both sites and models, we initialized the model state in the first year of

simulations using field observations. The PPA-SiBGC model used an annual timestep while LANDIS-II NECN used a monthly timestep internally. Both models may be set to other timesteps if desired.

The areal extent of the single-site model intercomparisons were designed to correspond to available field measurements. At both sites, tree inventories were conducted in 10,000 m², or one-hectare, areas. All target metrics were converted to an annual areal basis to ease interpretation, comparison, and transferability of results. Importantly, an areal conversion will allow comparison to other sites around the world. While flux tower measurements for both sites were already provided on an areal (m⁻²) basis, many other variables were converted to harmonize metrics between models and study sites. For example, moles CO₂ measurements were converted to moles C through well-described molecular weights, all other measures of mass were converted to kg, and all areal and flux measurements were harmonized to m⁻². A table of metrics and units used in the intercomparison of LANDIS-II and PPA-SiBGC is provided in Table 5.

Table 5. Model intercomparison abbreviations, metrics, and units.

Abbreviation	Metric	Units
NEE	Net ecosystem exchange	kg C m ⁻² year ⁻¹
B _{AG}	Aboveground biomass	kg mass m ⁻²
C _{AG}	Aboveground C	kg C m ⁻²
N _{AG}	Aboveground N	kg N m ⁻²
B _{BG}	Belowground biomass	kg mass m ⁻²
C _{BG}	Belowground C	kg C m ⁻²
N _{BG}	Belowground N	kg N m ⁻²
C _{SO}	Soil organic C	kg C m ⁻²
N _{SO}	Soil organic N	kg N m ⁻²
r _{soil}	Soil respiration C	kg C m ⁻² year ⁻¹
ANPP	Aboveground net primary production	kg mass m ⁻² year ⁻¹
B _{Sp}	Species aboveground biomass	kg mass m ⁻²
n _{Sp}	Species relative abundance	%

In the subsequent section, we describe the model intercomparison methodology.

2.5. Model Intercomparison

Intercomparison of the PPA-SiBGC and LANDIS-II models at the HF-EMS and JERC-RD EC flux tower sites was conducted using a collection of object-oriented functional programming scripts written in the R language for statistical computing [83]. These scripts were designed to simplify model configuration, parameterization, operation, calibration/validation, plotting, and error calculation. The scripts and our parameters are available on GitHub (<https://github.com/adam-erickson/ecosystem-model-comparison>), making our results fully and efficiently reproducible. The directory structure of the repository is shown in Figure S1 in the Supplementary Materials. The R scripts are also designed to automatically load and parse the results from previous model simulations, in order to avoid reproducibility issues stemming from model stochasticity. We use standard regression metrics applied to the time-series of observation and simulation data to assess model fitness. The metrics used include the coefficient of determination (R^2), root mean squared error (RMSE), mean absolute error (MAE), and mean error (ME) or bias, calculated using simulated and observed values. Our implementation of R^2 follows the Bravais–Pearson interpretation as the squared correlation coefficient between observed and predicted values [130]. This implementation is provided in Equation (2).

$$R^2 = r^2 = \left(\frac{\sum_{i=1}^n (y_i - \bar{y})(\hat{y}_i - \bar{\hat{y}})}{\sqrt{\sum_{i=1}^n (y_i - \bar{y})^2(\hat{y}_i - \bar{\hat{y}})^2}} \right)^2 \quad (2)$$

where n is the sample size, y_i is the i th observed value, \hat{y}_i is the i th predicted value, \bar{y} is the mean observed value, and $\bar{\hat{y}}$ is the mean predicted value. The calculation of RMSE follows the standard formulation, as shown in Equation (3).

$$\text{RMSE} = \sqrt{\frac{1}{n} \sum_{t=1}^n e_t^2} \quad (3)$$

where n is the sample size and e_t is the error for the t th value, or the difference between observed and predicted values. The calculation of MAE is similarly unexceptional, per Equation (4).

$$\text{MAE} = \frac{1}{n} \sum_{t=1}^n |e_t| \quad (4)$$

where again n is the sample size and e_t is the error for the t th value. Our calculation of mean error (ME) or bias is the same as MAE, but without taking the absolute value.

While Nash–Sutcliffe efficiency (NSE) is often used in a simulation model context, we selected the Bravais–Pearson interpretation of R^2 over NSE to simplify the interpretation of results. The NSE metric replaces $1 - (SS_{\text{predictions}} / SS_{\text{observations}})$ with $(SS_{\text{observations}} - SS_{\text{predictions}}) / SS_{\text{observations}}$, where SS is the sum of squares. Thus, NSE is analogous to the standard R^2 coefficient of determination used in regression analysis [131]. The implementation of R^2 that we selected is important to note, as its results are purely correlative and quantify only dispersion, ranging in value between zero and one. This has some desirable properties in that no negative or large values are produced, and that it is insensitive to differences in scale. Regardless of the correlation metric used, complementary metrics are needed to quantify the direction (i.e., bias) and/or magnitude of error. We rely on RMSE and MAE to provide information on error or residual magnitude, and ME to provide information on bias. We utilize a visual analysis to assess error directionality over time, as this can be poorly characterized by a single coefficient, masking periodicity.

We compute R^2 , RMSE, MAE, and ME for time-series of the metrics described in Table 5 on page 13. These include NEE, above- and below-ground biomass, C, and N, soil organic C and N, soil respiration (r_{soil}), aboveground net primary production (ANPP), and, species aboveground biomass and relative abundance. All of these metrics are pools with the exception of NEE, r_{soil} , and ANPP fluxes. Finally, we diagnose the ability of both models to meet a range of logistical criteria related to deployment: Model usability, performance, and transferability. Model usability is assessed per four criteria:

1. Ease of installation
2. Ease of parameterization
3. Ease of program operation
4. Ease of parsing outputs

Model software performance is assessed per a single metric: The speed of program execution for each site for the predefined simulation duration. The durations are 11 years and five years for the HF-EMS and JERC-RD EC flux tower sites, respectively. Simulation results are output at annual temporal resolution, the standard resolution for both models, while NECN operates on a monthly timestep, and most other modules of LANDIS-II are annual. Finally, model transferability is assessed per the following five criteria:

1. Model generalizability
2. Availability of parameterization data
3. Size of the program
4. Cross-platform support
5. Ease of training new users

Each of these logistical criteria are compared in a qualitative analysis, with the exception of software performance.

3. Results

Both PPA-SiBGC and LANDIS-II NECN showed strong performance for pools at the two model intercomparison sites, frequently achieving R^2 values approaching unity. Yet, both models showed weak performance for fluxes. The models failed to accurately predict ANPP, while PPA-SiBGC showed stronger r_{soil} performance and LANDIS-II NECN showed stronger NEE performance. The R^2 values for both models and sites are visualized in Figure 5.

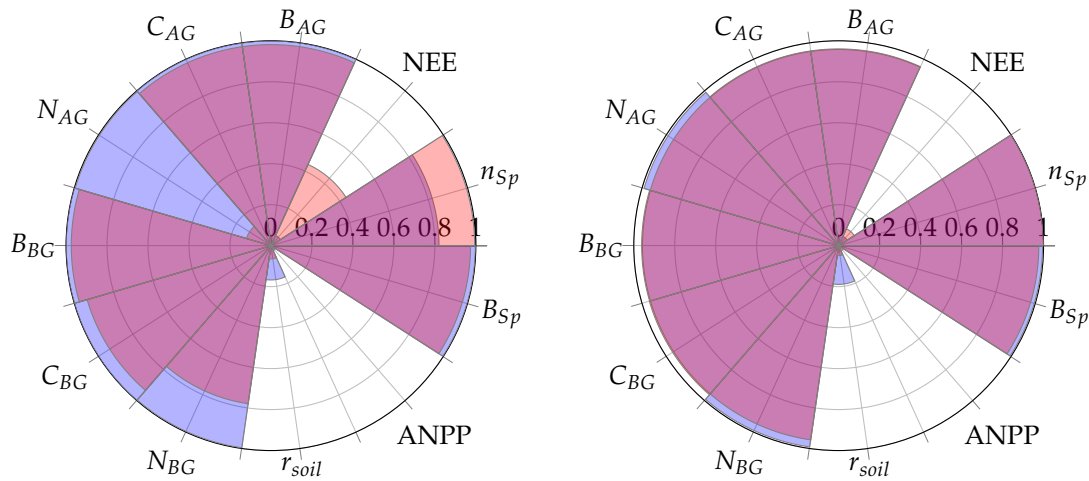


Figure 5. Overall model performance (R^2) for both models and sites; left = HF-EMS; right = JERC-RD; periwinkle = PPA-SiBGC; pink = LANDIS-II NECN; violet = intersection.

On average, PPA-SiBGC outperformed LANDIS-II NECN across the sites and metrics tested, showing higher correlations, lower error, and less bias overall (HF-EMS $\bar{R^2} = 0.73, +0.07$, $\bar{RMSE} = 4.68, -9.96$, $\bar{ME} = -0.84, -5.96$; JERC-RD $\bar{R^2} = 0.73, +0.01$, $\bar{RMSE} = 2.18, -1.64$, $\bar{ME} = 1.33, +1.03$). This result is based on calculating mean values for R^2 , RMSE, MAE, and ME in order to clearly translate the overall results. The two models produced the following mean values for each of the four statistical metrics and two sites:

As shown in Table 6, PPA-SiBGC yielded higher R^2 values and lower RMSE, MAE, and ME values in comparison to LANDIS-II, on average, across all sites and metrics tested. Below, we provide model intercomparison results individually for the two sites, HF-EMS and JERC-RD.

Table 6. Overall mean values across each of the sites and metrics tested.

Metric	PPA-SiBGC				LANDIS-II NECN			
	R^2	RMSE	MAE	ME	R^2	RMSE	MAE	ME
Mean	0.73	3.43	3.24	0.24	0.69	9.23	8.36	2.71

3.1. HF-EMS

For the HF-EMS site, PPA-SiBGC showed higher R^2 values and lower RMSE, MAE, and ME values compared to LANDIS-II NECN across the range of metrics. While PPA-SiBGC predicted NEE and species relative abundance showed weaker correlations with observed values compared to LANDIS-II NECN, the magnitude of error was lower, as evidenced by lower RMSE, MAE, and ME values. While LANDIS-II NECN showed a lower magnitude of error for belowground N, this is the only metric where this is the case, while the correlation of this metric to observed values was also lower than that of PPA-SiBGC. Overall results for the HF-EMS site model intercomparison are shown in Table 7.

Table 7. Model fitness for HF-EMS.

Metric	PPA-SiBGC				LANDIS-II NECN			
	R ²	RMSE	MAE	ME	R ²	RMSE	MAE	ME
NEE	0.05	0.78	0.76	0.76	0.44	0.49	0.44	0.44
B _{AG}	1.00	10.31	10.30	10.30	0.98	2.48	2.48	-2.48
C _{AG}	1.00	0.05	0.05	0.05	0.98	1.24	1.24	-1.24
N _{AG}	1.00	1.44	1.44	-1.44	0.12	1.99	1.99	-1.99
B _{BG}	1.00	9.25	9.25	9.25	0.97	2.82	2.82	-2.82
C _{BG}	1.00	4.92	4.92	-4.92	0.94	6.99	6.99	-6.99
N _{BG}	1.00	0.56	0.56	0.56	0.78	0.12	0.12	-0.12
r _{soil}	0.17	0.63	0.62	-0.62	0.06	1.10	1.10	-1.10
ANPP	0.03	0.01	0.01	-0.01	0.0002	0.97	0.93	0.90
C _{SO}	...	26.49	26.49	-26.49	...	36.63	36.63	-36.63
N _{SO}	...	1.33	1.33	-1.33	...	1.60	1.60	-1.60
B _{Sp}	1.00	5.07	2.92	2.92	0.97	133.70	119.87	119.87
n _{Sp}	0.82	0.05	0.03	0	0.99	0.29	0.22	0.22
Mean	0.73	4.68	4.51	-0.84	0.66	14.65	13.57	5.11

Time-series figures allow a visual analysis of the temporal dynamics between observations and model predictions in order to assess the ability of models to capture interannual variability in carbon exchange. Both models effectively captured integrals of dynamics in biomass, C, and, species biomass and abundance. In Figure 6, the temporal differences in modeled NEE, aboveground C, ANPP, and soil respiration are shown for the two models in comparison to observations for the HF-EMS site. LANDIS-II NECN predicted NEE showed a higher correlation with observations while the magnitude of error and bias were lower. Furthermore, LANDIS-II NECN predicted that the HF-EMS site is a net C source, rather than sink, in contrary to observations. Meanwhile, PPA-SiBGC outperformed LANDIS-II NECN in aboveground C per both R² and RMSE. Both models overpredicted species cohort biomass, while LANDIS-II NECN underpredicted total aboveground C.

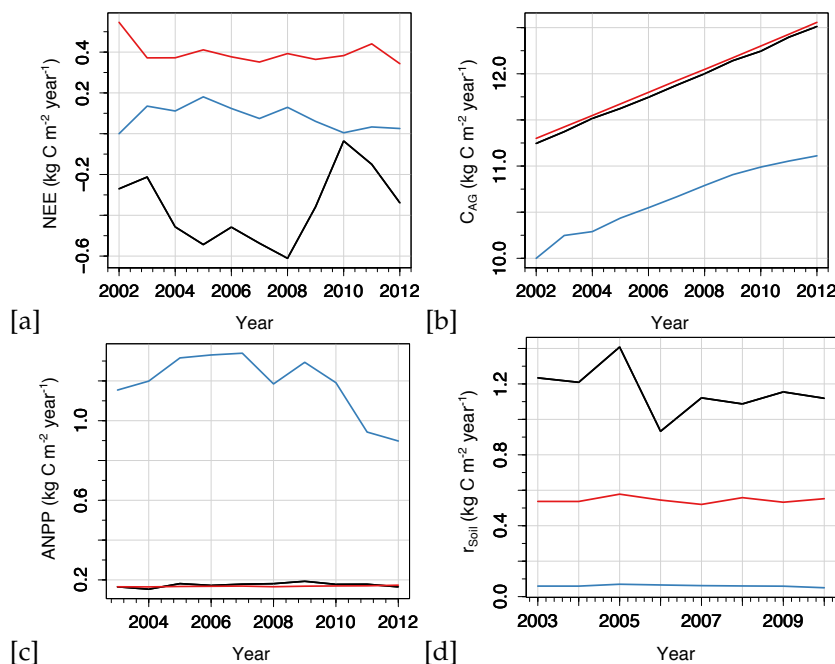


Figure 6. Simulated and observed NEE, C_{AG}, ANPP, and r_{Soil} for the HF-EMS site; black = observations; red = PPA-SiBGC; blue = LANDIS-II NECN; (a) = NEE; (b) = C_{AG}; (c) = ANPP; (d) = r_{Soil}.

An analysis of simulated species biomass and abundance also shows greater fidelity of the PPA-SiBGC model to data, as shown in Figure 7. As LANDIS-II NECN does not contain data on individual trees, species relative abundance is calculated based on the number of cohorts of each species. Two species were simulated in LANDIS-II NECN, as there are no explicit trees in the model and the number of cohorts appears to have no effect on the total biomass. Results for PPA-SiBGC indicate that species relative abundance may be improved in future studies by optimizing mortality and fecundity rates. Meanwhile, species biomass predictions output by LANDIS-II NECN were inverted from those of the observations.

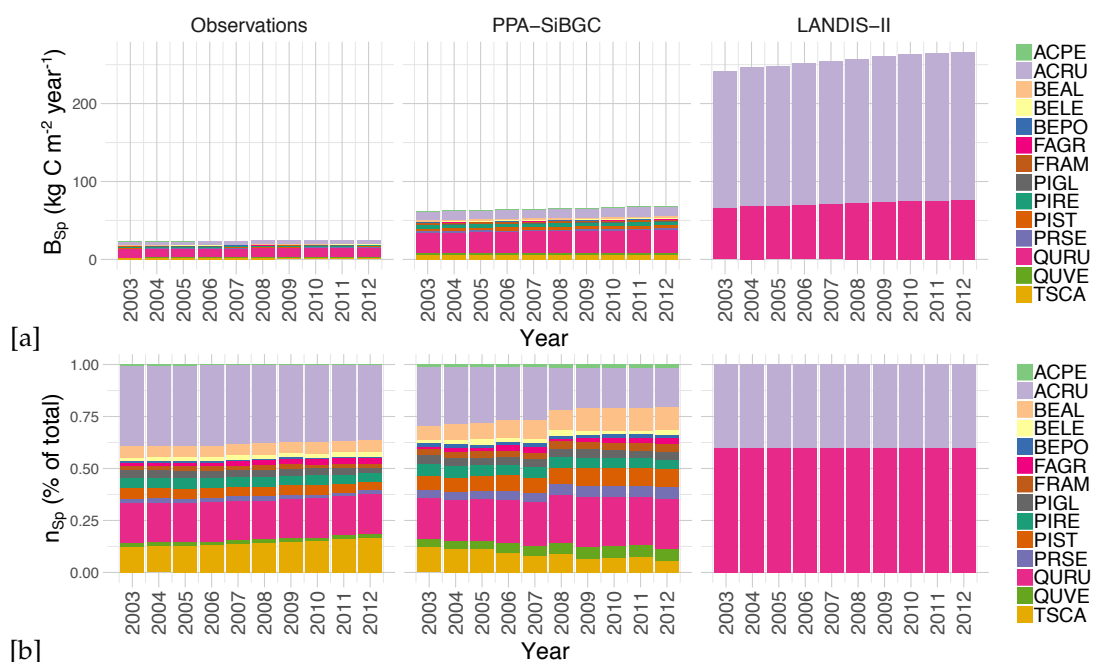


Figure 7. HF-EMS: Simulated and observed species aboveground biomass and relative abundance; (a) = biomass; (b) = abundance; left = observations, middle = PPA-SiBGC, right = LANDIS-II NECN; note that different scales are used for biomass.

3.2. JERC-RD

For the JERC-RD site, both models showed stronger fidelity to data than for the HF-EMS site. Again, PPA-SiBGC showed higher R^2 values and lower RMSE and MAE values compared to LANDIS-II NECN across the range of metrics tested. Yet, the margin between models was smaller for the JERC RD site. While PPA-SiBGC demonstrated higher correlations and lower errors for most metrics tested, LANDIS-II NECN outperformed PPA-SiBGC in a few cases. This includes a higher correlation for NEE, ANPP, and lower magnitude of error for aboveground N, belowground biomass, soil respiration, and SOC. PPA-SiBGC, however, showed correlations equal or higher for all metrics tested, and lower errors for all other metrics. Overall results for the JERC-RD site model intercomparison are shown in Table 8.

Table 8. Model fitness for JERC-RD.

Metric	PPA-SiBGC				LANDIS-II NECN			
	R ²	RMSE	MAE	ME	R ²	RMSE	MAE	ME
NEE	0.05	0.12	0.11	0.05	0.09	0.13	0.11	-0.05
B _{AG}	0.96	1.48	1.47	1.47	0.96	9.77	9.76	-9.76
C _{AG}	0.96	1.63	1.63	-1.63	0.96	4.88	4.88	-4.88
N _{AG}	0.99	0.29	0.29	0.29	0.96	0.05	0.05	-0.05
B _{BG}	0.96	10.84	10.83	10.83	0.96	1.37	1.20	1.20
C _{BG}	0.96	0.25	0.25	0.25	0.96	0.96	0.95	-0.95
N _{BG}	0.99	1.44	1.44	-1.44	0.96	1.60	1.60	-1.60
r _{soil}	0.19	0.98	0.97	-0.97	0.05	0.90	0.90	-0.90
ANPP	0.00	0.12	0.10	-0.10	0.03	0.62	0.60	0.49
C _{SO}	...	4.30	4.30	4.30	...	0.17	0.17	-0.17
N _{SO}	...	0.38	0.38	0.38	...	0.12	0.12	0.12
B _{Sp}	1.00	6.47	3.90	3.90	0.98	28.97	20.52	20.52
n _{Sp}	1.00	0.02	0.01	0	1.00	0.09	0.09	-0.02
Mean	0.73	2.18	1.98	1.33	0.72	3.82	3.15	0.30

Time-series carbon exchange metrics for the JERC-RD site, presented in Figure 8, show that modeled NEE values are positively correlated with each other rather than with observed NEE, while the magnitude of error varies from favoring PPA-SiBGC to LANDIS-II NECN. Overall, the PPA-SiBGC model shows a lower magnitude of error for NEE, ANPP, and C_{AG}, and slightly higher for r_{soil}. Again, for r_{soil} the two models show strong agreement, but underestimate observations by an order of magnitude. For C_{AG} and ANPP, PPA-SiBGC shows good overall fit.

While both models showed higher performance at the JERC-RD site in comparison to the HF-EMS site, an analysis of simulated species biomass and abundance again indicates greater fidelity of the PPA-SiBGC model to data, as shown in Figure 9. While LANDIS-II NECN greatly overpredicts the rate of longleaf pine growth, PPA-SiBGC matches observed species abundance and biomass trajectories for all species present. While the correlations are high, PPA-SiBGC overpredicts the magnitude of species biomass.

Our results for the HF-EMS and JERC-RD site model intercomparison exercise show strong performance for both models at both sites. Results for the JERC-RD site are particularly close between the two models. Next, we assess results related to the logistics of model deployment to new computers, users, and modeling sites.

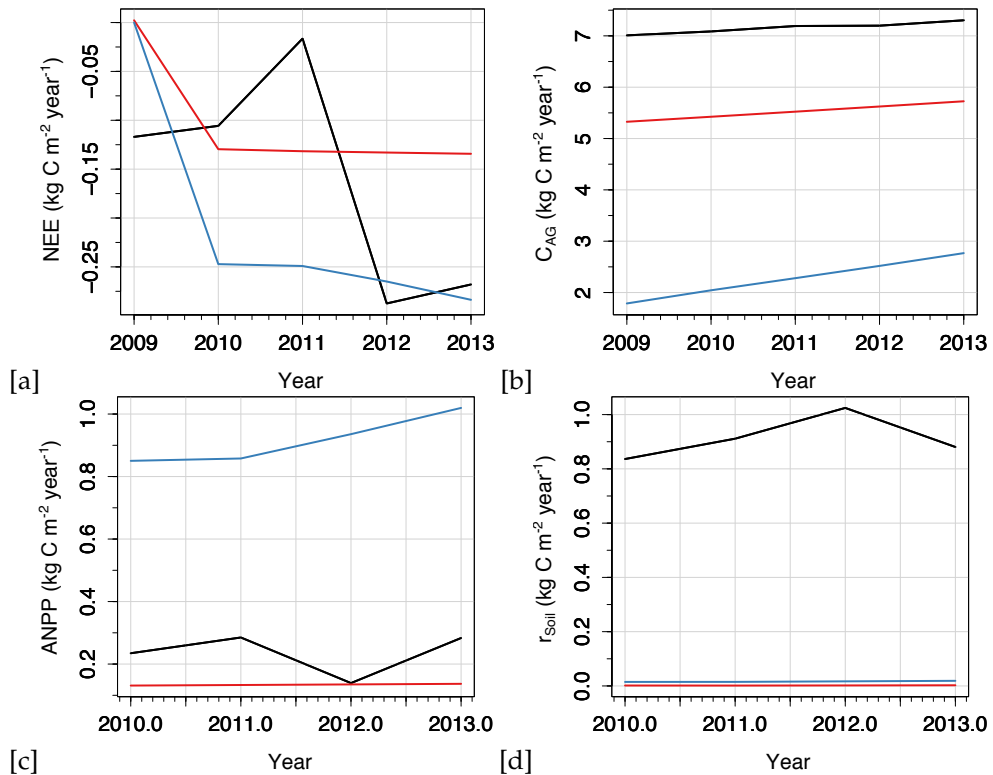


Figure 8. Simulated and observed NEE, C_{AG} , ANPP, and r_{Soil} for the JERC-RD site; black = observations; red = PPA-SiBGC; blue = LANDIS-II NECN; (a) = NEE; (b) = C_{AG} ; (c) = ANPP; (d) = r_{Soil} .

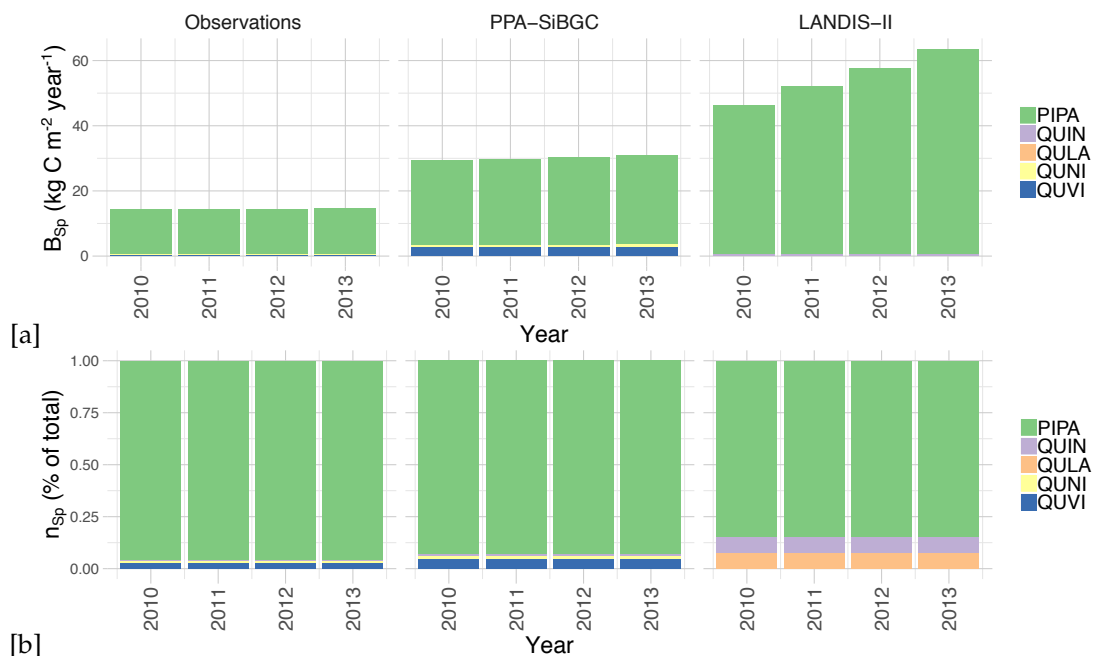


Figure 9. JERC-RD: Simulated and observed species aboveground biomass and relative abundance; (a) = biomass; (b) = abundance; left = observations, middle = PPA-SiBGC, right = LANDIS-II NECN; note that different scales are used for biomass.

3.3. Model Usability, Performance, and Transferability

While the two models share a similar basis in forest dynamics and biogeochemistry modeling, they differ in important practical and conceptual terms. The command-line version of the PPA-SiBGC model used in this work, version 5.0, consists of approximately 500 lines of R code and is thus readily

cross-platformed and portable. Meanwhile, the LANDIS-II model core and NECN succession extension are an estimated 2000 and 0.5 million lines of code, respectively. While this version of PPA-SiBGC fuses an explicit tree canopy geometry model with empirical data on fecundity, growth, mortality, and stoichiometry, the NECN extension of LANDIS-II borrows heavily from the process-based Century model [37], similar to the MAPSS-Century-1 (MC1) model [132]. This carries important implications for model parameterization needs. While PPA-SiBGC relies on typical forest inventory data, including tree species, age/size, and densities, LANDIS-II relies on species age/size and traits in the form of vital attributes, in addition to approximately 100 NECN parameters. Below, we summarize our findings regarding the logistics of model deployment.

3.3.1. Model Usability

In the following section, we provide an assessment of model usability based on four criteria.

1. *Ease of installation*

While LANDIS-II NECN requires the installation of two Windows programs, depending on the options desired, PPA-SiBGC is contained in a single R script and requires only a working R installation.

2. *Ease of parameterization*

While both models can be difficult to parameterize for regions with little to no observational data, the simple biogeochemistry in PPA-SiBGC requires an order of magnitude fewer parameters than LANDIS-II NECN. In addition, PPA-SiBGC uses commonly available forest inventory data while NECN requires a number of parameters that may be difficult to locate.

3. *Ease of program operation*

Both models use a command-line interface and are thus equally easy to operate. Yet, PPA-SiBGC is cross-platform and uses comma-separated-value (CSV) files for input tables, which are easier to work with than multiple tables nested within an unstructured text files. This additionally allows for simplification in designing model application programming interfaces (APIs), or model wrappers, a layer of abstraction above the models. These abstractions are important for simplifying model operation and reproducibility, and enable a number of research applications.

4. *Ease of parsing outputs*

All PPA-SiBGC outputs are provided in CSV files in a single folder while LANDIS-II NECN generates outputs in multiple formats in multiple folders. While the PPA-SiBGC format is simpler and easier to parse, the image output formats used by LANDIS-II carry considerable benefit for spatial applications. Both models may benefit by transitioning spatiotemporal data to the NetCDF scientific file format used by most general circulation and terrestrial biosphere models.

3.3.2. Model Performance

Next, we assess model performance in terms of the speed of operation on a consumer-off-the-shelf (COTS) laptop computer with a dual-core 2.8 GHz Intel Core i7-7600U CPU and 16 GB of DDR4-2400 RAM. We focus on a single performance metric, the timing of simulations. Other aspects of model performance in the form of precision and accuracy are described in previous sections. As shown in Table 9, PPA-SiBGC was between 1200 and 2800% faster than LANDIS-II NECN in our timing tests. This was surprising given that PPA-SiBGC models true cohorts (i.e., individual trees) in an interpreted language while LANDIS-II models theoretical cohorts (i.e., cohorts without a physical basis) in a compiled language. The difference in speed is likely attributable to the parsimony of the PPA-SiBGC model.

Table 9. Simulation timing results.

Site	Model	Duration (years)	Elapsed (s)
HF-EMS	PPA-SiBGC	11	8.51
HF-EMS	LANDIS-II NECN	11	101.15
JERC-RD	PPA-SiBGC	5	2.25
JERC-RD	LANDIS-II NECN	5	61.51

3.3.3. Model Transferability

Here, we discuss model transferability. In this section, we assess the effort required to transfer the models to new locations, new computer systems, or new users. All three are important logistical criteria for effective model deployment.

1. *Model generalization*

Both models appear to generalize effectively to different forested regions of the world, as both have shown strong performance in this study and others. No clear winner is evident in this regard. In terms of model realism, PPA-SiBGC has a more realistic representation of forest canopies while LANDIS-II NECN has more realistic processes, as it is a Century model variant.

2. *Availability of parameterization data*

While LANDIS-II NECN requires substantially greater parameterization data compared to PPA-SiBGC, it may often be possible to rely on previously published parameters. Meanwhile, the growth, mortality, and fecundity parameters used by PPA-SiBGC are easy to calculate using common field inventory data. PPA-SiBGC is simpler to transfer in this regard given the wide availability of forest inventory data.

3. *Size of the program*

PPA-SiBGC is approximately 500 lines of R code, while LANDIS-II NECN is estimated at 0.5 million lines of C# code.

4. *Cross-platform support*

While Linux support may soon be supported with Microsoft .NET Core, LANDIS-II NECN is written in C# and is thus limited to Microsoft Windows platforms. Meanwhile, PPA-SiBGC is written in standard R code and is fully cross-platform.

5. *Ease of training new users*

While both models have a learning curve, the practical simplicity of PPA-SiBGC may make it easier to train new users. While LANDIS-II NECN contains more mechanistic processes and related parameters, these come at the cost of confusing new users. The model wrapper library we developed as part of this work vastly eases the operation of both models. Future studies should measure the time required for new users to effectively operate both models.

4. Discussion

First, it is important to clarify some terms used in this analysis. Gross primary production (GPP) is the net rate of carboxylation and oxygenation by RuBisCO and is calculated as $GPP = P_g - R_p$, where P_g is gross photosynthesis and R_p is photorespiration. In EC flux data analyses, GPP is also known as gross ecosystem exchange (GEE) or gross ecosystem production (GEP) and is often estimated inversely from NEE or NEP flux tower retrievals as $GPP = NEE - R_e$, where R_e is ecosystem respiration or the sum of auto- and heterotrophic respiration components. Thus, $R_e = R_m + R_g + R_h$ where R_m is maintenance respiration, R_g is autotrophic growth respiration, and R_h is heterotrophic respiration. While GPP is the total amount of C fixed by plants in photosynthesis, NPP subtracts autotrophic respiration (R_a) as $NPP = GPP - R_a$ where $R_a = R_g + R_m$. NEE or net ecosystem production (NEP) is then calculated as NPP minus heterotrophic respiration, or $NEE = NPP - R_h$, which is equivalent

to $\text{NEE} = \text{GPP} - R_e$. During the day, $\text{NEE} = P_g + R_p + R_m + R_g + R_h$ while during the night, P_g and R_p are absent, making NEE approximate to ecosystem respiration, or R_e . Traditionally, gross or net exchange of CO_2 into the forest is negative and fluxes into the atmosphere are positive, while each constituent process is discussed with a positive sign. Thus, NEE is often calculated as $\text{NEE} = R_e - \text{GPP}$ where each constituent flux term is always positive [133–137].

All this is to say that there exists much difficulty in relating NPP from field inventories and soil respiration samples directly to NEE from EC flux towers, integrated over the year. In our analyses, we assume that the observed annual biomass growth increment is equivalent to ANPP and that soil respiration (r_{soil}) is equivalent to ecosystem respiration (R_e), or $\text{NEE} = \text{NPP} - r_{\text{soil}}$. Yet, there are known error contributions at multiple conversion points, making the comparison of models based on field data and EC flux tower measurements difficult. For example, field inventory estimates of ANPP contain known sources of error in converting DBH to biomass, both above- and belowground [115], and there are additional errors in converting biomass to C based on a fixed fraction for each biomass compartment. Meanwhile, unlike R_e , r_{soil} does not account for R_g or R_m , only R_h . Even if these fluxes were approximately similar, spatial biases in the EC flux tower footprint or contributing area [138–142] may make field inventory and tower measurements difficult to harmonize.

As others have noted [118,119], including a previous study on flux measurements at the HF-EMS site [88], it is evident that treating ANPP as the C fraction of woody biomass increment per allometric relations from field data is a loose proxy for ecosystem ANPP, given its visible disconnection from observed NEE and r_{soil} fluxes. Given the definition of NEE, the relation between these variables should be approximately linear. While others have reported hysteresis between peaks in NEE and growth increment at the HF-EMS site [88], we did not see evidence of this dynamic. Instead, flux tower NEE appears to have little to no connection to field data ANPP and observed r_{soil} fluxes at both sites in this analysis. Nevertheless, both models showed good agreement with net changes to C and N pools. This may partially reflect difficulties in accounting for belowground processes, which can contribute disproportionately to C fluxes, and in connecting flux tower NEE to forest stands where the contributing area extent is far greater than a one-hectare stand, as is often the case [138–140].

This issue can be seen in Figures 6 and 8. In this model intercomparison exercise, ANPP for the PPA-SiBGC model and field data are based on annual woody biomass increment, while ANPP in LANDIS-II NECN includes the Century process model for estimating ANPP. Rather than this basis making the NECN model purely process-based or mechanistic, species-specific growth is tightly constrained by empirical limits in a truncated logistic curve, with LAI and the number of cohorts present used as a proxy for growing space limitations and moisture and temperature used for physiological constraint based on Liebig's Law of the Minimum. In contrast, PPA-SiBGC is parameterized with mean observed growth and mortality rates from field data, which vary depending on the canopy position of a cohort. Understory cohorts assumed to be in full shade face higher mortality and lower growth, as is widely evident in field data, while overstory cohorts assumed to be in full sunlight have higher growth and lower mortality rates. While soil and root processes are explicitly simulated in Century and thus LANDIS-II NECN, PPA-SiBGC relies on simple stoichiometric and allometric relations from field data to model these pools. In other words, PPA-SiBGC is designed primarily to model pools rather than fluxes, as the former are of generally higher interest to foresters.

The strong empirical basis of parameterization of both PPA-SiBGC and LANDIS-II NECN explains why the two models are often in better agreement with each other than with observations. The similarity of outputs from the two models is perhaps surprising, given their differences in model architecture and theoretical basis. This shows that, despite any mechanistic process present, both models in their current form are closely fit to field data and are therefore strongly empirical, as evidenced by their representation of growth processes. Meanwhile, this design choice limits the representation of fluxes in both models, as detailed process models are absent. This is expected for PPA-SiBGC, which is intended primarily to be a simple empirical pool model. This work also shows that observations between field and tower measurements are substantially disconnected. We estimate

that fluxes are poorly represented by both models because they are tightly coupled to field inventory data rather than to tower-based measurements. Hence, patterns evident in field inventory data are reliably reproduced while fluxes appear wholly uncoupled.

The advancement of processor architectures has facilitated the development of increasingly complex forest models. Each new generation of processors allows researchers to conduct large-scale simulations faster and more efficiently than previous designs. As a result, forest models have grown into large, complex, analytically intractable programs. Rigorous intercomparison of models developed by different research groups, as well as the diagnosis of new versions of established models, is therefore a critical step in further advancing ecosystem models. This ensures that models are properly diagnosed and compared in a consistent, reliable, and transparent manner. Too often, model intercomparisons are conducted by each separate research group applying their own model in a manner that is, at best, inconsistent and opaque. In this work, we extended our model intercomparison by further providing wrapper functions that may be used to benchmark additional models or sites through a unified modeling framework. This ensures the consistency and transparency of intercomparison results.

The presented research is intended to establish the groundwork for future model intercomparison studies at both sites in order to advance the design of new models. Furthermore, we hope that this work will inspire a new generation of forest model intercomparisons in North America, which are sorely absent. Forest models have proven to be a critical testbed for improving the representation of vegetation dynamics in global terrestrial biosphere models [40,41,143], given the importance of forests in the global carbon cycle and the increased detail of local- to regional-scale models. Model benchmarking datasets and related results should be publicly shared and regularly updated with version-controlled software repositories (e.g., GitHub or GitLab), as is commonplace in the machine learning research community. Cloud computing providers may provide full reproducibility for cases where compute is limiting. In general, there is a broad disparity between modern software tools and existing forest models.

One important new forest model in development is a next-generation model from the SORTIE-PPA family of models, known as SORTIE-NG. This new model combines mechanistic representations of demographic processes, energetic and biogeochemical fluxes, and landscape disturbance dynamics, using hierarchical multiscale modeling with a modular component-based software framework [144]. Along with LM3-PPA [45], SORTIE-NG is among the first of a new class of hybrid models that we term ‘cohort-leaf’ models for their partitioning of energetic and biogeochemical fluxes amongst dynamic vegetation cohorts, instead of a single vertical ‘big-leaf’ profile. The SORTIE-NG model includes evolutionary optimality principles as well as phenotype plasticity and intraspecific genetic diversity through first-class support for probabilistic modeling, borrowing design principles from probabilistic programming languages (e.g., [145]). Thus, SORTIE-NG is intended to be the first forest model to bridge the divide between big-leaf, gap, and landscape models, and to be designed from the outset as a probabilistic modeling framework [144]. Future model extensions are in the planning stages, including the first machine learning processes included in an ecosystem model.

While implemented in a ‘close-to-metal’ language (i.e., C++17) and designed for efficiency, SORTIE-NG is more computationally demanding than the PPA-SiBGC model used in this paper. Yet, we anticipate that SORTIE-NG will be able to improve the fidelity to observed fluxes through reliance on detailed process models, which is the major shortcoming of both models considered in this paper. Similarly, there is a new version of the LANDIS-II NECN model in development known as NECN-Hydro, which remains a simplified variant of the Century model, but includes more detailed hydrological processes. The currently presented work provides not only an intercomparison of two current state-of-art models, but also open-source software and wrapper functions for simple and rapid comparison of our results with new models or sites. The selected forested ecosystems modeled in this work are among the best-studied model forests on Earth today. Specifically, the EMS EC flux tower at Harvard Forest is the longest running flux tower in the United States. Extensions of the presented

work will allow rigorous model comparison methodologies for forest models that will benefit the research community at large.

Extensions of this work may also address the robustness of model predictions to variations in parameter values. The parameterization of complex forest biogeochemistry models such as LANDIS-II NECN and PPA-SiBGC is an important problem for consideration. Models such as LANDIS-II NECN operate with an order of magnitude more parameters than PPA-SiBGC, which can each be estimated with different levels of accuracy. Often, we know only the range of parameter values while parameterization can also depend on the statistical approach employed. Meanwhile, authors routinely employ additional model calibration that consists of adjusting parameters in order to obtain improved fitness, which we explicitly avoided in this study.

Conducting such analyses through a unified software framework in a fully transparent and reproducible manner is therefore of the utmost importance. This is exactly the type of analyses that our provided software is designed to support. In a parallel line of research, we extend this base-level implementation into a generic application programming interface (API) and toolkit for geoscientific simulation models, known as Erde [146], supporting both R and Python. The Erde framework provides machine learning model emulation, robust loss estimation, parameter optimization, probabilistic parameterization, samplers such as Latin hypercube sampling and Markov Chain Monte Carlo, and a number of other helper methods designed for complex simulation models. We utilize the Erde framework in the design of Erde Gym, a toolkit for developing and comparing optimization algorithms in the geosciences with a focus on reinforcement learning [146]. For the first time, Erde Gym will allow us to model systems (e.g., evolutionary plant optimality) as intelligent agents able to navigate complex environments.

4.1. Limitations

This study, similar to most other modeling studies, was limited by the availability, quality, and quantity of observational data. The lack of temporal depth in this data poses substantial challenges in modeling the long-term effects of forest succession, as these processes can operate on a century timescale or longer. However, diagnosing succession was not the aim of this study, as we instead focus on near-term validation of forest models using field measurements and EC flux tower data. Another limitation is that these methods may be challenging to implement for sites that are less well-characterized, particularly in the absence of EC flux tower data and/or tree species parameters. A combination of tower-based and remote sensing observations may help overcome this challenge in the coming years with advances in machine learning. In addition, the poor performance of both tested models in capturing fluxes and excellent performance in capturing stocks indicate that the two current models should be applied in cases where stocks, rather than fluxes, are of primary interest.

4.2. Future Opportunities

Future studies should expand upon the PPA with a first-principles representation of energetic and biogeochemical above- and below-ground processes in a modern component-based software framework. This work should fuse the new state-of-the-art forest biogeochemistry model with a model wrapper API written in R or Python, in order to expand native model functions to include Monte Carlo methods, machine-learning model emulation, robust loss functions, and optimization through a simple API enabling reproducibility. This would combine a high-performance forest model written in a compiled language with a simple, user-friendly interface written in an interpreted language, combining the best of both worlds. We are currently conducting work along this line by fusing the SORTIE-NG model with the Erde framework in order to develop state-of-the-art and user-friendly modeling capabilities, inspired by the design of modern deep learning frameworks such as PyTorch [147] and the Keras API [148].

In addition, there is a clear opportunity to link individual-based models such as PPA-SiBGC and SORTIE-NG to remote sensing data including airborne laser scanning or high-resolution

multiview-stereo imagery (i.e., structure-from-motion), and hyperspectral indices of vegetation growth or stress. This line of work may assess opportunities for Bayesian data assimilation in addition to model parameterization and validation using detailed wall-to-wall forest structure maps. As models such as LES [32] provide more structural detail, spatially explicit data will be needed to parameterize the next generation of models. New data collection methods (e.g., [149]) will also be needed as the geometric realism of models advances toward the photorealistic detail offered by procedural models such as Lindenmayer- or L-systems [150,151].

5. Conclusions

In conclusion, the PPA-SiBGC and LANDIS-II NECN models represent vegetation dynamics previously absent in modeling studies at these sites. These include, "...long-term increases in tree biomass, successional change in forest composition, and disturbance events, processes not well represented in current models," which drive interannual variation in NEE [88]. While the timescale of our simulations were decidedly short-term due to data limitations, both models showed good performance. While PPA-SiBGC showed stronger performance across the range of metrics tested, including the logistics of model deployment, LANDIS-II NECN also performed well across the metrics tested. Further studies are needed to compare more aspects of these and other models based on an array of performance criteria.

Ultimately, we hope that this study serves as the foundation for future forest ecosystem model intercomparisons for the North American continent, similar in spirit to the former TDE Ecosystem Model Intercomparison project [54]. This may help create the impetus for a Global Forest Model Intercomparison Project (ForestMIP) together with modeling groups on other continents. The aims of this research were not to determine which model is 'best' for prognosis at two locations, but to improve the capabilities of existing models across a range of locations in order to advance earth system models. In this regard, there are beneficial aspects to both modeling approaches and the trade-offs presented largely depend on the desired application. Counter to the classical modeling trade-off of Levins [38], improvements in precision and generality resulted from realism.

Supplementary Materials: The following are available online at <http://www.mdpi.com/1999-4907/10/2/180/s1>. Parameter tables for both models and sites are provided in Appendix B (Tables A1–A30). All model, parameter, script files used in this model intercomparison exercise are available for download at the following public GitHub repository: <https://github.com/adam-erickson/ecosystem-model-comparison>. The repository provides tables containing parameter values and climate drivers used in the PPA-SiBGC and LANDIS-II NECN model simulations for the two model intercomparison sites. Tree species codes are adopted from the USDA PLANTS database, accessible at the following URL: <https://plants.usda.gov>. Scripts provided include a simple object-oriented forest biogeochemistry model wrapper library implemented in the R language [83]. The model wrapper library includes a number of features for simplifying the operation of this class of models, including functions for cleaning up and parsing model outputs into memory in a common format for comparison. Importantly, the wrapper library enables full reproducibility of results through the *hf_ems.r* and *jerc_rd.r* scripts. Using these scripts with the object-oriented *classes.r* model wrapper, it is possible to load pre-computed model results and calculate all intercomparison metrics for verification. The directory structure of the repository is shown in Figure S1.

Author Contributions: Individual contributions provided to complete this work include the following: conceptualization, N.S.; methodology, A.E. and N.S.; software, A.E.; validation, A.E.; formal analysis, A.E.; investigation, A.E.; resources, N.S.; data curation, A.E.; writing—original draft preparation, A.E.; writing—review and editing, A.E. and N.S.; visualization, A.E.; supervision, N.S.; project administration, N.S.; funding acquisition, N.S.

Funding: This research was funded by United States Army Corps of Engineers (USACE) contract number W912HQ-18-C-0007.

Acknowledgments: We would like to thank U.S. Department of Defense, Army Corps of Engineers, and the Environmental Security Technology Certification Program (ESTCP) for providing support necessary to conduct this work. We also thank Harvard University and Jones Ecological Research Center for kindly providing data to conduct the analyses. We would further like to thank those that provided guidance on parameterization of the LANDIS-II model. We thank Drs. Louise Loudermilk of USDA Forest Service and Steven Flanagan of Tall Timbers Research Station for providing guidance on parameterization for the Red Dirt flux tower site at JERC, and Dr. Matthew Duveneck of New England Conservatory for providing guidance on parameterization for the HF-EMS EC flux tower site at Harvard Forest. We also acknowledge Drs. Melissa Lucash and Robert Scheller, who

provided comments. Last, we would like to thank Drs. Bradley Case, Hannah Buckley, Audrey Barket-Plotkin, David Orwig, Aaron Ellison, and Zachary Robbins for providing some of the crown allometry parameters for Harvard Forest.

Conflicts of Interest: The authors declare no conflict of interest. The funders had no role in the design of the study; in the collection, analyses, or interpretation of data; in the writing of the manuscript, or in the decision to publish the results.

Abbreviations

The following abbreviations are used in this manuscript:

3D-CMCC CNR-BGC	3-D Forest Ecosystem Model of the Euro-Mediterranean Centre for Climate Change with Carbon-Nitrogen-Respiration Biogeochemistry
3D-CMCC FEM	3-D Forest Ecosystem Model of the Euro-Mediterranean Centre for Climate Change
3-PG	Physiological Processes Predicting Growth model
4C/FORESEE	Forest Ecosystems in a Changing Environment model
ANAFORE	ANalysis of FORest Ecosystems model
ANPP	Aboveground net primary production
API	Application programming interface
BASFOR	BASic FORest simulator model
BGC	Biogeochemistry
Biome-BGC	Biome BioGeochemical Cycles model
CARAIB	CARbon Assimilation In the Biosphere model
CoFoLaMo	Comparison of Forest Landscape Models
COST	Cooperation in Science and Technology
CPU	Central processing unit
CSV	Comma-separated values
DLEM	Dynamic Land Ecosystem Model
DoD	Department of Defense
EC	Eddy covariance
ED/ED2	Ecosystem Demography model
EMS	Environmental Measurement Station
ForClim	Forests in a changing Climate model
ForHyCS	Forest and Hydrology Change in Switzerland model
FORMIND	Forest Model Individual-based
FVS	Forest Vegetation Simulator
GO+	GRAECO and ORCHIDEE plus CASTANEA model
GOTILWA+	Growth of Trees is Limited by Water model
GPGPU	General-purpose graphics processing unit
HF	Harvard Forest, Massachusetts, USA
IBIS2	Integrated Biosphere Simulator version 2
iLand	Individual-based forest landscape and disturbance model
ISIMIP/ISIMIP2	Inter-Sectoral Impact Model Intercomparison Project
JERC	Jones Ecological Research Center, Georgia, USA
JULES	Joint UK Land Environment Simulator
L-systems	Lindenmayer systems
LandClim	LANDIS-ForClim model
LANDIS	Landscape Disturbance and Succession model
LANDIS-II	Landscape Disturbance and Succession model, C# version
LM3	Land Model version 3
Landscape-DNDC	Landscape DeNitritification DeComposition model
LINKAGES	Linked forest productivity-soil process model

LPJ-GUESS	Lund-Potsdam-Jena General Ecosystem Simulator
LPJmL	Lund-Potsdam-Jena managed Land
MAE	Mean absolute error
MAESTRO/MAESTRA	Model of Assimilation, Evaporation, and Solar radiation TRansfer Operation
MC1	MAPSS-Century-1 model
ME	Mean error
MIP	Model Intercomparison Project
NECN	Net Ecosystem Carbon and Nitrogen model
NEE	Net ecosystem exchange
NSE	Nash-Sutcliffe efficiency
ORCHIDEE	Organising Carbon and Hydrology In Dynamic Ecosystems
PnET-II	Photosynthetic/EvapoTranspiration model
PnET-BGC	Photosynthetic/EvapoTranspiration Biogeochemistry model
PPA	Perfect Plasticity Approximation model
PPA-SiBGC	PPA with Simple Biogeochemistry model
PRELES	PREdict with LESs - or - PREdict Light-use efficiency, Evapotranspiration and Soil water
PROFOUND	Towards robust projections of European forests under climate change
RAM	Random access memory
RCP	Representative Concentration Pathway
RD	Red Dirt mesic flux tower site, JERC
RMSE	Root mean squared error
SAS	Size- and age-structured equations
SOC	Soil organic carbon
SON	Soil organic nitrogen
SPA	Soil-plant-atmosphere continuum model
TDE	Throughfall Displacement Experiment
TreeMig	Tree Migration model
VEGAS	VEgetation-Global-Atmosphere-Soil model
VISIT	Vegetation Integrative Simulator for Trace Gases

Appendix A. Eddy Covariance Flux Tower Measurements

Appendix A.1. HF-EMS EC Flux Tower

Recent historical mean daily fluxes of temperature ($^{\circ}\text{C}$), ecosystem respiration ($\mu\text{ mol CO}_2\text{ m}^{-2}$), and NEE ($\mu\text{ mol C m}^{-2}$) for the HF-EMS tower are shown in Figure A1.

Patterns in daytime and nighttime NEE are shown in Figure A2. This was calculated by taking daily mean NEE values for three-hour windows surrounding noon and midnight, respectively (1100–1300 and 2300–0100 h). These patterns are important to diagnose, as they demonstrate responses to a gradient of light and temperature conditions.

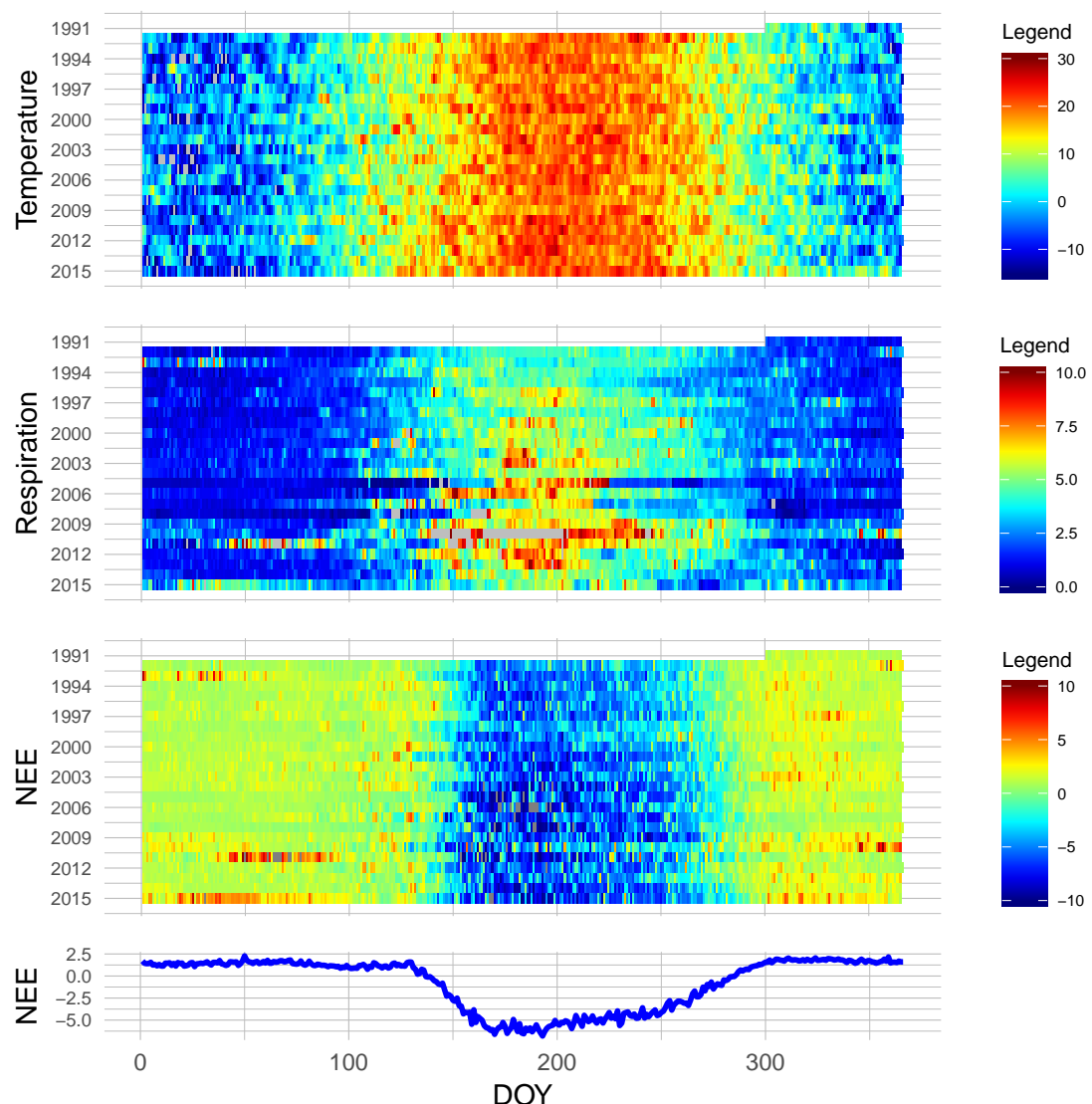


Figure A1. HF-EMS tower daily averages.

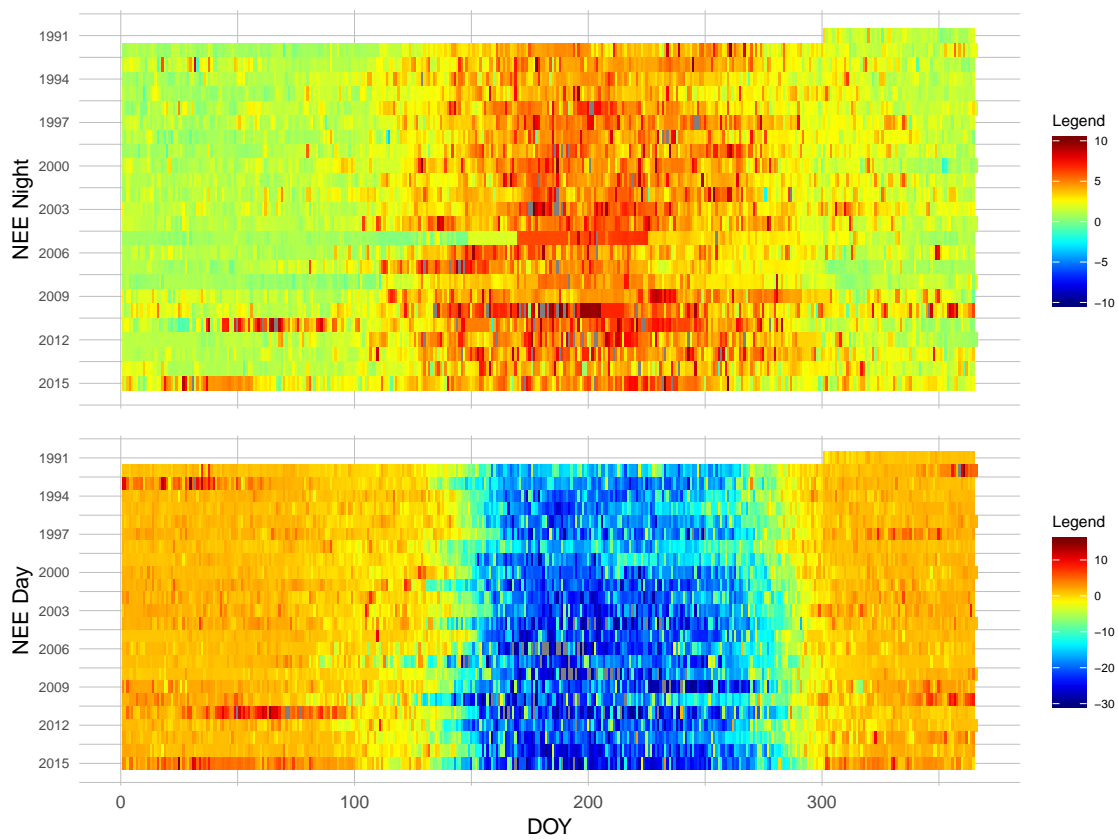


Figure A2. HF-EMS tower daily diurnal averages.

Appendix A.2. JERC-RD EC Flux Tower

Recent historical mean daily fluxes of latent heat flux (LE) (W m^{-2}), ecosystem respiration ($\mu \text{ mol CO}_2 \text{ m}^{-2}$), and NEE ($\mu \text{ mol C m}^{-2}$) for the RD flux tower are shown in Figure A3.

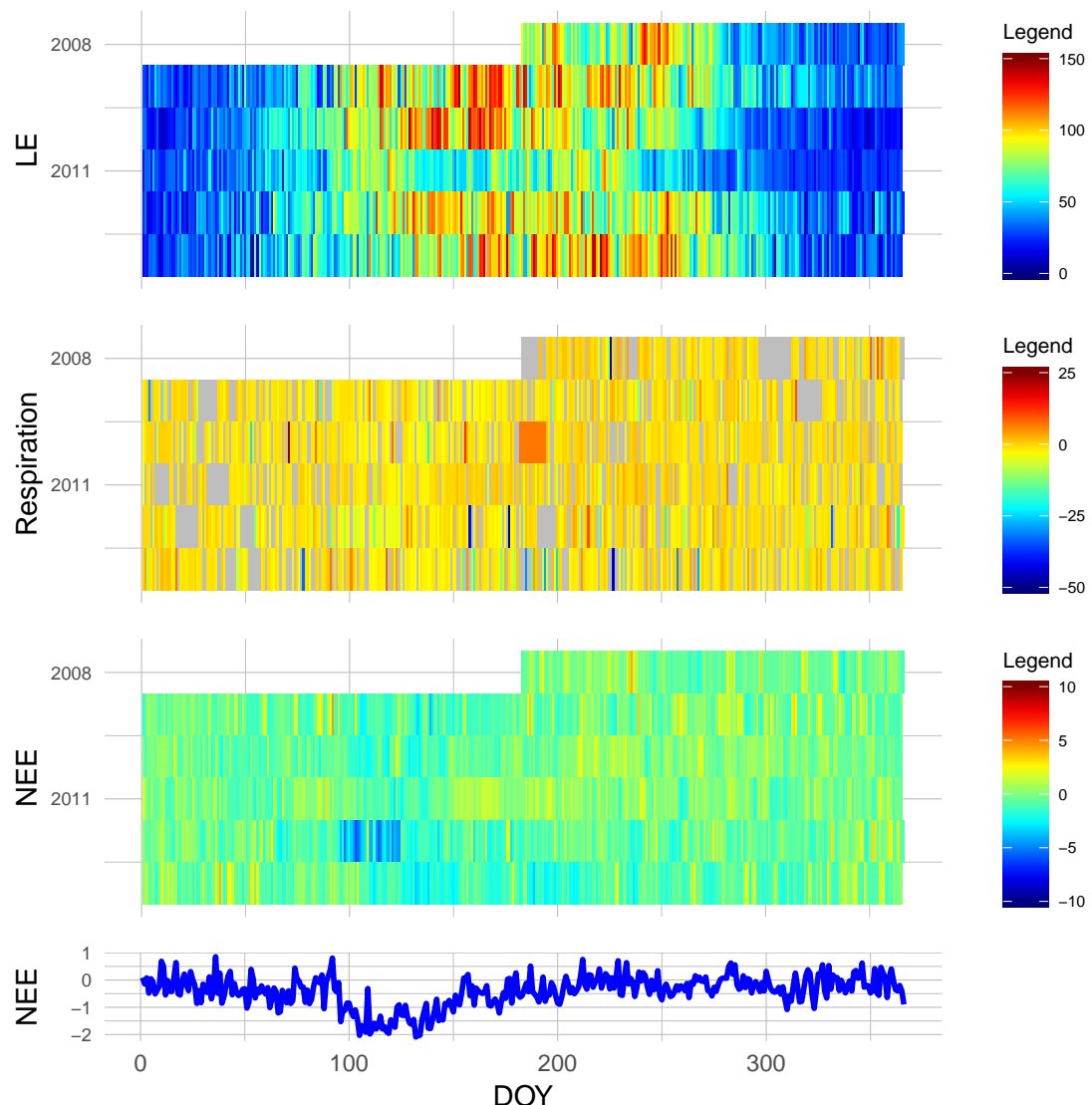


Figure A3. JERC-RD tower daily averages.

Patterns of daytime and nighttime NEE are shown in Figure A4. Again, this was calculated by taking daily mean NEE values for three-hour windows surrounding noon and midnight, respectively (1100–1300 and 2300–0100 h).

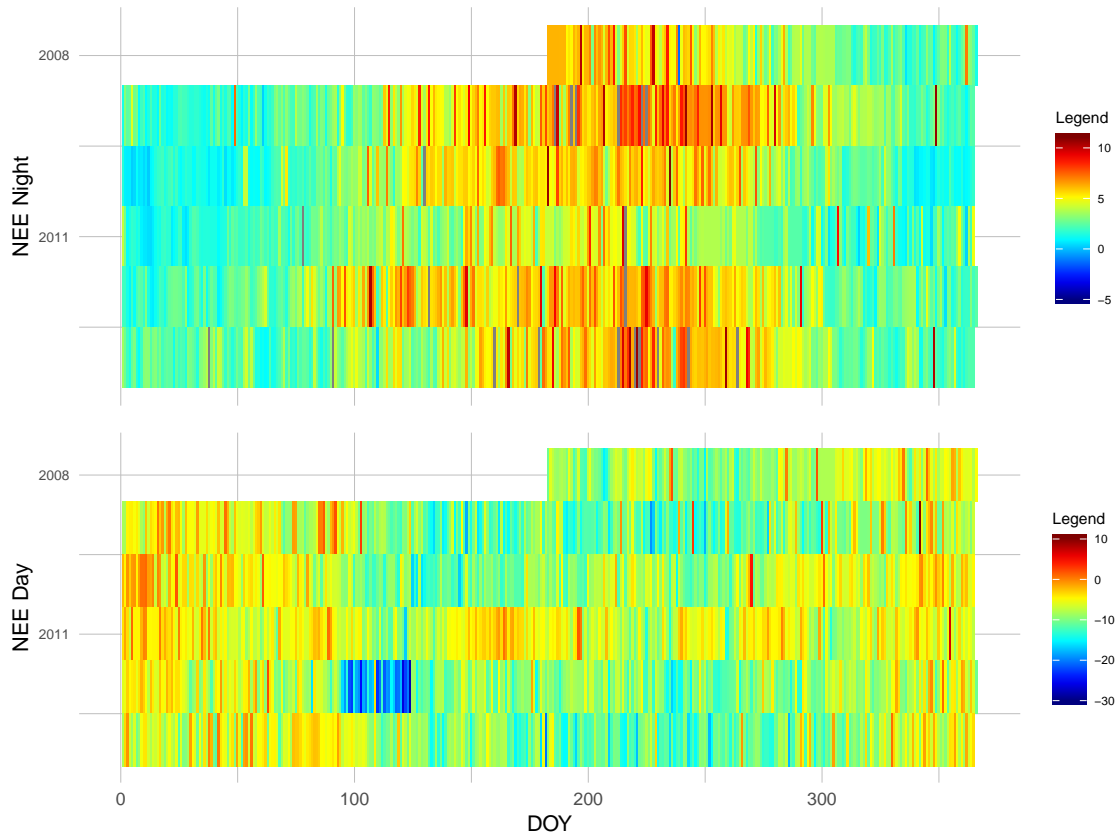


Figure A4. JERC-RD tower daily diurnal averages.

Appendix B. Model Parameters

Appendix B.1. HF-EMS

Appendix B.1.1. PPA-SiBGC

Table A1. Species crown allometry parameters.

Species	Type	h_{coeff}	cr_1	cr_2	cd
ACPE	adult	0.063	0.108	1	0.490
ACRU	adult	0.063	0.108	1	0.490
BEAL	adult	0.063	0.109	1	0.540
BELE	adult	0.024	0.109	1	0.540
BEPO	adult	0.063	0.109	1	0.540
FAGR	adult	0.035	0.152	1	0.664
FRAM	adult	0.056	0.095	1	0.319
PIGL	adult	0.033	0.087	1	0.413
PIRE	adult	0.033	0.087	1	0.413
PIST	adult	0.033	0.087	1	0.413
PRSE	adult	0.045	0.116	1	0.370
QURU	adult	0.042	0.119	1	0.413
QUVE	adult	0.042	0.119	1	0.413
TSCA	adult	0.024	0.100	1	0.846
ACPE	sapling	0.062	0.107	1	0.580
ACRU	sapling	0.063	0.108	1	0.490
BEAL	sapling	0.063	0.109	1	0.540
BELE	sapling	0.024	0.109	1	0.540
BEPO	sapling	0.063	0.109	1	0.540

Table A1. Cont.

Species	Type	h_{coeff}	cr_1	cr_2	cd
FAGR	sapling	0.035	0.152	1	0.664
FRAM	sapling	0.056	0.095	1	0.319
PIGL	sapling	0.033	0.087	1	0.413
PIRE	sapling	0.033	0.087	1	0.413
PIST	sapling	0.033	0.087	1	0.413
PRSE	sapling	0.045	0.116	1	0.370
QURU	sapling	0.042	0.119	1	0.413
QUVE	sapling	0.042	0.119	1	0.413
TSCA	sapling	0.024	0.100	1	0.846

Table A2. Species biomass equation parameters.

Species	b_0	b_1	f_{stem}	f_{branch}	f_{leaf}	f_{root}	f_{soil}
ACPE	-2.047	2.385	0.700	0.230	0.070	0.240	0.680
ACRU	-2.047	2.385	0.700	0.230	0.070	0.240	0.680
BEAL	-1.810	2.348	0.700	0.230	0.070	0.240	0.680
BELE	-1.810	2.348	0.700	0.230	0.070	0.240	0.680
BEPO	-2.227	2.451	0.700	0.230	0.070	0.240	0.680
FAGR	-2.070	2.441	0.700	0.230	0.070	0.240	0.680
FRAM	-1.838	2.352	0.700	0.230	0.070	0.240	0.680
PIGL	-2.136	2.323	0.700	0.230	0.070	0.240	0.680
PIRE	-2.618	2.464	0.700	0.230	0.070	0.240	0.680
PIST	-2.618	2.464	0.700	0.230	0.070	0.240	0.680
PRSE	-2.212	2.413	0.700	0.230	0.070	0.240	0.680
QURU	-2.070	2.441	0.700	0.230	0.070	0.240	0.680
QUVE	-2.070	2.441	0.700	0.230	0.070	0.240	0.680
TSCA	-2.348	2.388	0.700	0.230	0.070	0.240	0.680

Table A3. Biomass carbon fraction parameters.

f_{stem}	f_{branch}	f_{leaf}	f_{root}	f_{soil}
0.500	0.500	0.500	0.500	0.143

Table A4. Species DBH increment parameters.

Species	Type	I_{DBH}
ACPE	adult	0.277
ACRU	adult	0.312
BEAL	adult	0.280
BELE	adult	0.198
BEPO	adult	0.103
FAGR	adult	0.303
FRAM	adult	0.149
PIGL	adult	0.274
PIRE	adult	0.390
PIST	adult	0.277
PRSE	adult	0.120
QURU	adult	0.420
QUVE	adult	0.322
TSCA	adult	0.563

Table A4. *Cont.*

Species	Type	I_{DBH}
ACPE	sapling	0.895
ACRU	sapling	0.269
BEAL	sapling	0.520
BELE	sapling	0.201
BEPO	sapling	0.300
FAGR	sapling	0.530
FRAM	sapling	0.500
PIGL	sapling	0.353
PIRE	sapling	0.350
PIST	sapling	0.350
PRSE	sapling	0.200
QURU	sapling	0.098
QUVE	sapling	0.100
TSCA	sapling	0.509

Table A5. Species mortality parameters.

Species	Type	$p_{mortality}$
ACPE	adult	0.115
ACRU	adult	0.030
BEAL	adult	0.035
BELE	adult	0.009
BEPO	adult	0.032
FAGR	adult	0.015
FRAM	adult	0.004
PIGL	adult	0.074
PIRE	adult	0.023
PIST	adult	0.010
PRSE	adult	0.009
QURU	adult	0.007
QUVE	adult	0.001
TSCA	adult	0.022
ACPE	sapling	0.001
ACRU	sapling	0.873
BEAL	sapling	0.001
BELE	sapling	0.667
BEPO	sapling	0.001
FAGR	sapling	0.354
FRAM	sapling	0.001
PIGL	sapling	0.001
PIRE	sapling	0.001
PIST	sapling	0.001
PRSE	sapling	0.001
QURU	sapling	0.001
QUVE	sapling	0.001
TSCA	sapling	0.821

Table A6. Species fecundity parameters.

Species	Fecundity
ACPE	2
ACRU	29
BEAL	16
BELE	8
BEPO	2
FAGR	11
FRAM	5
PIGL	3
PIRE	3
PIST	11
PRSE	8
QURU	29
QUVE	9
TSCA	17

Table A7. Species C:N ratio parameters.

Species	CN _{stem}	CN _{branch}	CN _{leaf}	CN _{litter}	CN _{root}	CN _{soil}
ACPE	548.590	71.460	30.460	58.800	68.548	23.087
ACRU	548.590	71.460	30.460	58.800	68.548	23.087
BEAL	548.590	71.460	22.420	58.800	68.548	23.087
BELE	548.590	71.460	21.200	58.800	68.548	23.087
BEPO	548.590	71.460	21.560	58.800	68.548	23.087
FAGR	548.590	71.460	22.420	58.800	68.548	23.087
FRAM	548.590	71.460	21.910	58.800	68.548	23.087
PIGL	548.590	71.460	38	58.800	68.548	23.087
PIRE	548.590	71.460	33	58.800	68.548	23.087
PIST	548.590	71.460	38	58.800	68.548	23.087
PRSE	548.590	71.460	21.500	58.800	68.548	23.087
QURU	548.590	71.460	21.920	58.800	68.548	23.087
QUVE	548.590	71.460	21.920	58.800	68.548	23.087
TSCA	548.590	71.460	42.520	58.800	68.548	23.087

Appendix B.1.2. LANDIS-II NECN

Table A8. NECN adjustment parameters.

Parameter	Value
p_{est} modifier	0.1
$N_{mineral}$ initial	3.0
$Fuels_{fine}$ initial	0.1
N_{atmos} slope	0.007
N_{atmos} intercept	0.011
$Latitude_{deg}$	43.3
$r_{denitrification}$	0.001
r_{decay} surface	0.65
r_{decay} SOM1	1.0
r_{decay} SOM2	0.125
r_{decay} SOM3	0.0002

Table A9. NECN maximum LAI parameters.

<i>Class_{shade}</i>	<i>LAI_{max}</i>
1	1
2	2.5
3	3.5
4	6
5	8

Table A10. NECN light establishment parameters.

<i>Class_{shade}</i>	<i>Shade₀</i>	<i>Shade₁</i>	<i>Shade₂</i>	<i>Shade₃</i>	<i>Shade₄</i>	<i>Shade₅</i>
1	1	1	0.25	0.1	0	0
2	0.5	0.5	1	0.25	0.1	0
3	0.1	0.5	1	1	0.5	0.1
4	0.1	0.25	0.5	0.5	1	0.25
5	0	0.1	0.25	0.25	0.5	1

Table A11. NECN species parameters.

Species	PFT	<i>N_{fix}</i>	<i>GDD_{min}</i>	<i>GDD_{max}</i>	<i>T_{min}</i>	<i>D_{max}</i>	<i>Longleaf</i>	<i>R_{eipi}</i>	<i>L_{leaf}</i>	<i>L_{root_r}</i>	<i>L_{wood}</i>	<i>L_{root_c}</i>	<i>CN_{leaf}</i>	<i>CN_{root_r}</i>	<i>CN_{wood}</i>	<i>CN_{root_c}</i>	<i>CN_{litter}</i>	<i>ANPP_{max}</i>	<i>B_{max}</i>
ACRU	3	N	1260	6600	-18	0.23	1	N	0.183	0.334	0.125	0.312	28.20	26	565	50	55	440	25000
QURU	2	N	1100	4571	-17	0.2025	1	N	0.249	0.334	0.225	0.303	18.50	58	398	113	32	380	25000

Table A12. Functional group parameters.

PFT	Index	<i>T_{mean}</i>	<i>T_{max}</i>	<i>T_{shape}</i>	<i>T_{shape}</i>	<i>f_{Cf}</i>	<i>BTOLAI</i>	<i>kLAI</i>	<i>LAI_{max}</i>	<i>PPRPTS₂</i>	<i>PPRPTS₃</i>	<i>r_{decayw}</i>	<i>m_{wood}</i>	<i>m_{shape}</i>	<i>drop_{month}</i>	<i>f_{root_c}</i>	<i>f_{root_f}</i>
Oaks	2	25	40	1.5	2.5	0.6	-0.9	10000	9	0.1	0.8	0.5	0.0006	15	9	0.2	0.5
NorthHardwoods	3	25	40	1.5	2.5	0.6	-0.9	7000	10	1.5	0.96	0.7	0.0006	15	9	0.2	0.5

Table A13. Fire reduction parameters; inactive.

<i>Class_{severity}</i>	<i>Reduction_{wood}</i>	<i>Reduction_{litter}</i>	<i>Reduction_{SOM}</i>
1	0.0	0.5	1.0
2	0.05	0.75	1.0
3	0.2	1.0	1.0
4	0.5	1.0	1.0
5	0.8	1.0	1.0

Table A14. Harvest reduction parameters; inactive.

Class	<i>Reduction_{wood}</i>	<i>Reduction_{litter}</i>	<i>Reduction_{SOM}</i>	<i>Removal_{leaf}</i>	<i>Removal_{wood}</i>
HandThinning	0.05	1.0	1.0	1.0	1.0
MechThinning	0.05	1.0	1.0	0.85	1.0

Table A15. Species parameters; only ACRU and QURU were simulated.

Species	Longevity	Maturity	T_{shade}	T_{fire}	D_{eff}	D_{max}	p_{veg}	S_{min}	S_{max}	R_{fire}
ABBA	200	25	5	1	30	160	0	0	0	none
ACRU	235	5	4	1	100	200	0.75	0	150	none
ACSA	300	40	5	1	100	200	0.1	0	60	none
BEAL	300	40	3	2	100	400	0.1	0	180	none
BELE	250	40	4	2	100	400	0.1	0	0	none
BEPA	150	40	4	2	100	600	0.75	0	150	none
BEPO	150	40	4	2	100	400	0.1	0	0	none
CAGL	200	30	3	2	50	100	0.25	0	200	resprout
FAGR	350	10	5	1	30	300	0.4	10	200	resprout
FRAM	300	30	2	1	70	140	0.1	0	70	none
FRNI	150	30	4	2	200	2000	0.8	10	140	resprout
LALA	180	35	2	2	100	400	0.2	0	0	none
OSVI	110	25	4	2	100	200	0.15	0	100	resprout
PIGL	300	25	3	2	30	200	0	0	0	none
PIMA	215	30	3	3	79	158	0	0	0	none
PIRU	350	15	5	2	80	125	0	0	0	none
PIRE	250	15	2	4	100	275	0.1	0	20	none
PIRI	200	10	2	4	90	150	0.5	10	100	resprout
PIST	400	25	3	3	60	210	0	0	0	none
POBA	150	10	1	2	100	200	0.8	10	80	resprout
POGR	110	20	1	1	1000	5000	0.9	0	100	resprout
POTR	110	20	1	1	1000	5000	0.9	0	100	resprout
PRSE	200	10	2	3	100	200	0.5	20	90	resprout
QUAL	400	25	3	2	30	800	0.1	20	200	resprout
QUCO	150	20	2	3	50	100	0.5	20	100	resprout
QUPR	300	20	3	3	50	150	0.5	10	200	resprout
QURU	250	30	3	2	30	800	0.5	20	200	resprout
QUVE	120	20	3	2	70	150	0.1	20	90	resprout
THOC	800	30	2	1	45	100	0.5	0	200	none
TIAM	250	15	4	1	75	150	0.8	10	240	resprout
TSCA	500	20	5	2	30	100	0	0	0	none
ULAM	85	20	4	2	90	400	0.3	5	70	resprout

Appendix B.2. JERC-RD**Appendix B.2.1. PPA-SiBGC****Table A16.** Species crown allometry parameters.

Species	Type	h_{coeff}	$cr1$	$cr2$	cd
PIPA	adult	0.033	0.087	1	0.413
QUIN	adult	0.042	0.119	1	0.413
QUNI	adult	0.042	0.119	1	0.413
QUVI	adult	0.042	0.119	1	0.413
PIPA	sapling	0.033	0.087	1	0.413
QUIN	sapling	0.042	0.119	1	0.413
QUNI	sapling	0.042	0.119	1	0.413
QUVI	sapling	0.042	0.119	1	0.413

Table A17. Species biomass equation parameters.

Species	<i>b</i> 0	<i>b</i> 1	<i>f_{stem}</i>	<i>f_{branch}</i>	<i>f_{leaf}</i>	<i>f_{root}</i>	<i>f_{soil}</i>
PIPA	-3.051	2.647	0.700	0.230	0.070	0.240	0.680
QUIN	-2.070	2.441	0.700	0.230	0.070	0.240	0.680
QUNI	-2.070	2.441	0.700	0.230	0.070	0.240	0.680
QUVI	-2.070	2.441	0.700	0.230	0.070	0.240	0.680

Table A18. Biomass carbon fraction parameters.

<i>f_{stem}</i>	<i>f_{branch}</i>	<i>f_{leaf}</i>	<i>f_{root}</i>	<i>f_{soil}</i>
0.500	0.500	0.500	0.500	0.143

Table A19. Species DBH increment parameters.

Species	Type	<i>I_{DBH}</i>
PIPA	adult	0.261
QUIN	adult	0.119
QUNI	adult	0.994
QUVI	adult	0.276
PIPA	sapling	0.197
QUIN	sapling	0.100
QUNI	sapling	0.440
QUVI	sapling	0.271

Table A20. Species mortality parameters.

Species	Type	<i>p_{mortality}</i>
PIPA	adult	0.001
QUIN	adult	0.001
QUNI	adult	0.001
QUVI	adult	0.001
PIPA	sapling	0.174
QUIN	sapling	0.333
QUNI	sapling	0.143
QUVI	sapling	0.111

Table A21. Species fecundity parameters.

Species	Fecundity
PIPA	2
QUIN	0
QUNI	0
QUVI	0

Table A22. Species C:N ratio parameters.

Species	<i>CN_{stem}</i>	<i>CN_{branch}</i>	<i>CN_{leaf}</i>	<i>CN_{litter}</i>	<i>CN_{root}</i>	<i>CN_{soil}</i>
PIPA	133.721	133.721	255.103	255.103	133.721	23.087
QUIN	96.370	96.370	85.259	85.259	96.370	23.087
QUNI	96.370	96.370	85.259	85.259	96.370	23.087
QUVI	96.370	96.370	85.259	85.259	96.370	23.087

Appendix B.2.2. LANDIS-II NECN

Table A23. NECN adjustment parameters.

Parameter	Value
p_{est} modifier	0.4
$N_{mineral}$ initial	0.5
$Fuels_{fine}$ initial	0.1
N_{atmos} slope	0.004
N_{atmos} intercept	0.017
$Latitude_{deg}$	31.220731
$r_{denitrification}$	0.02
r_{decay} surface	0.70
r_{decay} SOM1	0.81
r_{decay} SOM2	0.05
r_{decay} SOM3	0.00006

Table A24. NECN maximum LAI parameters.

<i>Class_{shade}</i>	<i>LAI_{max}</i>
1	1
2	2.5
3	3.5
4	6
5	8

Table A25. NECN light establishment parameters.

<i>Class_{shade}</i>	<i>Shade₀</i>	<i>Shade₁</i>	<i>Shade₂</i>	<i>Shade₃</i>	<i>Shade₄</i>	<i>Shade₅</i>
1	1	1	0.25	0.1	0	0
2	0.5	0.5	1	0.25	0.1	0
3	0.1	1	1	1	0.5	0.1
4	0.1	0.25	0.5	0.5	1	0.25
5	0	0.1	0.25	0.25	0.5	1

Table A26. NECN species parameters.

Species	PFT	N_{fix}	GDD_{min}	GDD_{max}	T_{min}	D_{max}	<i>Longleaf</i>	R_{epi}	L_{leaf}	L_{root_f}	L_{wood}	L_{root_c}	CN_{leaf}	CN_{root_f}	CN_{wood}	CN_{root_c}	CN_{litter}	$ANPP_{max}$	B_{max}
QUIN	2	N	3915	7000	1	0.423	1	N	0.293	0.23	0.23	0.35	24	48	500	333	55	250	15,000
QULA	2	N	3915	7000	1	0.423	1	N	0.293	0.23	0.23	0.35	24	48	500	333	55	250	15,000
PIPA	1	N	3915	7000	1	0.423	2	N	0.2	0.2	0.35	0.35	50	50	380	170	100	500	15,000

Table A27. Functional group parameters.

PFT	Index	T_{mean}	T_{max}	T_{shape}	T_{shape}	f_{C_f}	$BTOLAI$	$kLAI$	LAI_{max}	$PPRPTS_2$	$PPRPTS_3$	r_{decay_w}	m_{wood}	m_{shape}	$month_{drop}$	f_{root_c}	f_{root_f}
Pine	1	28	45	3.0	2.5	0.37	-0.9	2000	10	1	0.8	0.6	0.001	15	9	0.31	0.56
Oaks	2	27	45	2.2	2.5	0.5	-0.9	2000	20	0.1	0.75	0.6	0.001	15	9	0.21	0.59

Table A28. Fire reduction parameters; inactive.

<i>Class_{severity}</i>	<i>Reduction_{wood}</i>	<i>Reduction_{litter}</i>	<i>Reduction_{SOM}</i>
1	0.0	0.5	1.0
2	0.05	0.75	1.0
3	0.2	1.0	1.0
4	0.5	1.0	1.0
5	0.8	1.0	1.0

Table A29. Harvest reduction parameters; inactive.

<i>Class_{severity}</i>	<i>Reduction_{wood}</i>	<i>Reduction_{litter}</i>	<i>Reduction_{SOM}</i>	<i>Removal_{leaf}</i>	<i>Removal_{wood}</i>
HandThinning	0.05	1.0	1.0	1.0	1.0
MechThinning	0.05	1.0	1.0	0.85	1.0

Table A30. Species parameters.

Species	Longevity	Maturity	<i>T_{shade}</i>	<i>T_{fire}</i>	<i>D_{eff}</i>	<i>D_{max}</i>	<i>p_{veg}</i>	<i>S_{min}</i>	<i>S_{max}</i>	<i>R_{fire}</i>
QUIN	150	10	4	5	50	3000	0.75	5	40	resprout
QULA	150	20	4	3	50	3000	0.75	5	40	resprout
PIPA	400	20	1	5	20	200	0.0	0	5	none

References

1. von Carlowitz, H.C.; Bernigeroth, M. *Sylvicultura Oeconomica Oder Haufwirthliche Nachricht und Naturmäßige Anweisung zur Wilden Baum-Zucht*; Johann Friedrich Braun: Leipzig, Deutschland, 1713; p. 414.
2. Mikesell, M.W. The Deforestation of Mount Lebanon. *Geogr. Rev.* **1969**, *59*, 1–28. [[CrossRef](#)]
3. Hansman, J. Gilgamesh, Humbaba and the Land of the Erin-Trees. *Iraq* **1976**, *38*, 23–35. [[CrossRef](#)]
4. Holling, C.S. Resilience and Stability of Ecological Systems. *Annu. Rev. Ecol. Syst.* **1973**, *4*, 1–23. [[CrossRef](#)]
5. Levin, S.A. Ecosystems and the biosphere as complex adaptive systems. *Ecosystems* **1998**, *1*, 431–436. [[CrossRef](#)]
6. Vehkämäki, S. The concept of sustainability in modern times. In *Sustainable Use of Renewable Natural Resources*; Jalkanen, A., Nygren, P., Eds.; Helsingin Yliopiston Metsäkologian Laitoksen Julkaisuja, Helsingin Yliopisto, Metsäkologian Laitos: Helsinki, Finland, 2005; Chapter 2, pp. 23–35.
7. Rowe, J.S.; Scotter, G.W. Fire in the boreal forest. *Quat. Res.* **1973**, *3*, 444–464. [[CrossRef](#)]
8. Franklin, J.F.; Spies, T.A.; Pelt, R.V.; Carey, A.B.; Thornburgh, D.A.; Berg, D.R.; Lindenmayer, D.B.; Harmon, M.E.; Keeton, W.S.; Shaw, D.C.; et al. Disturbances and structural development of natural forest ecosystems with silvicultural implications, using Douglas-fir forests as an example. *For. Ecol. Manag.* **2002**, *155*, 399–423. [[CrossRef](#)]
9. Ripple, W.J.; Beschta, R.L. Restoring Yellowstone's aspen with wolves. *Biol. Conserv.* **2007**, *138*, 514–519. [[CrossRef](#)]
10. Nitschke, C.R.; Innes, J.L. Integrating climate change into forest management in South-Central British Columbia: An assessment of landscape vulnerability and development of a climate-smart framework. *For. Ecol. Manag.* **2008**, *256*, 313–327. [[CrossRef](#)]
11. Erickson, A.M.; Nitschke, C.R.; Coops, N.C.; Cumming, S.G.; Stenhouse, G.B. Past-century decline in forest regeneration potential across a latitudinal and elevational gradient in Canada. *Ecol. Model.* **2015**, *313*, 94–102. [[CrossRef](#)]
12. Aitken, S.N.; Yeaman, S.; Holliday, J.A.; Wang, T.; Curtis-McLane, S. Adaptation, migration or extirpation: climate change outcomes for tree populations. *Evolut. Appl.* **2008**, *1*, 95–111. [[CrossRef](#)]
13. Aitken, S.N.; Whitlock, M.C. Assisted Gene Flow to Facilitate Local Adaptation to Climate Change. *Annu. Rev. Ecol. Evolut. Syst.* **2013**, *44*, 367–388. [[CrossRef](#)]
14. Erickson, A. Turing biocircuits for biosphere optimization. *ResearchGate* **2015**. [[CrossRef](#)]

15. Attiwill, P.M. The disturbance of forest ecosystems: The ecological basis for conservative management. *For. Ecol. Manag.* **1994**, *63*, 247–300. [[CrossRef](#)]
16. Vuokila, Y. *Functions for Variable Density Yield Tables of Pine Based on Temporary Sample Plots*; Technical Report; Finnish Forest Research Institute: Helsinki, Finland, 1965.
17. Usher, M.B. A Matrix Approach to the Management of Renewable Resources, with Special Reference to Selection Forests. *J. Appl. Ecol.* **1966**, *3*, 355–367. [[CrossRef](#)]
18. Stage, A.R. *Prognosis Model for Stand Development. Res. Pap. INT-RP-137*; Technical Report; U.S. Dept. of Agriculture, Forest Service, Intermountain Forest and Range Experiment Station: Ogden, UT, USA, 1973.
19. Crookston, N.L.; Dixon, G.E. The forest vegetation simulator: A review of its structure, content, and applications. *Comput. Electron. Agric.* **2005**, *49*, 60–80. [[CrossRef](#)]
20. Bugmann, H.K.M. A Simplified Forest Model to Study Species Composition Along Climate Gradients. *Ecology* **1996**, *77*, 2055–2074. [[CrossRef](#)]
21. Keane, R.E.; Cary, G.J.; Davies, I.D.; Flannigan, M.D.; Gardner, R.H.; Lavorel, S.; Lenihan, J.M.; Li, C.; Rupp, T. A classification of landscape fire succession models: Spatial simulations of fire and vegetation dynamics. *Ecol. Model.* **2004**, *179*, 3–27. [[CrossRef](#)]
22. Mladenoff, D.J. LANDIS and forest landscape models. *Ecol. Model.* **2004**, *180*, 7–19. [[CrossRef](#)]
23. He, H.S. Forest landscape models: Definitions, characterization, and classification. *For. Ecol. Manag.* **2008**, *254*, 484–498. [[CrossRef](#)]
24. Xi, W.; Coulson, R.N.; Birt, A.G.; Shang, Z.B.; Waldron, J.D.; Lafon, C.W.; Cairns, D.M.; Tchakerian, M.D.; Klepzig, K.D. Review of forest landscape models: Types, methods, development and applications. *Acta Ecol. Sin.* **2009**, *29*, 69–78. [[CrossRef](#)]
25. Shifley, S.R.; He, H.S.; Lischke, H.; Wang, W.J.; Jin, W.; Gustafson, E.J.; Thompson, J.R.; Thompson, F.R.; Dijak, W.D.; Yang, J. The past and future of modeling forest dynamics: From growth and yield curves to forest landscape models. *Landscape Ecol.* **2017**, *32*, 1307–1325. [[CrossRef](#)]
26. Sellers, P.J.; Mintz, Y.; Sud, Y.C.; Dalcher, A. A Simple Biosphere Model (SIB) for Use within General Circulation Models. *J. Atmos. Sci.* **1986**, *43*, 505–531. [[CrossRef](#)]
27. Fisher, J.B.; Huntzinger, D.N.; Schwalm, C.R.; Sitch, S. Modeling the Terrestrial Biosphere. *Annu. Rev. Environ. Resour.* **2014**, *39*, 91–123. [[CrossRef](#)]
28. Fisher, R.A.; Koven, C.D.; Anderegg, W.R.L.; Christoffersen, B.O.; Dietze, M.C.; Farrior, C.E.; Holm, J.A.; Hurtt, G.C.; Knox, R.G.; Lawrence, P.J.; et al. Vegetation demographics in Earth System Models: A review of progress and priorities. *Glob. Chang. Biol.* **2018**, *24*, 35–54. [[CrossRef](#)] [[PubMed](#)]
29. Kimmins, J.; Mailly, D.; Seely, B. Modelling forest ecosystem net primary production: the hybrid simulation approach used in forecast. *Ecol. Model.* **1999**, *122*, 195–224. [[CrossRef](#)]
30. Mäkelä, A.; Landsberg, J.; Ek, A.R.; Burk, T.E.; Ter-Mikaelian, M.; Ågren, G.I.; Oliver, C.D.; Puttonen, P. Process-based models for forest ecosystem management: current state of the art and challenges for practical implementation. *Tree Physiol.* **2000**, *20*, 289–298. [[CrossRef](#)] [[PubMed](#)]
31. Duursma, R.A.; Medlyn, B.E. MAESPA: A model to study interactions between water limitation, environmental drivers and vegetation function at tree and stand levels, with an example application to CO₂ x drought interactions. *Geosci. Model Dev.* **2012**, *5*, 919–940. [[CrossRef](#)]
32. Liénard, J.; Strigul, N. An individual-based forest model links canopy dynamics and shade tolerances along a soil moisture gradient. *R. Soc. Open Sci.* **2016**, *3*, 150589. [[CrossRef](#)] [[PubMed](#)]
33. Landsberg, J.J.; Waring, R.H. A generalised model of forest productivity using simplified concepts of radiation-use efficiency, carbon balance and partitioning. *For. Ecol. Manag.* **1997**, *95*, 209–228. [[CrossRef](#)]
34. Farquhar, G.D.; von Caemmerer, S.; Berry, J.A. A biochemical model of photosynthetic CO₂ assimilation in leaves of C3 species. *Planta* **1980**, *149*, 78–90. [[CrossRef](#)]
35. Sulman, B.N.; Moore, J.A.M.; Abramoff, R.; Averill, C.; Kivlin, S.; Georgiou, K.; Sridhar, B.; Hartman, M.D.; Wang, G.; Wieder, W.R.; et al. Multiple models and experiments underscore large uncertainty in soil carbon dynamics. *Biogeochemistry* **2018**, *141*, 109–123. [[CrossRef](#)]
36. Parton, W.J., Anderson, D.W.; Cole, C.V.; Stewart, J.W.B. *Simulation of organic matter formation and mineralization in semi-arid agroecosystems*; Nutrient cycling in agricultural ecosystems. Special publication no. 23; The University of Georgia Press: Athens, GA, USA, 1983; pp. 533–550.
37. Parton, W.J.; Schimel, D.S.; Cole, C.V.; Ojima, D.S. Analysis of Factors Controlling Soil Organic Matter Levels in Great Plains Grasslands1. *Soil Sci. Soc. Am. J.* **1987**, *51*, 1173–1179. [[CrossRef](#)]

38. Levins, R. The Strategy of Model Building in Population Biology. *Am. Sci.* **1966**, *54*, 421–431.
39. Kimmings, H.; Blanco, J.A.; Seely, B.; Welham, C.; Scoullar, K. *Forecasting Forest Futures: A Hybrid Modelling Approach to the Assessment of Sustainability of Forest Ecosystems and Their Values*; Taylor & Francis Group: Boca Raton, FL, USA, 2010; p. 296.
40. Fisher, R.; McDowell, N.; Purves, D.; Moorcroft, P.; Sitch, S.; Cox, P.; Huntingford, C.; Meir, P.; Ian Woodward, F. Assessing uncertainties in a second-generation dynamic vegetation model caused by ecological scale limitations. *New Phytol.* **2010**, *187*, 666–681. [[CrossRef](#)] [[PubMed](#)]
41. Ahlström, A.; Xia, J.; Arneth, A.; Luo, Y.; Smith, B. Importance of vegetation dynamics for future terrestrial carbon cycling. *Environ. Res. Lett.* **2015**, *10*, 054019. [[CrossRef](#)]
42. Sitch, S.; Smith, B.; Prentice, I.C.; Arneth, A.; Bondeau, A.; Cramer, W.; Kaplan, J.O.; Levis, S.; Lucht, W.; Sykes, M.T.; et al. Evaluation of ecosystem dynamics, plant geography and terrestrial carbon cycling in the LPJ dynamic global vegetation model. *Glob. Chang. Biol.* **2003**, *9*, 161–185. [[CrossRef](#)]
43. Moorcroft, P.R.; Hurtt, G.C.; Pacala, S.W. A method for scaling vegetation dynamics: The ecosystem demography model (ED). *Ecol. Monogr.* **2001**, *71*, 557–586. [[CrossRef](#)]
44. Medvigy, D.; Wofsy, S.C.; Munger, J.W.; Hollinger, D.Y.; Moorcroft, P.R. Mechanistic scaling of ecosystem function and dynamics in space and time: Ecosystem Demography model version 2. *J. Geophys. Res. Biogeosci.* **2009**, *114*, doi:10.1029/2008JG000812. [[CrossRef](#)]
45. Weng, E.S.; Malyshev, S.; Lichstein, J.W.; Farrior, C.E.; Dybzinski, R.; Zhang, T.; Shevliakova, E.; Pacala, S.W. Scaling from individual trees to forests in an Earth system modeling framework using a mathematically tractable model of height-structured competition. *Biogeosciences* **2015**, *12*, 2655–2694. [[CrossRef](#)]
46. Strigul, N.; Pristinski, D.; Purves, D.; Dushoff, J.; Pacala, S. Scaling from trees to forests: Tractable macroscopic equations for forest dynamics. *Ecol. Monogr.* **2008**, *78*, 523–545. [[CrossRef](#)]
47. Purves, D.W.; Lichstein, J.W.; Strigul, N.; Pacala, S.W. Predicting and understanding forest dynamics using a simple tractable model. *Proc. Natl. Acad. Sci. USA* **2008**, *105*, 17018–17022. [[CrossRef](#)] [[PubMed](#)]
48. Davis, A.V. Testing LANDIS-II to Stochastically Model Spatially Abstract Vegetation Trends in the Contiguous United States. Master’s Thesis, University of Southern California, Los Angeles, CA, USA, 2013.
49. Strigul, N. Individual-based models and scaling methods for ecological forestry: Implications of tree phenotypic plasticity. In *Sustainable Forest Management*; Garcia, J., Casero, J., Eds.; InTech: Rijeka, Croatia, 2012; pp. 359–384.
50. Seidl, R.; Rammer, W.; Scheller, R.M.; Spies, T.A. An individual-based process model to simulate landscape-scale forest ecosystem dynamics. *Ecol. Model.* **2012**, *231*, 87–100. [[CrossRef](#)]
51. Warszawski, L.; Frieler, K.; Huber, V.; Piontek, F.; Serdeczny, O.; Schewe, J. The Inter-Sectoral Impact Model Intercomparison Project (ISI-MIP): Project framework. *Proc. Natl. Acad. Sci. USA* **2014**, *111*, 3228–3232. [[CrossRef](#)] [[PubMed](#)]
52. Lischke, H.; Speich, M.; Schmatz, D.; Vacchiano, G.; Mairotta, P.; Leronni, V.; Schuler, L.; Bugmann, H.; Bruna, J.; Thom, D.; et al. CoFoLaMo: Comparing forest landscape model simulations under different climate, interaction- and land use scenarios. *EGU Gen. Assem. Conf. Abstr.* **2016**, *18*, EPSC2016-13867.
53. Hanson, P.J.; Todd, D.E.; Huston, M.A.; Joslin, J.D.; Croker, J.L.; Auge, R.M. *Description and Field Performance of the Walker Branch Throughfall Displacement Experiment: 1993–1996*; Technical Report; Oak Ridge National Laboratory: Oak Ridge, TN, USA, 1998.
54. Hanson, P.J.; Amthor, J.S.; Wullschleger, S.D.; Wilson, K.B.; Grant, R.F.; Hartley, A.; Hui, D.; Hunt, E.R.; Johnson, D.W.; Kimball, J.S.; et al. Oak Forest Carbon and Water Simulations: Model Intercomparisons and Evaluations against Independent Data. *Ecol. Monogr.* **2004**, *74*, 443–489. [[CrossRef](#)]
55. Aber, J.D.; Ollinger, S.V.; Federer, C.A.; Reich, P.B.; Goulden, M.L.; Kicklighter, D.W.; Melillo, J.M.; Lathrop, R.G. Predicting the effects of climate change on water yield and forest production in the northeastern United States. *Clim. Res.* **1995**, *5*, 207–222. [[CrossRef](#)]
56. Williams, M.; Rastetter, E.B.; Fernandes, D.N.; Goulden, M.L.; Wofsy, S.C.; Shaver, G.R.; Melillo, J.M.; Munger, J.W.; Fan, S.M.; Nadelhoffer, K.J. Modelling the soil-plant-atmosphere continuum in a Quercus-Acer stand at Harvard Forest: The regulation of stomatal conductance by light, nitrogen and soil/plant hydraulic properties. *Plant Cell Environ.* **1996**, *19*, 911–927. [[CrossRef](#)]
57. Running, S.; Coughlan, J. A general model of forest ecosystem processes for regional applications I. Hydrologic balance, canopy gas exchange and primary production processes. *Ecol. Model.* **1988**, *42*, 125–154. [[CrossRef](#)]

58. Post, W.M.; Pastor, J. Linkages—An individual-based forest ecosystem model. *Clim. Chang.* **1996**, *34*, 253–261. [[CrossRef](#)]
59. Wang, Y.P.; Jarvis, P.G. Description and validation of an array model—MAESTRO. *Agric. For. Meteorol.* **1990**, *51*, 257–280. [[CrossRef](#)]
60. Warnant, P.; François, L.; Strivay, D.; Gérard, J.C. CARAIB: A global model of terrestrial biological productivity. *Glob. Biogeochem. Cycles* **1994**, *8*, 255–270. [[CrossRef](#)]
61. Tian, H.; Chen, G.; Zhang, C.; Liu, M.; Sun, G.; Chappelka, A.; Ren, W.; Xu, X.; Lu, C.; Pan, S.; et al. Century-Scale Responses of Ecosystem Carbon Storage and Flux to Multiple Environmental Changes in the Southern United States. *Ecosystems* **2012**, *15*, 674–694. [[CrossRef](#)]
62. Best, M.J.; Pryor, M.; Clark, D.B.; Rooney, G.G.; Essery, R.L.H.; Ménard, C.B.; Edwards, J.M.; Hendry, M.A.; Porson, A.; Gedney, N.; et al. The Joint UK Land Environment Simulator (JULES), model description—Part 1: Energy and water fluxes. *Geosci. Model Dev.* **2011**, *4*, 677–699. [[CrossRef](#)]
63. Clark, D.B.; Mercado, L.M.; Sitch, S.; Jones, C.D.; Gedney, N.; Best, M.J.; Pryor, M.; Rooney, G.G.; Essery, R.L.H.; Blyth, E.; et al. The Joint UK Land Environment Simulator (JULES), model description—Part 2: Carbon fluxes and vegetation dynamics. *Geosci. Model Dev.* **2011**, *4*, 701–722. [[CrossRef](#)]
64. Smith, B.; Wårland, D.; Arneth, A.; Hickler, T.; Leadley, P.; Siltberg, J.; Zaehle, S. Implications of incorporating N cycling and N limitations on primary production in an individual-based dynamic vegetation model. *Biogeosciences* **2014**, *11*, 2027–2054. [[CrossRef](#)]
65. Bondeau, A.; Smith, P.C.; Zaehle, S.; Schaphoff, S.; Lucht, W.; Cramer, W.; Gerten, D.; Lotze-Campen, H.; Müller, C.; Reichstein, M.; et al. Modelling the role of agriculture for the 20th century global terrestrial carbon balance. *Glob. Chang. Biol.* **2007**, *13*, 679–706. [[CrossRef](#)]
66. Krinner, G.; Viovy, N.; de Noblet-Ducoudré, N.; Ogée, J.; Polcher, J.; Friedlingstein, P.; Ciais, P.; Sitch, S.; Prentice, I.C. A dynamic global vegetation model for studies of the coupled atmosphere-biosphere system. *Glob. Biogeochem. Cycles* **2005**, *19*, doi:10.1029/2003GB002199. [[CrossRef](#)]
67. Zeng, N.; Qian, H.; Munoz, E.; Iacono, R. How strong is carbon cycle-climate feedback under global warming? *Geophys. Res. Lett.* **2004**, *31*, doi:10.1029/2004GL020904. [[CrossRef](#)]
68. Inatomi, M.; Ito, A.; Ishijima, K.; Murayama, S. Greenhouse Gas Budget of a Cool-Temperate Deciduous Broad-Leaved Forest in Japan Estimated Using a Process-Based Model. *Ecosystems* **2010**, *13*, 472–483. [[CrossRef](#)]
69. Chang, J.; Ciais, P.; Wang, X.; Piao, S.; Asrar, G.; Betts, R.; Chevallier, F.; Dury, M.; François, L.; Frieler, K.; et al. Benchmarking carbon fluxes of the {ISIMIP}2a biome models. *Environ. Res. Lett.* **2017**, *12*, 45002. [[CrossRef](#)]
70. Frieler, K.; Lange, S.; Piontek, F.; Reyer, C.P.O.; Schewe, J.; Warszawski, L.; Zhao, F.; Chini, L.; Denvil, S.; Emanuel, K.; et al. Assessing the impacts of 1.5 °C global warming—Simulation protocol of the Inter-Sectoral Impact Model Intercomparison Project (ISIMIP2b). *Geosci. Model Dev.* **2017**, *10*, 4321–4345. [[CrossRef](#)]
71. Collalti, A.; Perugini, L.; Santini, M.; Chiti, T.; Nolè, A.; Matteucci, G.; Valentini, R. A process-based model to simulate growth in forests with complex structure: Evaluation and use of 3D-CMCC Forest Ecosystem Model in a deciduous forest in Central Italy. *Ecol. Model.* **2014**, *272*, 362–378. [[CrossRef](#)]
72. Collalti, A.; Marconi, S.; Ibrom, A.; Trotta, C.; Anav, A.; D’Andrea, E.; Matteucci, G.; Montagnani, L.; Gielen, B.; Mammarella, I.; et al. Validation of 3D-CMCC Forest Ecosystem Model (v.5.1) against eddy covariance data for 10 European forest sites. *Geosci. Model Dev.* **2016**, *9*, 479–504. [[CrossRef](#)]
73. Marconi, S.; Chiti, T.; Nolè, A.; Valentini, R.; Collalti, A. The Role of Respiration in Estimation of Net Carbon Cycle: Coupling Soil Carbon Dynamics and Canopy Turnover in a Novel Version of 3D-CMCC Forest Ecosystem Model. *Forests* **2017**, *8*, 220. [[CrossRef](#)]
74. Lasch, P.; Badeck, F.W.; Suckow, F.; Lindner, M.; Mohr, P. Model-based analysis of management alternatives at stand and regional level in Brandenburg (Germany). *For. Ecol. Manag.* **2005**, *207*, 59–74. [[CrossRef](#)]
75. Deckmyn, G.; Verbeeck, H.; de Beeck, M.O.; Vansteenkiste, D.; Steppe, K.; Ceulemans, R. ANAFORE: A stand-scale process-based forest model that includes wood tissue development and labile carbon storage in trees. *Ecol. Model.* **2008**, *215*, 345–368. [[CrossRef](#)]
76. Van Oijen, M.; Rougier, J.; Smith, R. Bayesian calibration of process-based forest models: Bridging the gap between models and data. *Tree Physiol.* **2005**, *25*, 915–927. [[CrossRef](#)]

77. Köhler, P.; Huth, A. The effects of tree species grouping in tropical rainforest modelling: Simulations with the individual-based model Formind. *Ecol. Model.* **1998**, *109*, 301–321. [[CrossRef](#)]
78. Loustau, D.; Bosc, A.; Colin, A.; Ogée, J.; Davi, H.; François, C.; Dufrêne, E.; Déqué, M.; Cloppet, E.; Arrouays, D.; et al. Modeling climate change effects on the potential production of French plains forests at the sub-regional level. *Tree Physiol.* **2005**, *25*, 813–823. [[CrossRef](#)]
79. Nadal-Sala, D.; Keenan, T.F.; Sabaté, S.; Gracia, C. *Forest Eco-Physiological Models: Water Use and Carbon Sequestration BT—Managing Forest Ecosystems: The Challenge of Climate Change*; Springer International Publishing: Berlin, Germany, 2017; pp. 81–102.
80. Haas, E.; Klatt, S.; Fröhlich, A.; Kraft, P.; Werner, C.; Kiese, R.; Grote, R.; Breuer, L.; Butterbach-Bahl, K. LandscapeDNDC: A process model for simulation of biosphere–atmosphere–hydrosphere exchange processes at site and regional scale. *Landscape Ecol.* **2013**, *28*, 615–636. [[CrossRef](#)]
81. Gbondo-Tugbawa, S.S.; Driscoll, C.T.; Aber, J.D.; Likens, G.E. Evaluation of an integrated biogeochemical model (PnET-BGC) at a northern hardwood forest ecosystem. *Water Resour. Res.* **2001**, *37*, 1057–1070. [[CrossRef](#)]
82. Minunno, F.; Peltoniemi, M.; Launiainen, S.; Aurela, M.; Lindroth, A.; Lohila, A.; Mammarella, I.; Minkkinen, K.; Mäkelä, A. Calibration and validation of a semi-empirical flux ecosystem model for coniferous forests in the Boreal region. *Ecol. Model.* **2016**, *341*, 37–52. [[CrossRef](#)]
83. R Core Team. *R: A Language and Environment for Statistical Computing*; R Foundation for Statistical Computing: Vienna, Austria, 2018.
84. Schumacher, S.; Bugmann, H.; Mladenoff, D.J. Improving the formulation of tree growth and succession in a spatially explicit landscape model. *Ecol. Model.* **2004**, *180*, 175–194. [[CrossRef](#)]
85. Speich, M.; Lischke, H.; Scherstjanoi, M.; Zappa, M. FORHYCS—A coupled, spatially distributed eco-hydrological model for assessing climate and land use change impact in Switzerland at landscape scale. *EGU Gen. Assem. Conf. Abstr.* **2016**, *18*, EPSC2016-12988.
86. Lischke, H.; Zimmermann, N.E.; Bolliger, J.; Riekebusch, S.; Löffler, T.J. TreeMig: A forest-landscape model for simulating spatio-temporal patterns from stand to landscape scale. *Ecol. Model.* **2006**, *199*, 409–420. [[CrossRef](#)]
87. Scheller, R.M.; Domingo, J.B.; Sturtevant, B.R.; Williams, J.S.; Rudy, A.; Gustafson, E.J.; Mladenoff, D.J. Design, development, and application of LANDIS-II, a spatial landscape simulation model with flexible temporal and spatial resolution. *Ecol. Model.* **2007**, *201*, 409–419. [[CrossRef](#)]
88. Urbanski, S.; Barford, C.; Wofsy, S.; Kucharik, C.; Pyle, E.; Budney, J.; McKain, K.; Fitzjarrald, D.; Czikowsky, M.; Munger, J.W. Factors controlling CO₂ exchange on timescales from hourly to decadal at Harvard Forest. *J. Geophys. Res. Biogeosci.* **2007**, *112*. [[CrossRef](#)]
89. Hawkins, D.M. The Problem of Overfitting. *J. Chem. Inf. Comput. Sci.* **2004**, *44*, 1–12. [[CrossRef](#)]
90. Mladenoff, D.J.; Host, G.E.; Boeder, J.; Crow, T.R. LANDIS: A model of forest landscape succession and management at multiple scales. In Proceedings of the Annual US Landscape Ecology Symposium, Oak Ridge, TN, USA, 24–27 March 1993; p. 77.
91. Mladenoff, D.J.; He, H.S. Design, behavior and application of LANDIS, an object-oriented model of forest landscape disturbance and succession. In *Spatial Modeling of Forest Landscape Change: Approaches and Applications*; Cambridge University Press: Cambridge, UK, 1999; pp. 125–162.
92. He, H.S.; Mladenoff, D.J.; Boeder, J. An object-oriented forest landscape model and its representation of tree species. *Ecol. Model.* **1999**, *119*, 1–19. [[CrossRef](#)]
93. Wang, W.J.; He, H.S.; Fraser, J.S.; Thompson, F.R.; Shifley, S.R.; Spetich, M.A. LANDIS PRO: A landscape model that predicts forest composition and structure changes at regional scales. *Ecography* **2014**, *37*, 225–229. [[CrossRef](#)]
94. Pennanen, J.; Kuuluvainen, T. A spatial simulation approach to natural forest landscape dynamics in boreal Fennoscandia. *For. Ecol. Manag.* **2002**, *164*, 157–175. [[CrossRef](#)]
95. Pennanen, J.; Greene, D.F.; Fortin, M.J.; Messier, C. Spatially explicit simulation of long-term boreal forest landscape dynamics: incorporating quantitative stand attributes. *Ecol. Model.* **2004**, *180*, 195–209. [[CrossRef](#)]
96. Roberts, D.W.; Betz, D.W. Simulating landscape vegetation dynamics of Bryce Canyon National Park with the vital attributes/fuzzy systems model VAFS/LANDSIM. In *Spatial Modeling of Forest Landscape Change: Approaches and Applications*; Cambridge University Press: Cambridge, UK, 1999; pp. 99–123.

97. Von Neumann, J.; Burks, A.W. Theory of self-reproducing automata. *IEEE Trans. Neural Netw.* **1966**, *5*, 3–14.
98. Noble, I.; Slatyer, R. The use of vital attributes to predict successional changes in plant communities subject to recurrent disturbances. *Vegetatio* **1980**, *43*, 5–21. [[CrossRef](#)]
99. Rothermel, R.C. *A Mathematical Model for Predicting Fire Spread in Wildland Fuels. Res. Pap. INT-115*; Technical Report; U.S. Department of Agriculture, Intermountain Forest and Range Experiment Station: Ogden, UT, USA, 1972.
100. ISO. *ISO/IEC 14882:1998: Programming Languages — C++*; ISO: Geneva, Switzerland, 1998; p. 732.
101. Scheller, R.M.; Hua, D.; Bolstad, P.V.; Birdsey, R.A.; Mladenoff, D.J. The effects of forest harvest intensity in combination with wind disturbance on carbon dynamics in Lake States Mesic Forests. *Ecol. Model.* **2011**, *222*, 144–153. [[CrossRef](#)]
102. Manabe, S. Climate and the Ocean Circulation. *Mon. Weather Rev.* **1969**, *97*, 739–774. [[CrossRef](#)]
103. Thompson, J.R.; Foster, D.R.; Scheller, R.; Kittredge, D. The influence of land use and climate change on forest biomass and composition in Massachusetts, USA. *Ecol. Appl. Publ. Ecol. Soc. Am.* **2011**, *21*, 2425–2444. [[CrossRef](#)]
104. Duveneck, M.J.; Thompson, J.R.; Gustafson, E.J.; Liang, Y.; de Brujin, A.M.G. Recovery dynamics and climate change effects to future New England forests. *Landsc. Ecol.* **2017**, *32*, 1385–1397. [[CrossRef](#)]
105. Duveneck, M.J.; Scheller, R.M.; White, M.A.; Handler, S.D.; Ravenscroft, C. Climate change effects on northern Great Lake (USA) forests: A case for preserving diversity. *Ecosphere* **2014**, *5*, art23. [[CrossRef](#)]
106. Lucash, M.S.; Scheller, R.M.; Gustafson, E.J.; Sturtevant, B.R. Spatial resilience of forested landscapes under climate change and management. *Landsc. Ecol.* **2017**, *32*, 953–969. [[CrossRef](#)]
107. Pacala, S.W.; Canham, C.D.; Silander, J.A., Jr. Forest models defined by field measurements: I. The design of a northeastern forest simulator. *Can. J. For. Res.* **1993**, *23*, 1980–1988. [[CrossRef](#)]
108. Ribbens, E.; Silander, J.A.; Pacala, S.W. Seedling recruitment in forests: calibrating models to predict patterns of tree seedling dispersion. *Ecology* **1994**, *75*, 1794–1806. [[CrossRef](#)]
109. Hurtt, G.C.; Moorcroft, P.R.; And, S.W.P.; Levin, S.A. Terrestrial models and global change: Challenges for the future. *Glob. Chang. Biol.* **1998**, *4*, 581–590. [[CrossRef](#)]
110. Robbins, Z.; Scheller, R.; Case, B.; Strigul, N. The parameterization of PPA formulas using a SORTIE-ND Model for Harvard Forest. Abstracts of the AMS Spring Western Sectional Meeting, 2018. Available online: http://www.ams.org/amsmtgs/2248_abstracts/1137-92-206.pdf (accessed on 1 September 2018).
111. García, O. Can plasticity make spatial structure irrelevant in individual-tree models? *For. Ecosyst.* **2014**, *1*, 16. [[CrossRef](#)]
112. Lee, M.J.; García, O. Plasticity and extrapolation in modeling mixed-species stands. *For. Sci.* **2016**, *62*, 1–8. [[CrossRef](#)]
113. Canham, C.D.; Coates, K.D.; Bartemucci, P.; Quaglia, S. Measurement and modeling of spatially explicit variation in light transmission through interior cedar-hemlock forests of British Columbia. *Can. J. For. Res.* **1999**, *29*, 1775–1783. [[CrossRef](#)]
114. Case, B.S.; Buckley, H.L.; Barker-Plotkin, A.A.; Orwig, D.A.; Ellison, A.M. When a foundation crumbles: forecasting forest dynamics following the decline of the foundation species *Tsuga canadensis*. *Ecosphere* **2017**, *8*, e01893. [[CrossRef](#)]
115. Chojnacky, D.C.; Heath, L.S.; Jenkins, J.C. Updated generalized biomass equations for North American tree species. *For. Int. J. For. Res.* **2014**, *87*, 129–151. [[CrossRef](#)]
116. Raich, J.W.; Potter, C.S.; Bhagawati, D. Interannual variability in global soil respiration, 1980–94. *Global Change Biology* **2002**, *8*, 800–812. [[CrossRef](#)]
117. Domke, G.M.; Perry, C.H.; Walters, B.F.; Nave, L.E.; Woodall, C.W.; Swanston, C.W. Toward inventory-based estimates of soil organic carbon in forests of the United States. *Ecol. Appl.* **2017**, *27*, 1223–1235. [[CrossRef](#)]
118. Valentini, R.; De Angelis, P.; Matteucci, G.; Monaco, R.; Dore, S.; Mucnozza, G.E.S. Seasonal net carbon dioxide exchange of a beech forest with the atmosphere. *Glob. Chang. Biol.* **1996**, *2*, 199–207. [[CrossRef](#)]
119. Clark, D.a.; Brown, S.; Kicklighter, D.W.; Chambers, J.Q.; Thominson, J.R.; Ni, J. Measuring Net Primary Production in Forests: Concepts and Field Methods. *Ecol. Appl.* **2001**, *11*, 356–370. [[CrossRef](#)]

120. Barford, C.C.; Wofsy, S.C.; Goulden, M.L.; Munger, J.W.; Pyle, E.H.; Urbanski, S.P.; Hutyra, L.; Saleska, S.R.; Fitzjarrald, D.; Moore, K. Factors Controlling Long- and Short-Term Sequestration of Atmospheric CO₂ in a Mid-latitude Forest. *Science* **2001**, *294*, 1688–1691. [CrossRef] [PubMed]
121. Reineke, L.H. Perfecting a stand-density index for even-aged forests. *J. Agric. Res.* **1933**, *46*, 627–638.
122. Giasson, M.A.; Ellison, A.M.; Bowden, R.D.; Crill, P.M.; Davidson, E.A.; Drake, J.E.; Frey, S.D.; Hadley, J.L.; et al. Soil respiration in a northeastern US temperate forest: A 22-year synthesis. *Ecosphere* **2013**, *4*, art140. [CrossRef]
123. Hendricks, J.J.; Hendrick, R.L.; Wilson, C.A.; Mitchell, R.J.; Pecot, S.D.; Guo, D. Assessing the patterns and controls of fine root dynamics: an empirical test and methodological review. *J. Ecol.* **2005**, *94*, 40–57. [CrossRef]
124. Drew, M.B.; Kirkman, L.K.; Angus K.; Gholson, J. The Vascular Flora of Ichauway, Baker County, Georgia: A Remnant Longleaf Pine/Wiregrass Ecosystem. *Castanea* **1998**, *63*, 1–24.
125. Goebel, P.C.; Hix, D.M. Changes in the composition and structure of mixed-oak, second-growth forest ecosystems during the understory reinitiation stage of stand development. *Ecoscience* **1997**, *4*, 327–339. [CrossRef]
126. Mitchell, R.J.; Kirkman, L.K.; Pecot, S.D.; Wilson, C.A.; Palik, B.J.; Boring, L.R. Patterns and controls of ecosystem function in longleaf pine—Wiregrass savannas. I. Aboveground net primary productivity. *Can. J. For. Res.* **1999**, *29*, 743–751. [CrossRef]
127. Whelan, A.; Mitchell, R.; Staudhammer, C.; Starr, G. Cyclic Occurrence of Fire and Its Role in Carbon Dynamics along an Edaphic Moisture Gradient in Longleaf Pine Ecosystems. *PLoS ONE* **2013**, *8*, e54045. [CrossRef]
128. Wiesner, S.; Staudhammer, C.L.; Loescher, H.W.; Baron-Lopez, A.; Boring, L.R.; Mitchell, R.J.; Starr, G. Interactions Among Abiotic Drivers, Disturbance and Gross Ecosystem Carbon Exchange on Soil Respiration from Subtropical Pine Savannas. *Ecosystems* **2018**. [CrossRef]
129. Starr, G.; Staudhammer, C.L.; Loescher, H.W.; Mitchell, R.; Whelan, A.; Hiers, J.K.; O'Brien, J.J. Time series analysis of forest carbon dynamics: recovery of *Pinus palustris* physiology following a prescribed fire. *New For.* **2015**, *46*, 63–90. [CrossRef]
130. Krause, P.; Boyle, D.P.; Bäse, F. Comparison of different efficiency criteria for hydrological model assessment. *Adv. Geosci.* **2005**, *5*, 89–97. [CrossRef]
131. Nash, J.; Sutcliffe, J. River flow forecasting through conceptual models part I — A discussion of principles. *J. Hydrol.* **1970**, *10*, 282–290. [CrossRef]
132. Bachelet, D.; Lenihan, J.M.; Daly, C.; Neilson, R.P.; Ojima, D.S.; Parton, W.J. MC1: A dynamic vegetation model for estimating the distribution of vegetation and associated ecosystem fluxes of carbon, nutrients, and water. In *Pacific Northwest Station General Technical Report PNW-GTR-508*; USDA Forest Service: Corvallis, OR, USA, 2001.
133. Waring, R.H.; Law, B.E.; Goulden, M.L.; Bassow, S.L.; McCreight, R.W.; Wofsy, S.C.; Bazzaz, F.A. Scaling gross ecosystem production at Harvard Forest with remote sensing: A comparison of estimates from a constrained quantum-use efficiency model and eddy correlation. *Plant Cell Environ.* **1995**, *18*, 1201–1213. [CrossRef]
134. Goulden, M.L.; Daube, B.C.; Fan, S.M.; Sutton, D.J.; Bazzaz, A.; Munger, J.W.; Wofsy, S.C. Physiological responses of a black spruce forest to weather. *J. Geophys. Res. Atmos.* **1997**, *102*, 28987–28996. [CrossRef]
135. Law, B.E.; Waring, R.H.; Anthoni, P.M.; Aber, J.D. Measurements of gross and net ecosystem productivity and water vapour exchange of a *Pinus ponderosa* ecosystem, and an evaluation of two generalized models. *Glob. Chang. Biol.* **2000**, *6*, 155–168. [CrossRef]
136. Stoy, P.C.; Katul, G.G.; Siqueira, M.B.S.; Juang, J.Y.; Novick, K.A.; Uebelherr, J.M.; Oren, R. An evaluation of models for partitioning eddy covariance-measured net ecosystem exchange into photosynthesis and respiration. *Agric. For. Meteorol.* **2006**, *141*, 2–18. [CrossRef]
137. Piao, S.; Luyssaert, S.; Ciais, P.; Janssens, I.A.; Chen, A.; Cao, C.; Fang, J.; Friedlingstein, P.; Luo, Y.; Wang, S. Forest annual carbon cost: a global-scale analysis of autotrophic respiration. *Ecology* **2010**, *91*, 652–661. [CrossRef]
138. Foken, T.; Leclerc, M.Y. Methods and limitations in validation of footprint models. *Agric. For. Meteorol.* **2004**, *127*, 223–234. [CrossRef]

139. Sogachev, A.; Rannik, Ü.; Vesala, T. Flux footprints over complex terrain covered by heterogeneous forest. *Agric. For. Meteorol.* **2004**, *127*, 143–158. [[CrossRef](#)]
140. Kljun, N.; Calanca, P.; Rotach, M.W.; Schmid, H.P. A simple two-dimensional parameterisation for Flux Footprint Prediction (FFP). *Geosci. Model Dev.* **2015**, *8*, 3695–3713. [[CrossRef](#)]
141. Wang, H.; Jia, G.; Zhang, A.; Miao, C. Assessment of Spatial Representativeness of Eddy Covariance Flux Data from Flux Tower to Regional Grid. *Remote Sens.* **2016**, *8*, 742. [[CrossRef](#)]
142. Arriga, N.; Rannik, Ü.; Aubinet, M.; Carrara, A.; Vesala, T.; Papale, D. Experimental validation of footprint models for eddy covariance CO₂ flux measurements above grassland by means of natural and artificial tracers. *Agric. For. Meteorol.* **2017**, *242*, 75–84. [[CrossRef](#)]
143. Friend, A.D.; Lucht, W.; Rademacher, T.T.; Keribin, R.; Betts, R.; Cadule, P.; Ciais, P.; Clark, D.B.; Dankers, R.; Falloon, P.D.; et al. Carbon residence time dominates uncertainty in terrestrial vegetation responses to future climate and atmospheric CO₂. *Proc. Natl Acad. Sci. USA* **2014**, *111*, 3280–3285. [[CrossRef](#)] [[PubMed](#)]
144. Erickson, A.; Strigul, N. Design and Application of a Next-Generation Forest Biogeochemistry Model, Sortie-NG; ForestSAT 2018; Association for Forest Spatial Analysis Technologies: College Park, MD, USA, 2018.
145. Bingham, E.; Chen, J.P.; Jankowiak, M.; Obermeyer, F.; Pradhan, N.; Karaletsos, T.; Singh, R.; Szerlip, P.; Horsfall, P.; Goodman, N.D. Pyro: Deep Universal Probabilistic Programming. *J. Mach. Learn. Res.* **2018**, arXiv:1810.09538.
146. Erickson, A.; Strigul, N. TBM Gym: A toolkit for developing and comparing terrestrial biosphere models and non-convex optimization algorithms. In *AGU Fall Meeting 2018*; American Geophysical Union: Washington, DC, USA, 2018.
147. Paszke, A.; Gross, S.; Chintala, S.; Chanan, G.; Yang, E.; DeVito, Z.; Lin, Z.; Desmaison, A.; Antiga, L.; Lerer, A. Automatic Differentiation in PyTorch. In Proceedings of the 31st Conference on Neural Information Processing Systems (NIPS 2017), Long Beach, CA, USA, 4–9 December 2017.
148. Chollet, F. Keras. 2015. Available online: <https://keras.io> (accessed on 1 September 2018).
149. Liénard, J.; Vogt, A.; Gatziolis, D.; Strigul, N. Embedded, real-time UAV control for improved, image-based 3D scene reconstruction. *Measurement* **2016**, *81*, 264–269. [[CrossRef](#)]
150. Lindenmayer, A. Mathematical models for cellular interactions in development II. Simple and branching filaments with two-sided inputs. *J. Theor. Biol.* **1968**, *18*, 300–315. [[CrossRef](#)]
151. Stava, O.; Pirk, S.; Kratt, J.; Chen, B.; Měch, R.; Deussen, O.; Benes, B. Inverse Procedural Modelling of Trees. *Comput. Gr. Forum* **2014**, *33*, 118–131. [[CrossRef](#)]



© 2019 by the authors. Licensee MDPI, Basel, Switzerland. This article is an open access article distributed under the terms and conditions of the Creative Commons Attribution (CC BY) license (<http://creativecommons.org/licenses/by/4.0/>).